UNCLASSIFIED

AD 278 810

Reproduced
by the

ARMED SERVICES TECHNICAL INFORMATION AGENCY
ARLINGTON HALL STATION
ARLINGTON 12, VIRGINIA

UNCLASSIFIED

NOTICE: When government or other drawings, specifications or other data are used for any purpose other than in connection with a definitely related government procurement operation, the U. S. Government thereby incurs no responsibility, nor any obligation whatsoever; and the fact that the Government may have formulated, furnished, or in any way supplied the said drawings, specifications, or other data is not to be regarded by implication or otherwise as in any manner licensing the holder or any other person or corporation, or conveying any rights or permission to manufacture, use or sell any patented invention that may in any way be related thereto.

62-4-4

278 810

TDR-62-324

THE DEVELOPMENT OF A LOW TEMPERATURE VAPOR FILLED THERMIONIC CONVERTER

TECHNICAL DOCUMENTARY REPORT NO. ASD-TDR-62-324
June 1962

Flight Accessories Laboratory
Aeronautical Systems Division
Air Force Systems Command
Wright-Patterson Air Force Base, Ohio

Project No. 3145, Task No. 314509

(Prepared under Contract No. AF 33(616)-7903
by Radio Corporation of America, Lancaster, Pennsylvania.
Authors: F. G. Block and J. J. O'Grady.)

NOX

NOTICES

When Government drawings, specifications, or other data are used for any purpose other than in connection with a definitely related Government procurement operation, the United States Government thereby incurs no responsibility nor any obligation whatsoever; and the fact that the Government may have formulated, furnished, or in any way supplied the said drawings, specifications, or other data, is not to be regarded by implication or otherwise as in any manner licensing the holder or any other person or corporation, or conveying any rights or permission to manufacture, use, or sell any patented invention that may in any way be related thereto.

Information furnished by RCA is believed to be accurate and reliable. However, no responsibility is assumed by RCA for its use; nor for any infringements of patents or other rights of third parties which may result from its use. No license is granted by implication or otherwise under any patent rights of RCA.

Qualified requesters may obtain copies of this report from the Armed Services Technical Information Agency, (ASTIA), Arlington Hall Station, Arlington 12, Virginia.

This report has been released to the Office of Technical Services, U.S. Department of Commerce, Washington 25, D.C., in stock quantities for sale to the general public.

Copies of this report should not be returned to the Aeronautical Systems Division unless return is required by security considerations, contractual obligations, or notice on a specific document.

200 - August 1962 - 44-2013 & 2014

FOREWORD

This report was prepared by the Radio Corporation of America, Lancaster, Pennsylvania on Air Force Contract AF33(616)-7903, under Task Number 314509 of Project Number 3145, "The Development of a Low-Temperature, Vapor-Filled Thermionic Converter". The work was administered under the direction of D. R. Warnock and J. D. Murrell, Flight Accessories Laboratory, Aeronautical Systems Division.

The studies presented began in January 1961, were concluded in January 1962 and represent the effort of the Thermionic Energy Conversion group of Space Components Engineering, RCA, Lancaster, Pennsylvania. Mr. F. G. Block, as Project Leader, was assisted in the technical direction of the program by the following engineering personnel: G. Y. Eastman, W. B. Hall, P. R. Liller, R. W. Longsderff, T. C. Loser, J. J. Moscony and J. C. Turnbull. Special assistance was obtained from Dr. K. G. Hernqvist and P. Rappaport of the RCA Laboratories, Princeton, New Jersey.

This report is the Final Technical Report and it concludes the work on Contract AF33(616)-7903.

This report is unclassified.

ABSTRACT

This report covers a one year program of applied research toward developing a low-temperature, plasma, thermionic converter. The converter uses a third electrode to ionize plasma so as to neutralize the space charge. The lower temperature thus achieved should significantly prolong the life of the converter and contribute to the development of a more reliable power supply for space application.

The program was directed toward optimizing geometry and operating characteristics and investigating the effects of temperature and pressure, starting pulse, magnetic fields, and operation in both series and parallel circuitry. Materials were investigated to achieve practical electrodes by determining compatibility of material, atmospheric corrosion, and gas permeation. Converters were fabricated, evaluated, and life tested with the parameters optimized by the test program.

TABLE OF CONTENTS

LIST OF APPENDICES

LIST OF ILLUSTRATIONS

LIST OF ILLUSTRATIONS
(Continued)

LIST OF SYMBOLS

a = anode

A = area-cm^2

c = cathode

e = electronic charge = 1.603×10^{-19} coulomb

G = temperature gradient, $\frac{dt}{ds}$ - degree K/cm

I_o = total current emitted from cathode-amperes

I = total current delivered to load-amperes

j_o = current density from cathode-amperes/cm^2

j = current density delivered to anode - amperes/cm^2

k = Boltzmann's constant - 1.38×10^{-23} joule/degree K

l = electrical length - cm

M_e = electron mass

M_{Cs} = ion mass

P_e = electron emission cooling power loss - watts

P_{Cs} = sum of electrical and thermal conduction power losses in cesium - watts

P_i = power required to generate cesium ions - watts

P_L = power loss in electrical leads - watts

P_o = output power - watts

P_r = cathode radiation power loss - watts

P_t = total power input to converter - watts

R_{Cs} = electrical resistance of cesium - ohms

R_L = electrical resistance of leads - ohms

s = distance - cm

T_a = anode temperature - °K

T_c = cathode temperature - °K

V_i = ionization potential of alkali gas

V_L = voltage drop in electrical leads

ϵ = total thermal emissivity

η = converter efficiency

κ = thermal conductivity - watts/°K/cm

ρ = electrical resistivity - ohm-cm

σ = Stephan-Boltzmann constant - 5.67×10^{-12} watts/cm^2/°K^4

ϕ_a = anode work function - electron volts

ϕ_c = cathode work function - electron volts

THE DEVELOPMENT OF A LOW-TEMPERATURE VAPOR-FILLED THERMIONIC CONVERTER

SECTION I

PURPOSE

The objective of the program was to carry the development to the point where a practical thermionic converter of the low-temperature plasma-type can be designed to meet specific Air Force requirements.

The purpose of this program was to provide for Applied Research toward the development of a low-temperature thermionic converter. The design under investigation utilized a third electrode for plasma ionization and the consequent space-charge neutralization. Lower temperatures are thus achieved which should significantly prolong the life of thermionic converters and contribute thereby to the development of more reliable power supplies for space application.

In order to accomplish the objectives of the program, the work was organized under three main headings: Parameter Evaluation; Materials Development; and Laboratory Models. The specific items of work, as detailed in the original program are as follows:

****

Manuscript released by the author (5 April 1962) for publication as an ASD Technical Documentary Report.

A Parameter Evaluation

(1) The optimum geometrical form of the three-element converter will be sought with consideration given to ease of manufacture, efficiency, and reliability.

(2) The effect on converter performance of anode temperature and plasma pressure shall be established.

(3) The starting pulse and magnetic field requirements and ion-generator bias limits shall be established.

(4) DC and AC operating characteristics will be determined for various loads, for different electrode and vapor temperatures and varying bias and magnetic field.

(5) Methods will be studied for supplying the starting pulse, bias voltage and magnetic field from a single heat source.

(6) Operation of converters in series and parallel connection shall be studied.

(7) Converters will be life tested to determine their stability.

B Materials Development

(1) Work will be directed toward the development of practical cathode materials for operation in the range 900° Centigrade to 1800° Centigrade.

(2) Lanthanum boride (LaB_6) will be investigated as a cathode material. This will include studies of diffusion into substrates, the determination of suitable substrate materials, the interaction with cesium, and the determination of the thermal emissivity.

(3) The performance of LaB_6 and standard cathodes of the matrix and thoria types will be studied in a low-temperature plasma-type converter.

(4) Assistance will be given to the RCA Laboratories in the search for anode materials with suitable low-work functions.

(5) Assistance will be given to the RCA Laboratories in the investigation of different ion emitter materials with high yield in the required temperature range.

(6) The compatibility of converter materials with alkali metals will be studied. This will include cathode, anode, ion emitter, and envelope materials.

(7) Investigations will be made of the atmospheric corrosion of the converter envelope, including cathode support and seal areas.

(8) Gas permeation of the vacuum envelope will be studied over the range 900° - 1800° Centigrade.

C Laboratory Models

(1) Experimental thermionic converters will be fabricated using the information obtained in the parameter evaluation and in the materials development phases.

(2) Important parameters will be optimized with emphasis on high conversion efficiency and long life.

(3) Converters will be life tested under a variety of conditions for extended periods up to 500 hours with periodic repetition of the initial testing procedure to determine the extent of any change in characteristics.

SECTION II

GENERAL FACTUAL DATA

A General

The plasma triode, in which a separate electrode is utilized for ion generation, was developed to the stage where thermionic energy conversion was demonstrated in a metal-ceramic envelope, with a single electrical heat source outside the converter envelope supplying heat to both the cathode and the ion generator electrode.

A net power density of 0.7 watt per square centimeter was demonstrated from such converters at a true operating temperature of 1180° Centigrade.

The operating characteristics with regard to load, cesium pressure, anode temperature, bias voltage and applied magnetic field were determined.

A suitable high-temperature electrical insulation technique was developed allowing cathode and auxiliary electrode to operate in close proximity and at nearly equal temperatures.

B Materials Investigation

Various cathode and ion-generating materials were studied for effectiveness of electron emission and ion generation over the temperature range of interest. Suitable and compatible cathode and ion-generating materials were found and proper processing schedules were developed.

To accomplish the above results, a total of 24 duo-emitter test diodes and 32 plasma triode converters were built and tested.

In addition, most commonly used tube construction materials were tested for compatibility with both liquid and vaporized cesium. While some materials were found to be excessively attacked by cesium, a sufficient number of materials were found to be usable under the conditions encountered in a plasma-triode energy converter.

Tube envelope materials, with and without protective coatings, were evaluated for their resistance to atmospheric corrosion and gas permeation at the operating temperatures of the various portions of a plasma-triode thermionic converter. Suitable materials of both forms were found to resist atmospheric attack at the temperature ranges of interest.

C Conclusions and Recommendations

The principle of plasma-triode converter operation was demonstrated to be sound. Life tests on electrodes and envelope materials appear to establish compatibility with each other and with cesium inside and atmospheric conditions outside the converter under certain operating conditions.

Improvements in converter operation are needed with respect to output power density and bias power requirements. These should be possible by optimizing geometry with regard to module size, ratio of cathode and ion-generating area, and relative positioning of electrodes. While graphite is a satisfactory material for the auxiliary electrode if certain precautions are taken with regard to contact with cesium, another more versatile material should be found. More extensive life testing is required to determine the stability and reliability of plasma-triode converters. Characteristics of converters operating in series must be obtained.

SECTION III
DETAILED FACTUAL DATA

A Introduction

The basic operation of a thermionic converter has been described in an earlier paper and also has been discussed in several RCA publications, such as the paper by Hernqvist, Kanefsky, and Norman, entitled "Thermionic Energy Converter".

In the method investigated herein for space-charge cancellation, which is based on space-charge neutralization by positive ion injection into the interelectrode space, this space becomes occupied with a plasma-like medium. Since in general the creation of electron-ion pairs requires electric power, it is very important for efficient converter operation to utilize an efficient ionization mechanism. Such a mechanism is the ion generation in cesium vapor due to resonance ionization at a hot high-work-function surface. Thus, by introducing cesium vapor in a thermionic diode, ions generated at the cathode surface will be injected into the interelectrode space. For efficient ion generation, the cathode work-function must be close to the ionization potential for cesium or about 3.9 volts. This high cathode work-function calls for high ($\sim$ 2000° Centigrade) cathode (and heat source) temperatures for efficient converter operation.

However, an invention made at the RCA Laboratories has made it possible to extend the principles used in the cesium diode to allow operation at the much lower cathode temperatures used for the close-spaced vacuum diode. Here a third electrode whose sole purpose is to generate ions, is introduced in close proximity to the cathode and the anode.

B Parameter Evaluation

1. Geometry Studies

For a plasma triode operating from a single heat source, heating both the electron emitter and the ion emitter, the prime design considerations are those of heat transfer to the emitters and of the electrical insulation between the emitters. Heat from the heat source must be conducted through an insulator to either the ion emitter or the electron emitter. This of course, will result in a temperature difference between the ion emitters and cathode which must be minimized. For high efficiency, it is desirable to operate the electron emitter at a temperature close to that of the heat source. As is seen from Figure 1, the performance of the ion emitter is better the higher its temperature. The temperature uniformity between ion emitters is also of paramount importance in order to obtain a uniform plasma density. The thermodynamic and insulation design requirements of the ion emitter cathode assembly cause mechanical design problems which greatly limited the study of the best ion emitter cathode geometry to give high power density.

High-density alumina ceramic insulators have good thermal conductivity at temperatures in the 1000-1500° Centigrade range (0.1 - 0.2 times that of molybdenum) and was therefore used as the insulating member. The most severe temperature drop appears across thermal barriers between the metal and insulator members. This temperature drop is caused by poor bond between the insulator and metal member which results in a high interface resistance to heat flow. In order to reduce the thermal barrier, three different

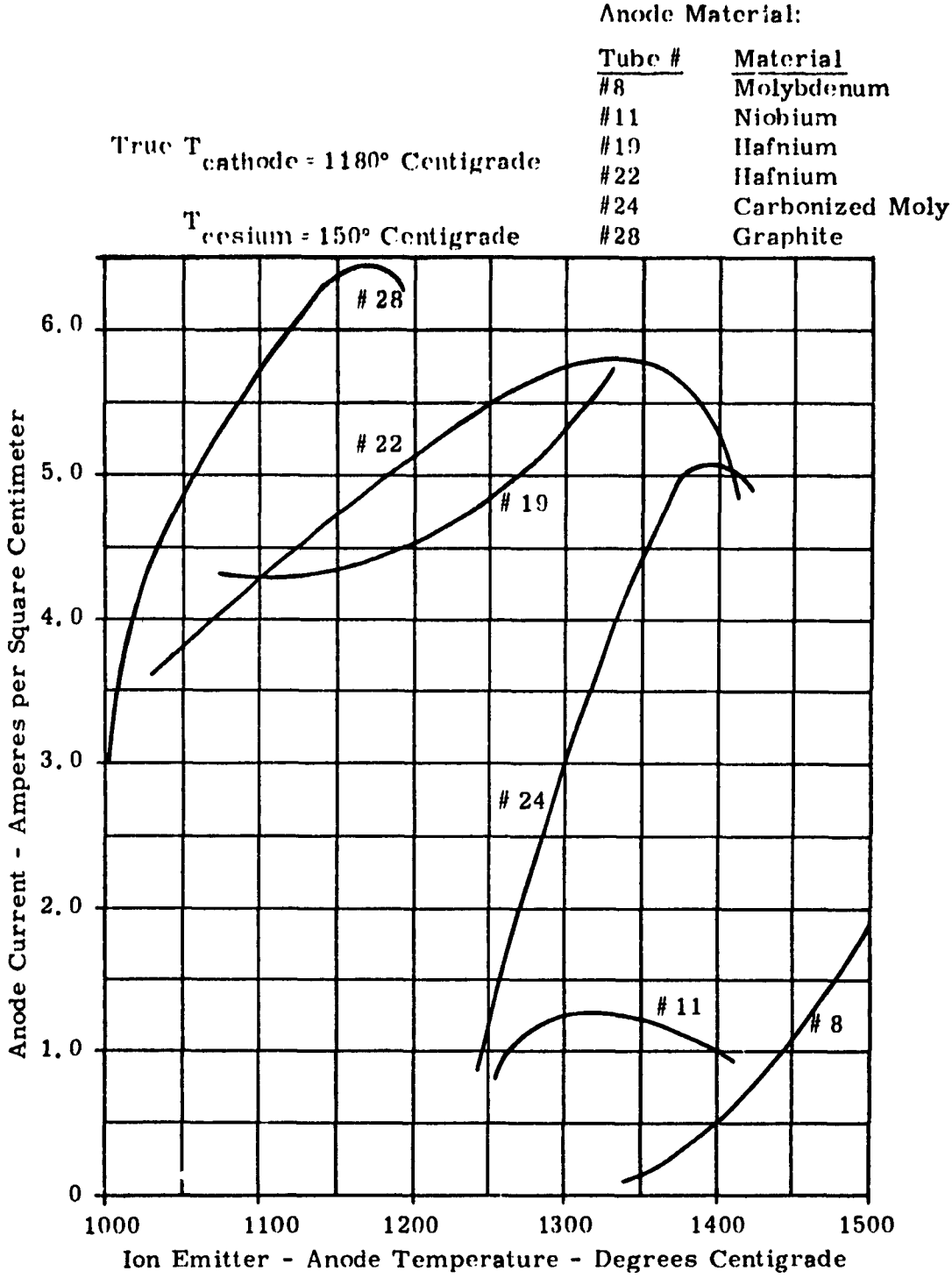

FIGURE 1 - ANODE CURRENT VERSUS ION EMITTER TEMPERATURE FOR VARIOUS ANODE MATERIALS

approaches were taken to fasten the ceramic to the metals: (1) melting of alumina, (2) high temperature sintering of the aluminum oxide, and (3) brazing of metalized ceramics with a nickel molybdenum powder mixture.

The ion emitter cathode assemblies shown in Figures 2 and 3 were made by melting aluminum oxide in hydrogen and allowing it to flow between the molybdenum ion emitters and the molybdenum assembly base. The base ion-emitter assemblies are made at 2300° Centigrade. The cathodes are then brazed in with nickel molybdenum brazing material at 1365° Centigrade. During the braze, alloying between the molybdenum base and the brazing material increases the melting temperature to 1500° Centigrade which is 300° Centigrade above cathode operating temperature. One experimental converter was made using this type of assembly. Excellent temperature uniformity was obtained. However, the converter performed poorly. After the first tests on duo-emitter diodes revealed that molybdenum is not a good ion emitter at 1180° Centigrade, the poor operation of the converter is easily explained. Later hafnium and graphite were found to be good ion emitters. These materials could not be used with this method of fabrication because they form alloys with the molybdenum assembly base and with aluminum oxide at the temperatures necessary to make the assembly. This method of fabrication was, therefore, abandoned.

The ion emitter cathode assemblies shown in Figures 4, 5, and 6 were made both by high-temperature sintering of aluminum oxide and by brazing to metalized ceramics. During high-temperature

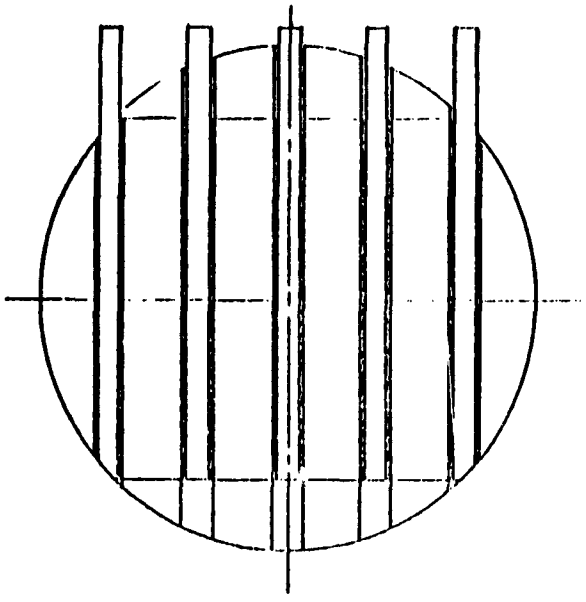

ION-EMITTER ASSEMBLY
RCA DEVELOPMENTAL
PART NUMBER 344-1580

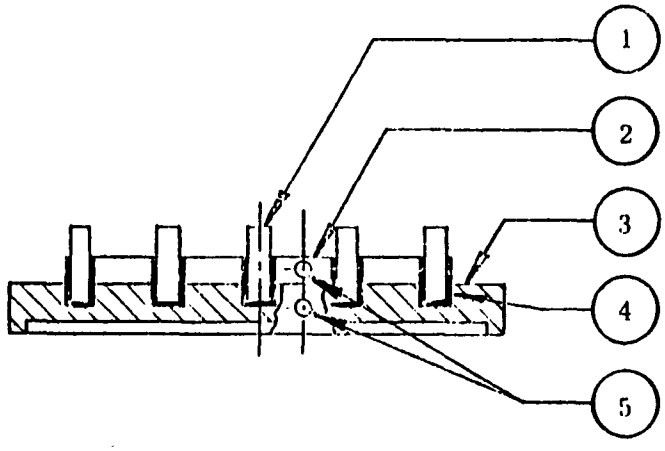

FIGURE 2 - ION EMITTER ASSEMBLY #344-1580
FOR PLASMA-TRIODE CONVERTER

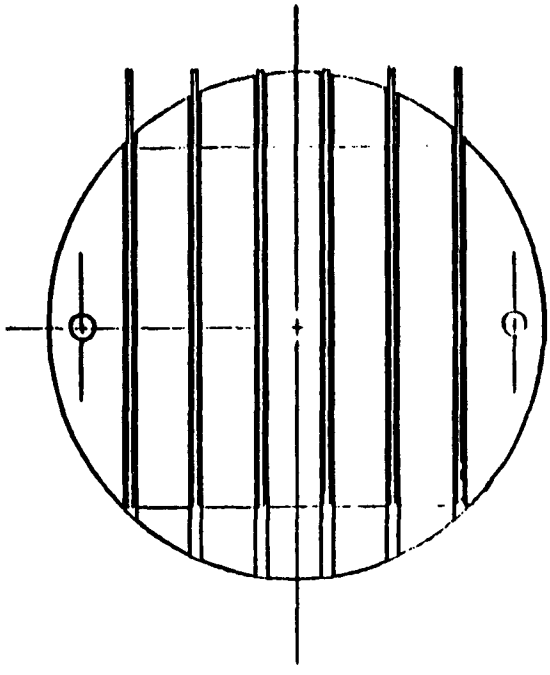

ION-EMITTER ASSEMBLY
RCA DEVELOPMENTAL
PART NUMBER 344-1662

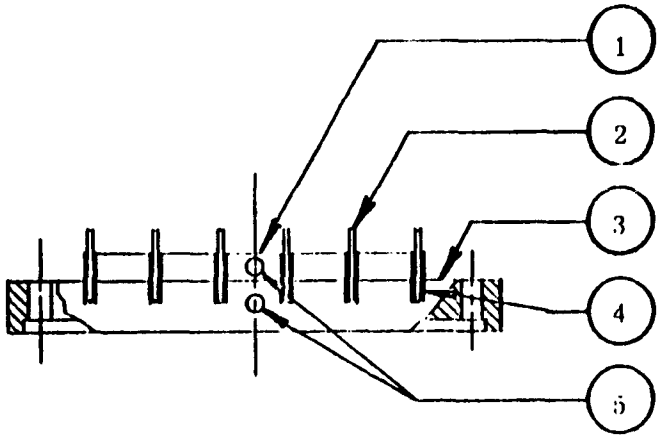

Cathode

Ion-Emitter

Assembly Base

Insulator

Black-Body Holes

FIGURE 3 - ION-EMITTER ASSEMBLY #344-1662
FOR PLASMA TRIODE CONVERTER

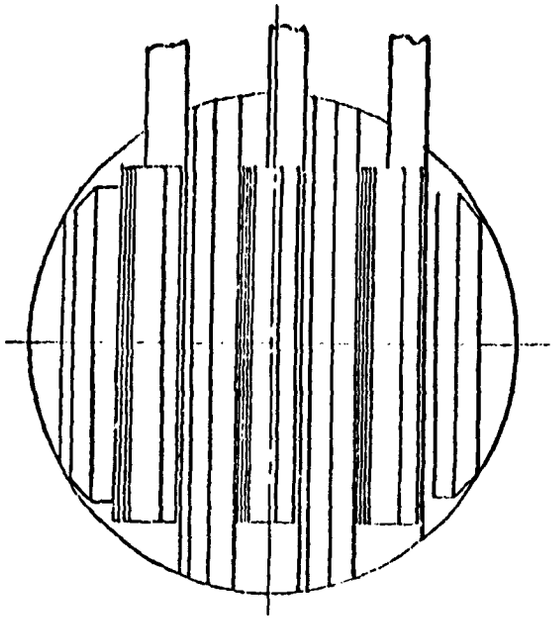

ION-EMITTER ASSEMBLY
RCA DEVELOPMENTAL
PART NUMBER 344-1599

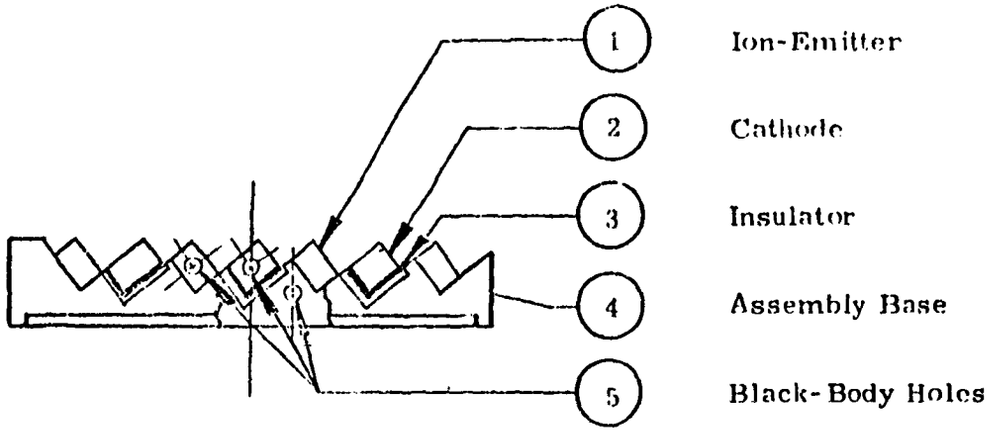

FIGURE 4 - ION-EMITTER ASSEMBLY #344-1599
FOR PLASMA-TRIODE CONVERTER

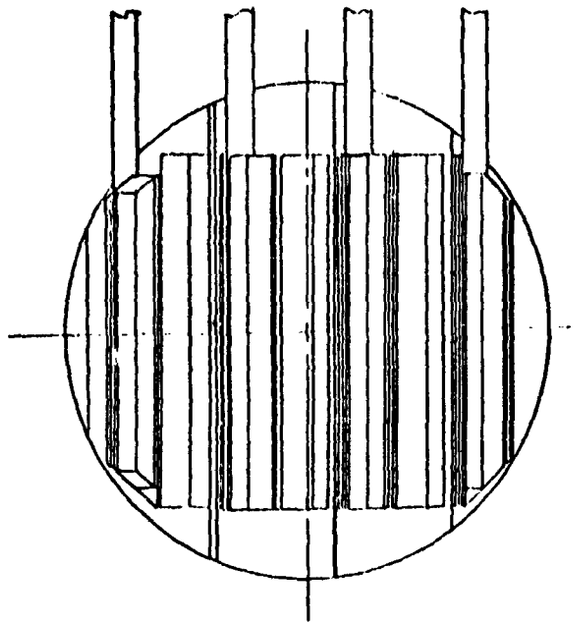

ION-EMITTER ASSEMBLY
RCA DEVELOPMENTAL
PART NUMBER 344-1641

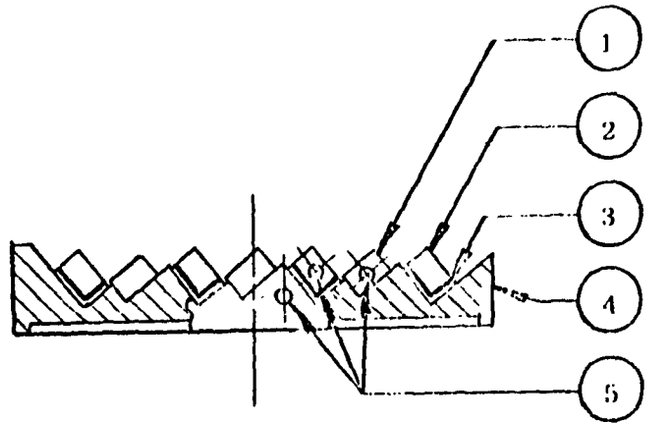

FIGURE 5 - ION EMITTER ASSEMBLY #344-1641
FOR PLASMA-TRIODE CONVERTER

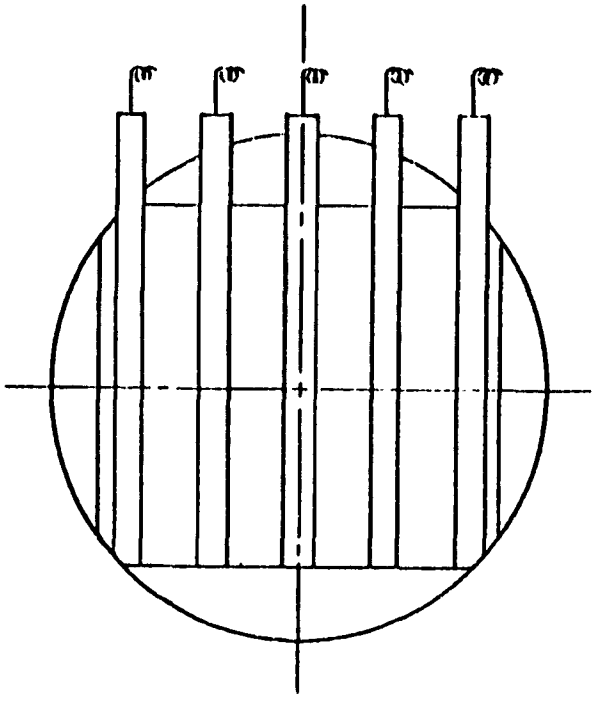

Ion-Emitter Assembly
RCA Developmental
Part Number 344-1686

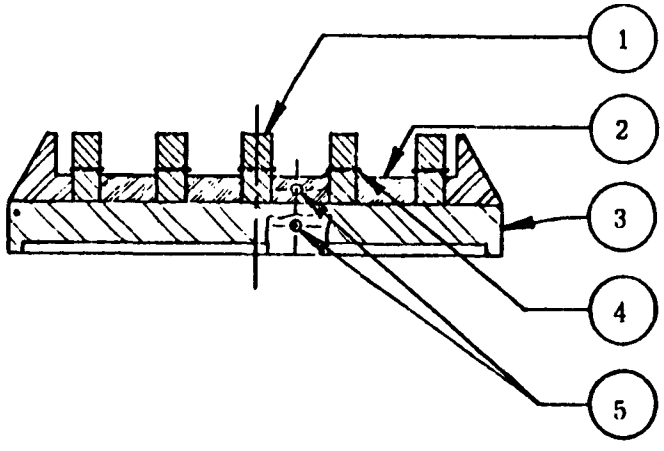

Ion Emitter

Cathode

Assembly Base

Insulator

Black-Body Holes

FIGURE 6 - ION-EMITTER ASSEMBLY #344-1686
FOR PLASMA-TRIODE CONVERTER

sintering of aluminum oxide to molybdenum at 1800° Centigarde, the quality of the sintered joint depends upon obtaining uniform pressure over the sintered area. Since uniform pressure could not always be maintained over the entire area to be joined, poor joints and a high-thermal barrier resulted. Therefore, the use of metalized ceramics was employed to improve the bond. The metalized ceramic was brazed to the assembly base and to the ion emitter with nickel molybdenum brazing material at 1365° Centigrade. Repeated thermal cycles from 20° Centigrade to 1180° Centigrade has shown these assemblies to be mechanically sound.

The ion emitter assembly shown in Figure 4 is designed with the cathode insulated from the assembly base. In this structure, the ion emitters operate 20° Centigrade hotter than the cathode. As better ion emitter materials were found that would operate effectively at a temperature below the cathode, this approach was no longer required and was not needed. The ion emitter assembly shown in Figure 5 proved to be the easiest to fabricate and gave the best converter performance. In this structure, as well as the one shown in Figure 6, the cathode is brazed to the substrate and the ion emitters are insulated. This approach has the advantage of requiring only one heavy-heat obtaining-lead from the cathode structure, the one carrying the converter current and forming the vacuum barrier. The ion emitter lead, carrying only a small current, may be made thin, thereby minimizing heat loss

2. Optimum Temperature Determination

Experiments to determine the optimum temperature at which the

ion emitter and the cathode should operate were conducted in the duo-emitter diodes. It was found from these experiments that the best ion emitter materials (graphite and hafnium) should operate at a temperature as close to the impregnated cathode operating temperature (1180° Centigrade) as possible. The optimum temperatures of the anode and cesium reservoir were investigated in laboratory model converters. The best anode temperature was found to be 250° Centigrade for an optimum cesium reservoir temperature of 150° Centigrade.

3. Starting Pulse, Bias Investigation and Magnetic Field Requirements
An experimental plasma triode was designed in the early stages of the contract to obtain a better understanding of converter operation and to give more reliable data on starting pulse, bias, and magnetic field requirements than could be obtained in converters built at the RCA Laboratories which had the heaters in the cesiated chamber. A cross-sectional drawing of this converter is shown in Figure 7. In order to obtain this information at an early stage in the program before laboratory models were designed compromises were made in the design of the converter geometry so that many standard RCA parts could be used. These compromises caused an unwanted low-voltage arc discharge between low and high-work functions on the support structure. This discharge prevented optimum bias from being applied to the ion emitter which resulted in poor converter operation. However, the data obtained from this converter did give a better understanding of the starting pulse, bias, and magnetic field requirements. The operation of this converter demonstrated that the operational theory of a plasma triode was sound

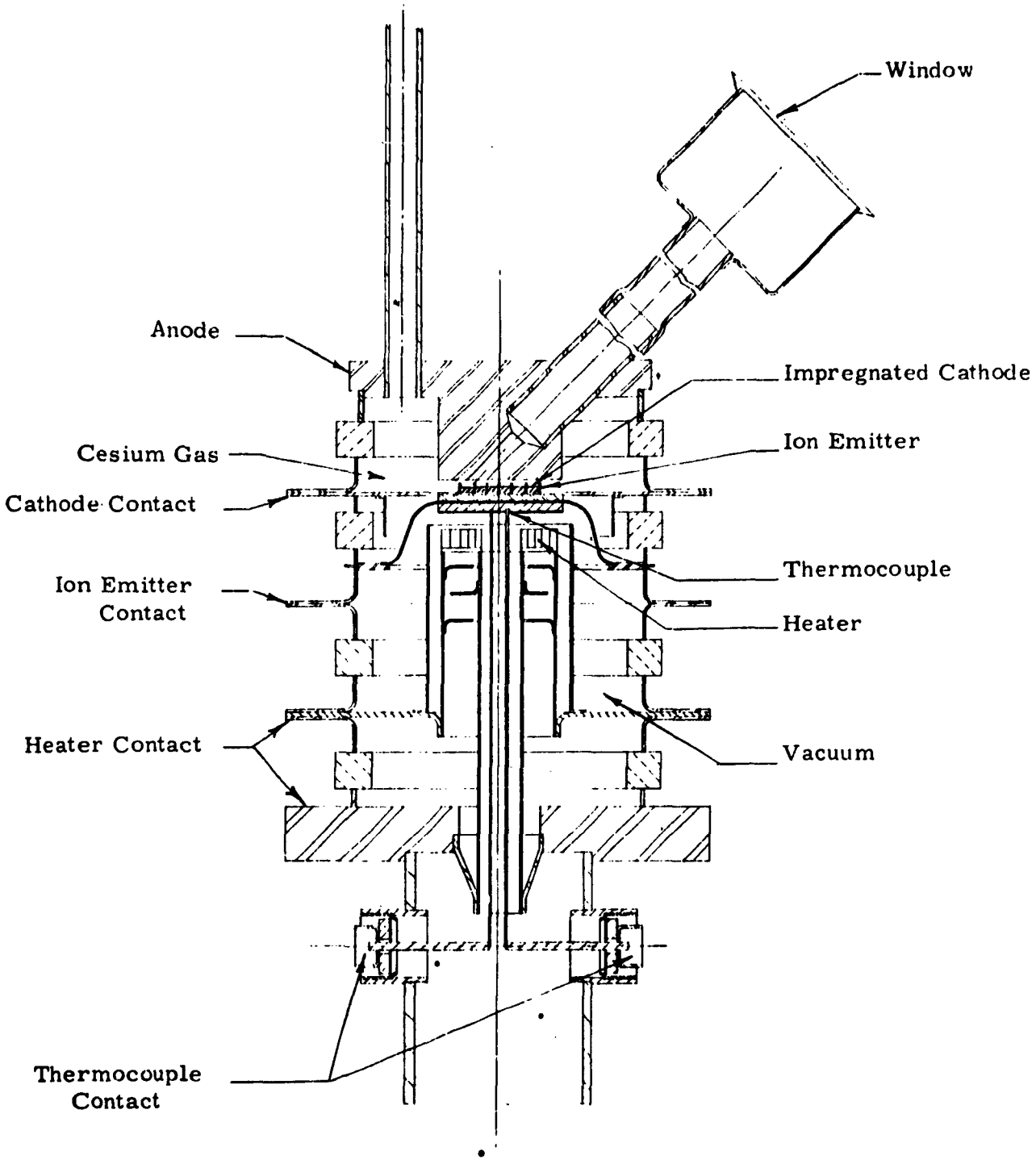

FIGURE 7 - EXPERIMENTAL CONVERTER ASSEMBLY DRAWING

and that neither a magnetic field nor a starting pulse is required. These results were verified from tests conducted on laboratory model converters (A1196). In addition, the laboratory model converter incorporated a method by which a longitudinal magnetic field could be impressed on the converter between the cathode-anode gap. The magnetic field improved the current division between the ion emitter and cathode but at the same time, the power output was reduced. With more advanced geometries the magnetic field may aid converter operation. Bias power is essential to converter operation and will therefore, always be required. The detailed effect of this magnetic field and the bias requirements are discussed and shown in Section III-D-3.

C Materials Development

1. Cathode Development

At the start of the work on plasma triode converters, little data was available on the temperature at which the ion emitter must be run to give sufficient ions, by contact ionization, to neutralize the space charge. Since the ion emitter and the cathode are heated from the same heat source, the operating temperature of the ion emitter determines the type of cathode to be employed. Therefore, two types of cathodes - lanthanum hexaboride (LaB_6) and tungsten impregnated cathodes were investigated for use in the plasma triode. The selection of these cathodes gave a temperature range of 1500° Centigrade for LaB_6 and 1180° Centigrade true for impregnated tungsten in which the ion emitter must operate. As the work on ion emitters progressed and more data became available on the ion emission properties of various materials, it

was found that sufficient ions could be obtained at 1180° Centigrade to neutralize the space charge and the work on LaB_6 was dropped in favor of tungsten impregnated cathodes. The work that was done on these two types of cathodes follows:

a. Lanthanum Hexaboride (LaB_6)

The excellent emission properties of LaB_6 has been known for some time, but the use of this material has always presented a problem in that boron diffuses into the substrate to which it is applied and is lost. Tests were performed to determine the relative rates of diffusion of boron from LaB_6 into various substrate materials. LaB_6 was cataphoretically coated onto tantalum strips, some of which had been previously carburized and/or coated with tantalum boride. After resistance heating these strips for 30 minutes at approximately 1700° Centigrade, the samples were cross-sectioned and micro-photographed for evaluation. Substrates of TaC and TaB_2 evidenced considerably less boron penetration after 30 minutes at temperature than did tantalum after only one minute. See Figures 8, 9, and 10. Although differences between the two were slight, TaB_2 seems to resist boron diffusion better than TaC. Initial attempts to test these substrates on filament cathodes mounted into standard RCA power tube (811A) failed. Tantalum boride peels after a few hours life and tantalum carbide causes the resistance of the filament to change with life. A tungsten matrix impregnated with tantalum boride was found to give excellent adherence. Therefore, tubes were made employing tungsten matrix impregnated with tantalum boride and coated with LaB_6. Additional

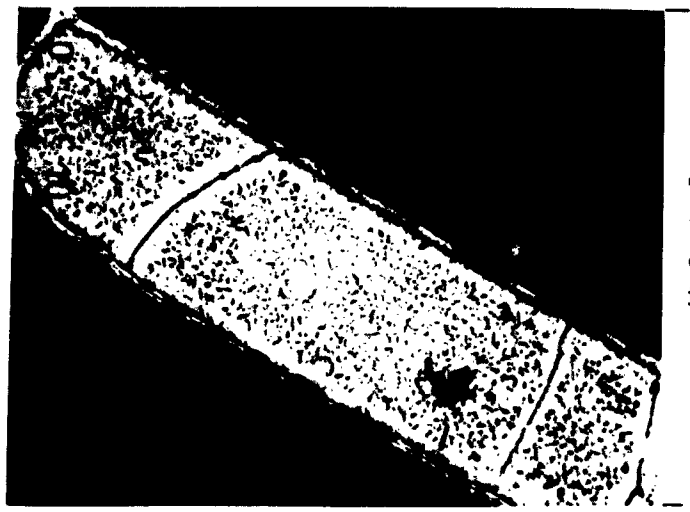

FIGURE 8

BORIDE PENETRATION SAMPLE #1

Tantalum Carbide cataphoretically coated with Tantalum Boride then cataphoretically coated with Lanthanum Hexaboride Magnification 194X.

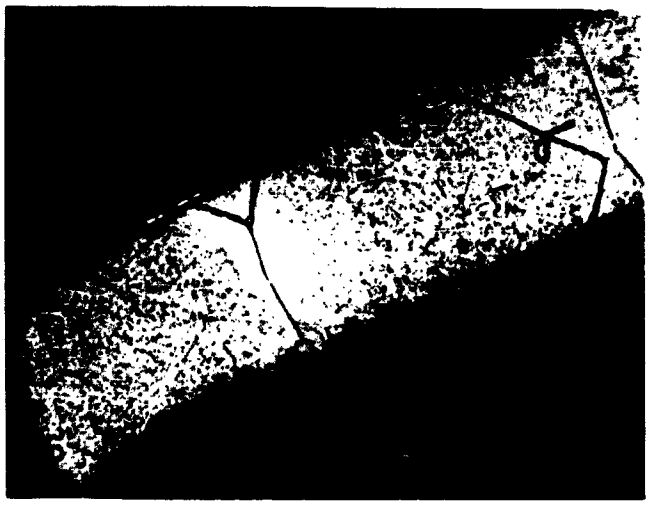

FIGURE 9

BORIDE PENETRATION SAMPLE #2

Tantalum Carbide cataphoretically coated with Lanthanum Hexaboride Magnification 194X.

FIGURE 10

BORIDE PENETRATION SAMPLE #3

Pure Tantalum cataphoretically coated with Lanthanum Hexaboride Magnification 194X.

control tubes were made with tungsten and rhenium coated with LaB_6. After processing, the peak emission was recorded and the tube placed on life test with the cathode operating at 1500° Centigrade true temperature. The peak emission was then taken at regular intervals during life. The data is shown below:

Tube Number 10

Base Material: Tungsten wire coated with LaB_6.

Time (hours)	Current Density (amps/cm^2)
0	0.82
25.6	0.52
436.1	0.69
1298.3	0.59
1855.7	0

Conclusion: LaB_6 had diffused into the tungsten substrate causing it to become very brittle.

Tube Number 21

Base Material: Tungsten matrix impregnated with tantalum boride coated with LaB_6.

Time (hours)	Current Density (amps/cm^2)
0	2.06
42.4	1.35
69.3	2.06
2130.6	2.06
2750.8	Open Heater

Conclusion: Tantalum boride prevents the diffusion of boron.

Tube Number 19

Base Material: Tungsten matrix impregnated with tantalum boride coated with LaB_6.

Time (hours)	Current Density (amps/cm^2)
0	2.85
11.0	1.01
58.4	1.67
279.9	1.92
2683.1	2.02
4032.1	2.06

Conclusion: Life test discontinued at end of contract. Tantalum boride prevents the diffusion of boron.

Tube Number 15

Base Material: Rhenium coated with LaB_6.

Time (hours)	Current Density (amps/cm^2)
0	2.56
42.4	1.70
69.3	1.09
461.5	1.41
2158.6	1.30
2778.8	0.89
4127.8	0.86

Conclusion: Life test discontinued at end of contract. The rate of diffusion of boron into rhenium is slower than in tungsten, but faster than into tantalum boride.

Tantalum boride appears to be a good diffusion barrier for boron. More tests would have to be run before LaB_6 could be used as a cathode in a thermionic converter. Better methods of applying LaB_6 to the base material would be desirable to reduce its spectral emissivity. The spectral thermal emissivity of cataphoretically coated LaB_6 was measured as:

$$\epsilon_{\lambda} = 0.85 \text{ at } 1000^{\circ} \text{ Centigrade}$$

where

ϵ = emissivity at wavelength

$\lambda = 0.66\mu$ (microns)

b. Tungsten Impregnated Cathode

The vendors of these cathodes indicated that the direct current emission density that they would deliver at true cathode temperature of 1180° Centigrade is 10 amperes per square centimeter. This conclusion was based on long-pulse peak emission data from impregnated cathodes operating in vacuum. No data was available on their operation under field free conditions in a cesium atmosphere. The duo-emitter diode, discussed in Section III-C-5 is an ideal test vehicle to investigate the use of impregnated cathodes in thermionic converters. All of the conditions to which a cathode would be subjected in converter operation are simulated in a duo-emitter. The cathode is subjected to ionized cesium at the same pressure and temperature that is encountered in converter operation and the emission is measured under direct-current field-free conditions. Under these simulated converter operating conditions, a current density of

8 amperes per square centimeter was achieved and maintained for 1700 hours. The actual operating conditions are discussed in Section III-C-5. All of the data that is presented in that Section applies to the performance of tungsten impregnated cathodes in simulated converter operating conditions. The tungsten impregnated cathode has proved to be easily fabricated and gives consistently high emission which can be easily maintained for many hours life.

2. Cesium Compatibility

In order to provide information pertinent to the development of a low-temperature thermionic converter, a program was initiated to test various materials in cesium liquid and vapor over a wide range of temperatures. The detailed Technical Discussion on this work appears in Appendix 1.

In general, many metals and ceramics were found to have good resistance to attack particularly at the lower temperatures. At the higher temperatures, certain metals showed good resistance only after adequate vacuum treatment. Brazing alloys containing gold and silver showed poor resistance even at the lower temperatures.

3. Atmospheric Corrosion of the Vacuum Envelope

In some applications it is desirable to operate all or a portion of the vacuum envelope of a thermionic energy converter in an oxidizing atmosphere at elevated temperatures. For this reason tests were performed to determine oxidation rates of various materials at 600° Centigrade and 1000° Centigrade.

A number of tube construction metals and alloys show atmospheric oxidation rates in excess of that desired for long-term applications. Protective coatings and/or suitable substitutes must be found to insure extended life. A method was developed that affords good protection for molybdenum against oxidation in air at 600° Centigrade. Silicized molybdenum coatings were not found practical for extended use at 1300° Centigrade. The detailed Technical Discussion of the work appears in Appendix III.

4. Gas Permeation Study of Material

This investigation was undertaken to enable the best choice of envelope materials for a thermionic energy converter to be heated by fossil fuels to temperatures of 1200° Centigrade or higher.

It was found that metals can not be used at high temperatures in contact with gases containing hydrogen, due to rapid permeation of the metals by hydrogen. The only material offering protection from gas permeation for all gases of interest was found to be an alumina ceramic. The detailed Technical Discussion of this work appears in Appendix II.

5. Ion Emitter Development

In order to study the details of plasma synthesis as it applies to a three-element converter, an idealized geometry was designed into test diodes. Such a geometry which qualitatively simulates the three-element converter geometry is the plane-parallel structure where electrons are emitted from one electrode and ions from the other. This structure, called the duo-emitter diode, facilitates a convenient evaluation of low-temperature electron and ion emitter

materials in a low-pressure cesium environment. Values for the contact difference in potential between the ion emitter and cathode, saturated ion emission, and saturated electron emission can be obtained from measurements using the diode. Since the operation of a converter is simulated in the diode, life test data from the diode can be used to determine the compatibility of a converter system.

A cross-sectional drawing of the duo-emitter diode is shown in Figure 11. The tube consists of two separate identical heater chambers which are under vacuum and are outside of the cesiated chamber. With this arrangement, there is no possibility of erroneous operation that can be caused by ionization of the cesium from applied heater potentials. The cathode and ion emitter materials to be tested are brazed separately to each of the heater chambers. Ions are produced by contact ionization with the ion emitter anode surface thus neutralizing the space charge. When a bias voltage, equal to the difference in work function between the ion emitter and cathode, is applied, field-free emission current flows across the structure. The test circuit use for the duo-emitter diode is shown in Figure 12. A typical volt-ampere characteristic of the duo-emitter diode is shown in Figure 13. Data from these diodes have shown that converter operation is successfully simulated.

Once the cathode material is chosen for a triode design, the choice of ion emitter material is limited. There are four basic requirements for an ion emitter suitable for a plasma triode: (1) it must have good ion emission and life at an operating temperature equal

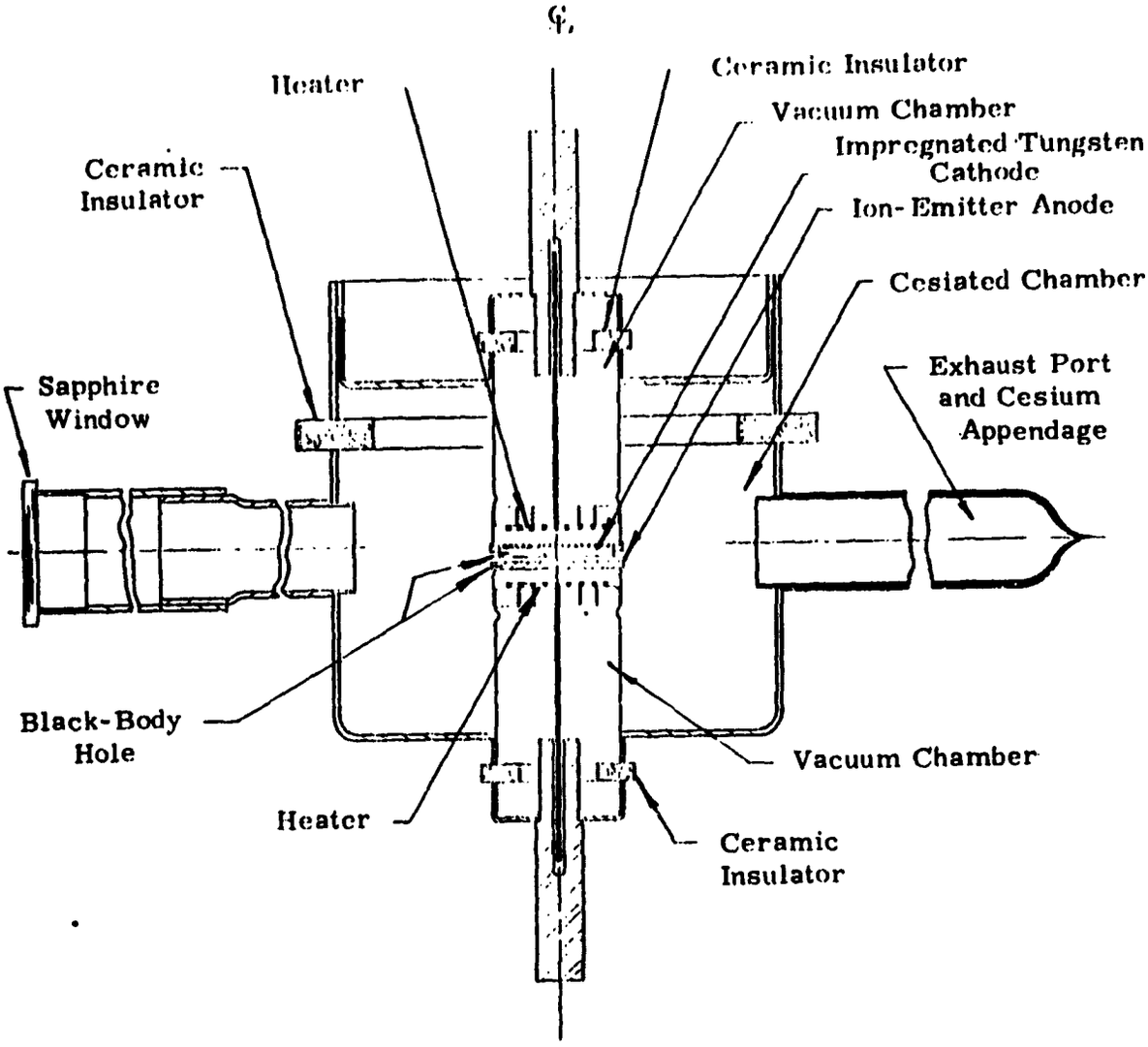

FIGURE 11- CROSS-SECTIONAL DRAWING
OF THE DUO-EMITTER DIODE

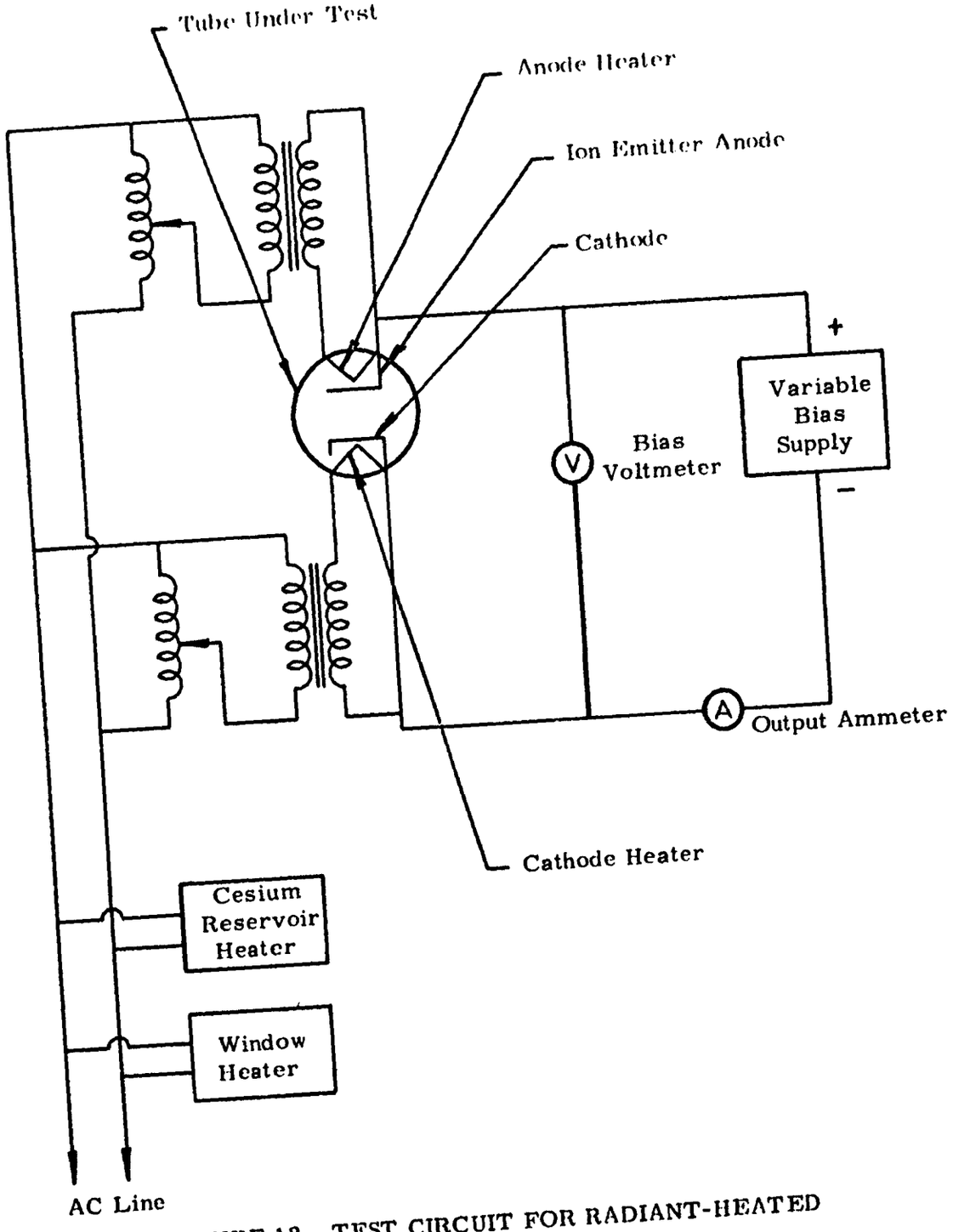

FIGURE 12 - TEST CIRCUIT FOR RADIANT-HEATED DUO-EMITTER DIODE

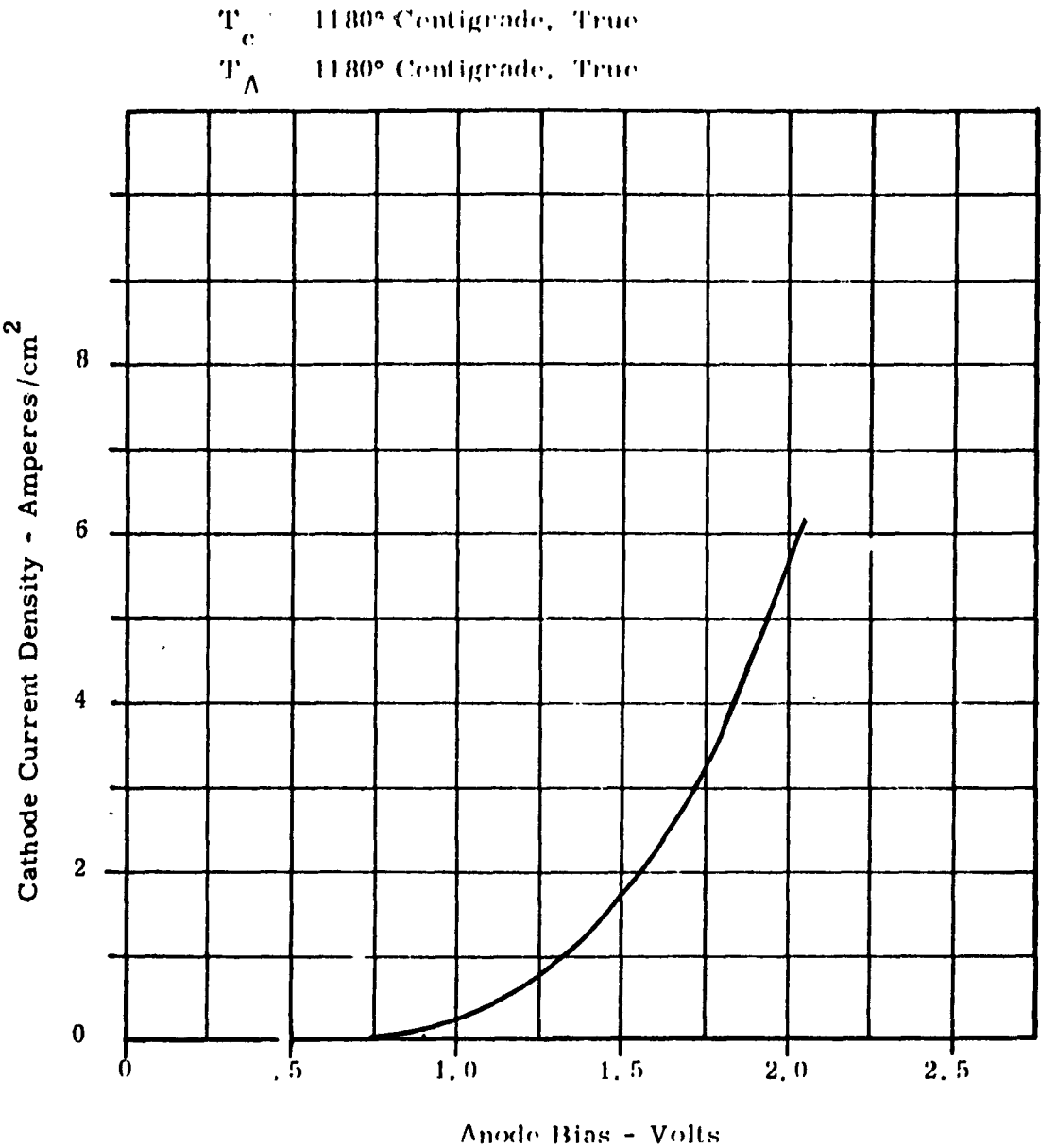

FIGURE 13 - VOLT-AMPERE CHARACTERISTIC
OF A DUO-EMITTER DIODE

to and preferably lower than the cathode operating temperature, (2) its properties as an ion emitter must not be affected by material transported from the electron emitter, (3) the ion emitter must be compatible with the cathode, (4) the ion emitter must be compatible with cesium vapor. Since the operating temperature (1550° Centigrade for high-current density) of lanthanum hexaboride was considered to be too high for most applications, the impregnated cathode, which operates at a lower temperature, (1180° Centigrade true) was selected for the ion emitter tests. When considering a triode design using the impregnated cathode, the question of contamination of the ion emitter by the impregnated evaporants becomes of great importance. The impregnated cathode gives off appreciable quantities of barium and barium oxide which, if they remain on the ion emitter surface, would lower its work function and reduce the ion emission. In order to study the performance of the ion emitter in the presence of impregnated cathode, the duo-emitter diode, meeting the basic requirements for temperature, was used. In these tests the impregnated cathode having an area of 1.8 square centimeters was designed to face the ion emitter in a low-pressure cesium environment.

The following ion emitter materials were evaluated: niobium, molybdenum, carburized molybdenum, hafnium, graphite and vapor deposited carbon. During these tests the impregnated cathode was operated at a true temperature of 1180° Centigrade as measured in a black body hole through a sapphire window. The temperature of the ion emitter was measured by the same method. The results of these studies are given in Figure 1. The diode current was plotted

as a function of ion-emitter temperature for the various materials. Graphite and hafnium gave excellent ion emission at true temperatures between 1100° and 1200° Centigrade. Carburized molybdenum, molybdenum, and niobium gave insufficient ionization at 1180° Centigrade (cathode operating temperature) to be of interest for use in the plasma triode. Vapor deposited carbon on molybdenum flaked from the substrate in the presence of cesium vapor and therefore could not be tested. This flaking was caused by cesium attack on carbon. Since graphite displayed the highest ion-emitter characteristics tested, it was chosen as the best material to use to prove out the principles of the plasma triode. Much work was done toward determining the best methods for its use. Cesium was found to attack graphite severely if liquid cesium came into contact with the graphite at temperatures below 1000° Centigrade. Special care was taken to keep the graphite above 1000° Centigrade in the presence of cesium. Extensive tests of graphite, as an ion-emitter material, were conducted with cathode at various temperatures, with various cesium reservoir temperatures, and with various anode temperatures. This information is shown in Figures 14, 15, 16, and 17.

Life tests were performed using graphite and hafnium as the ion-emitter material in the duo-emitter diode under conditions determined in the evaluation listed above. The life test conditions are as follows:

Ion-emitter anode true temperature	1180° Centigrade
Impregnated cathode true temperature	1180° Centigrade

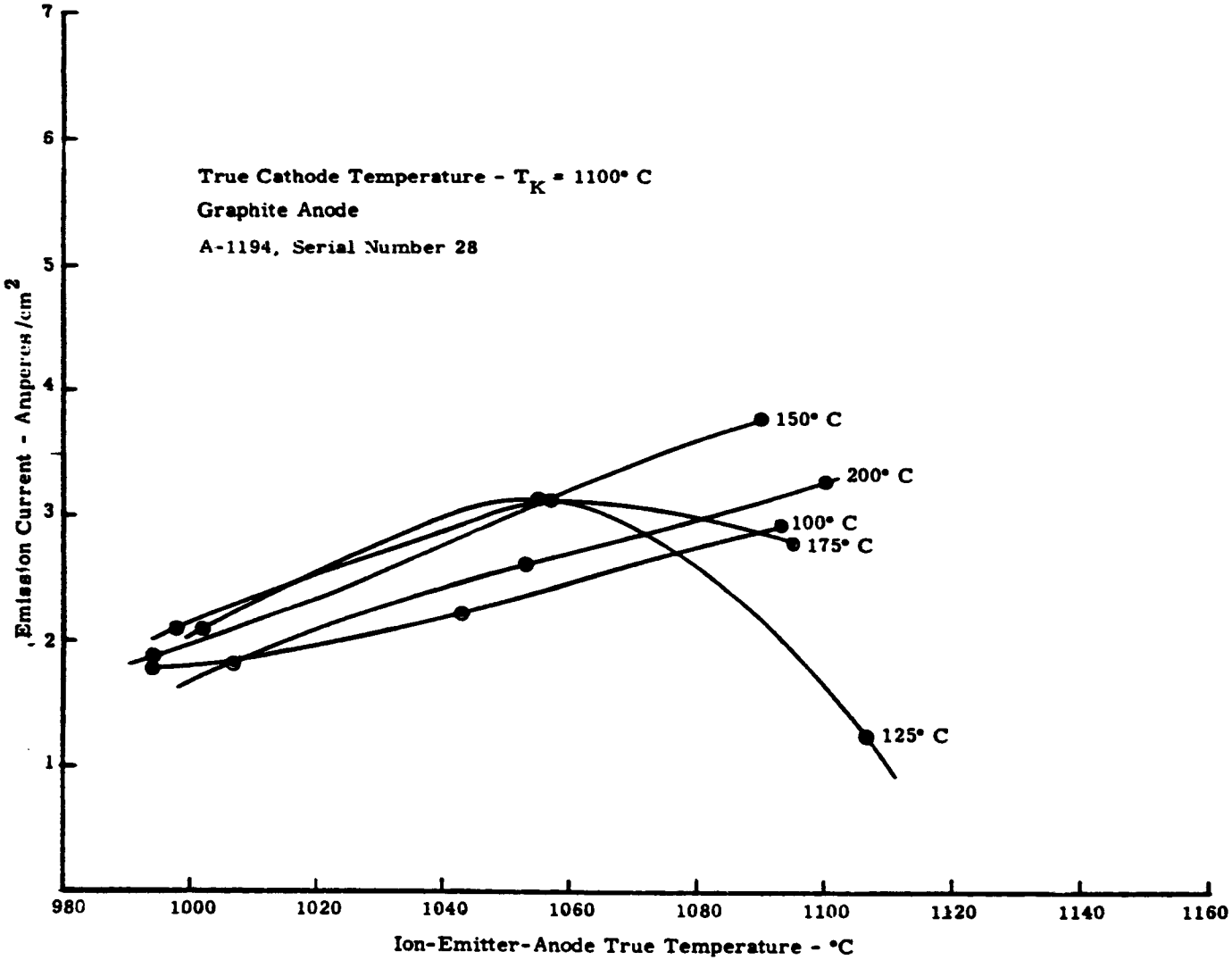

FIGURE 14 - EMISSION VERSUS ION-EMITTER TEMPERATURE - T_K = 1100° C

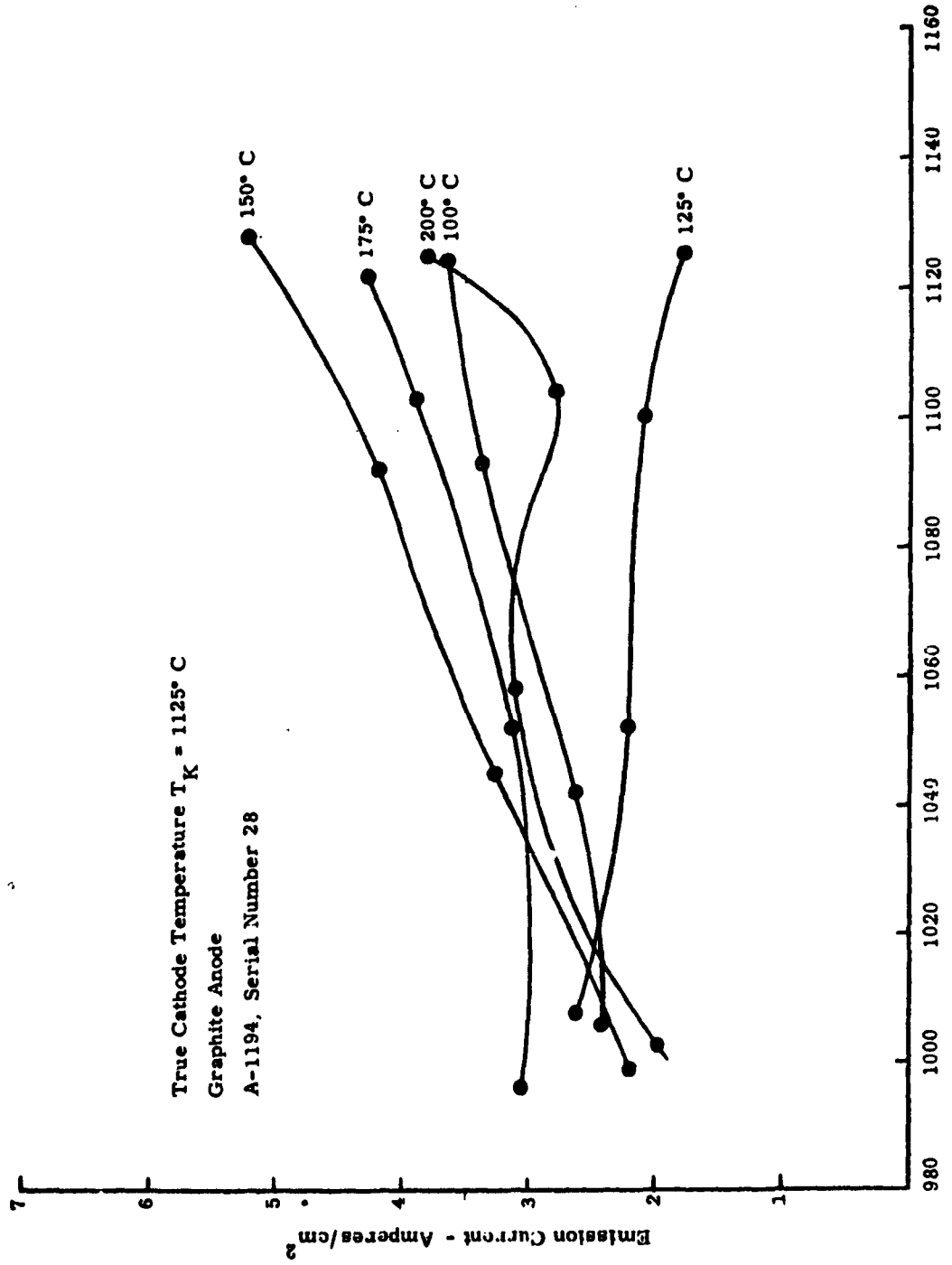

FIGURE 15 - EMISSION VERSUS ION-EMITTER TEMPERATURE - T_K = 1125° C

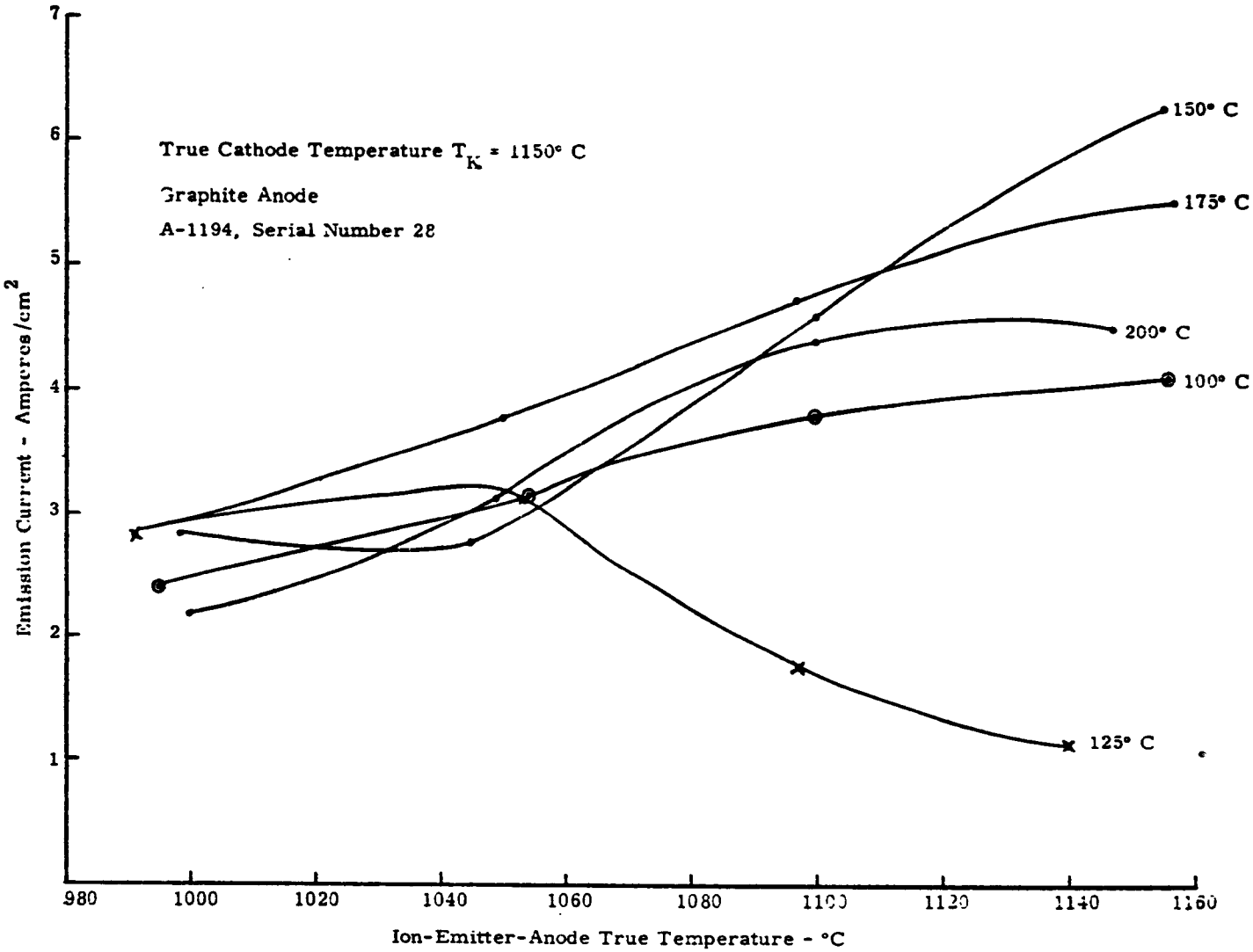

FIGURE 16- EMISSION VERSUS ION-EMITTER TEMPERATURE - T_K = 1150° C

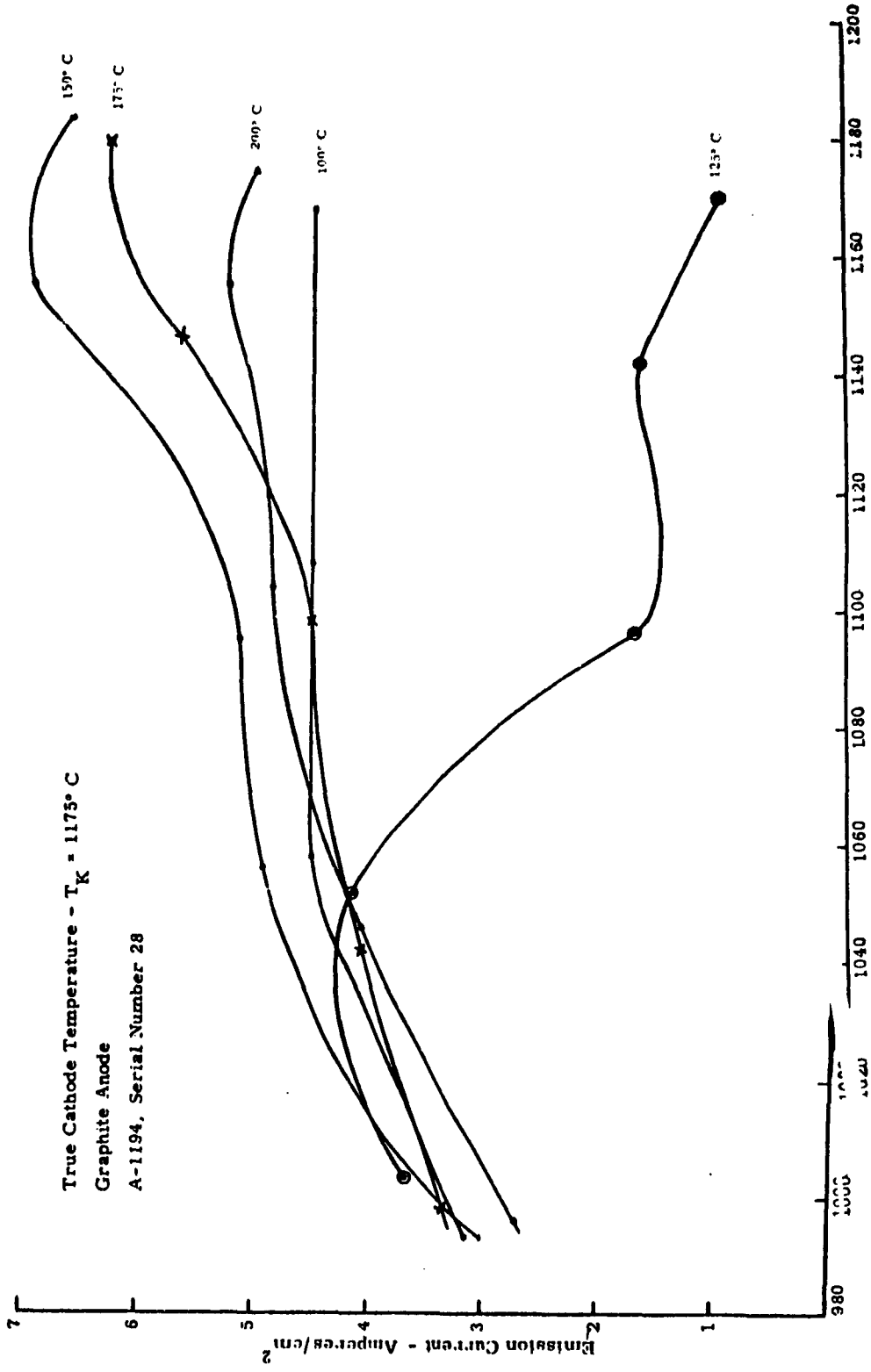

FIGURE 17 - EMISSION VERSUS ION-EMITTER TEMPERATURE - T_K = 1175° C

Cesium Reservoir temperature	150° Centigrade
Initial dc emission current density	2.8 amperes per square centimeter

Two duo-emitter diodes, serial numbers 19 and 22, employing hafnium ion emitter anodes, were life tested. The initial test conditions and the reduced characteristics after 317 hours life for tube number 19 are shown in Figure 18. In order to check the compatibility of the diode envelope with cesium, the life test was continued to 775 hours before a vacuum leak developed in the converter envelope. Since the current density had dropped to such a low value, after 317 hours, further characteristic data was not taken. The initial conditions for tube number 22 are shown in Figure 1. After only 45 hours of life, the emission density of this tube had dropped to less than one ampere per square centimeter. The characteristics of the tube indicated that the slump in emission density was caused by poisoned emission from the impregnated cathodes. However, after analysis the cause of the slump in emission density was accurately determined. The nickel from the nickel-molybdenum brazing material, used to braze the hafnium to the heater cup, had alloyed through the hafnium and poisoned its ion emission properties. Since graphite was found to be a more effective ion emitter, work with hafnium was stopped. One diode, (number 28) with a graphite anode-ion emitter, was extensively life tested. The initial conditions, the conditions at 1000 hours and the conditions at 1728 hours are shown in Figures 19, 20, and 21, respectively. This life test has shown that the emission from

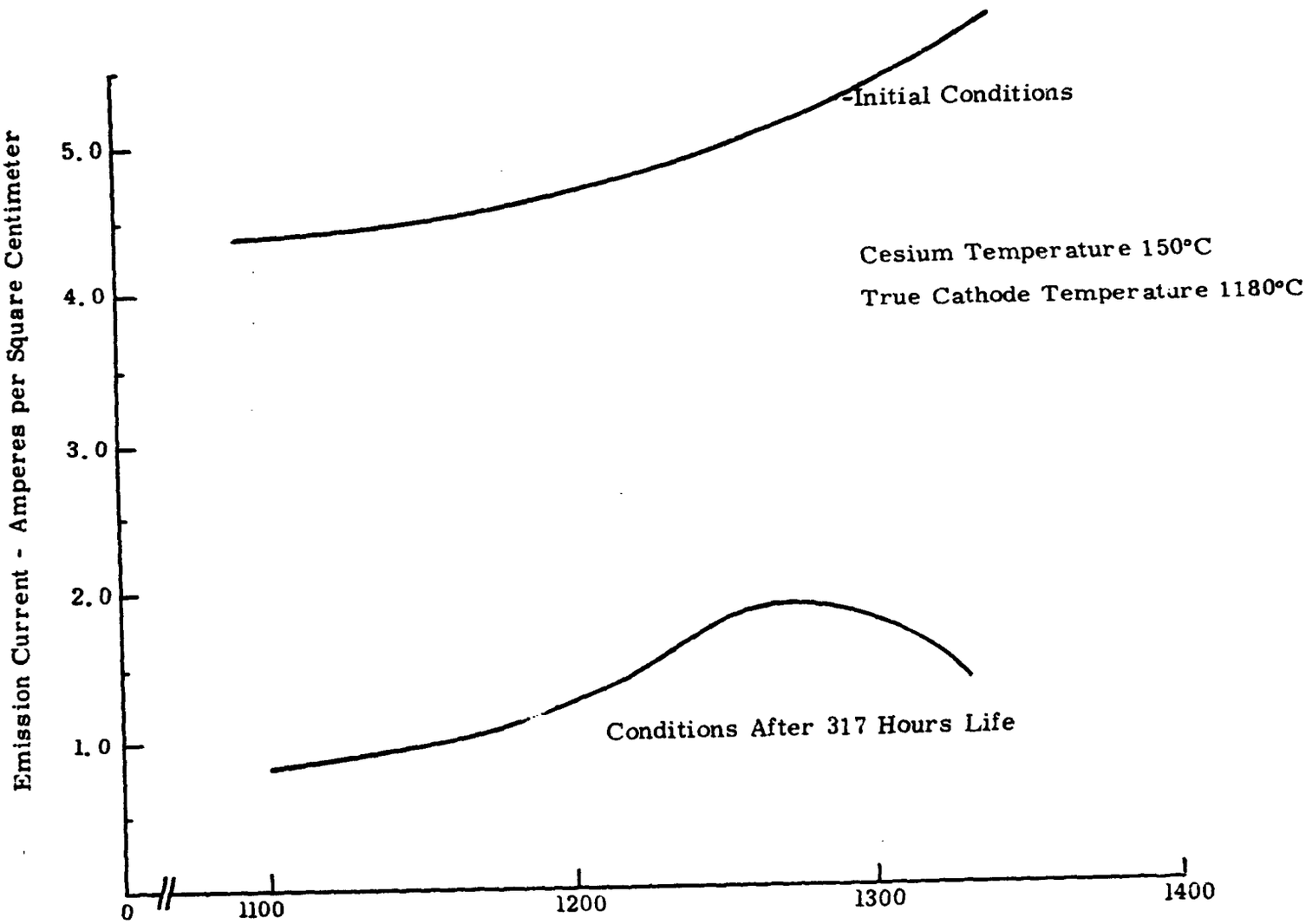

FIGURE 18 - EMISSION VERSUS ION-EMITTER TEMPERATURE

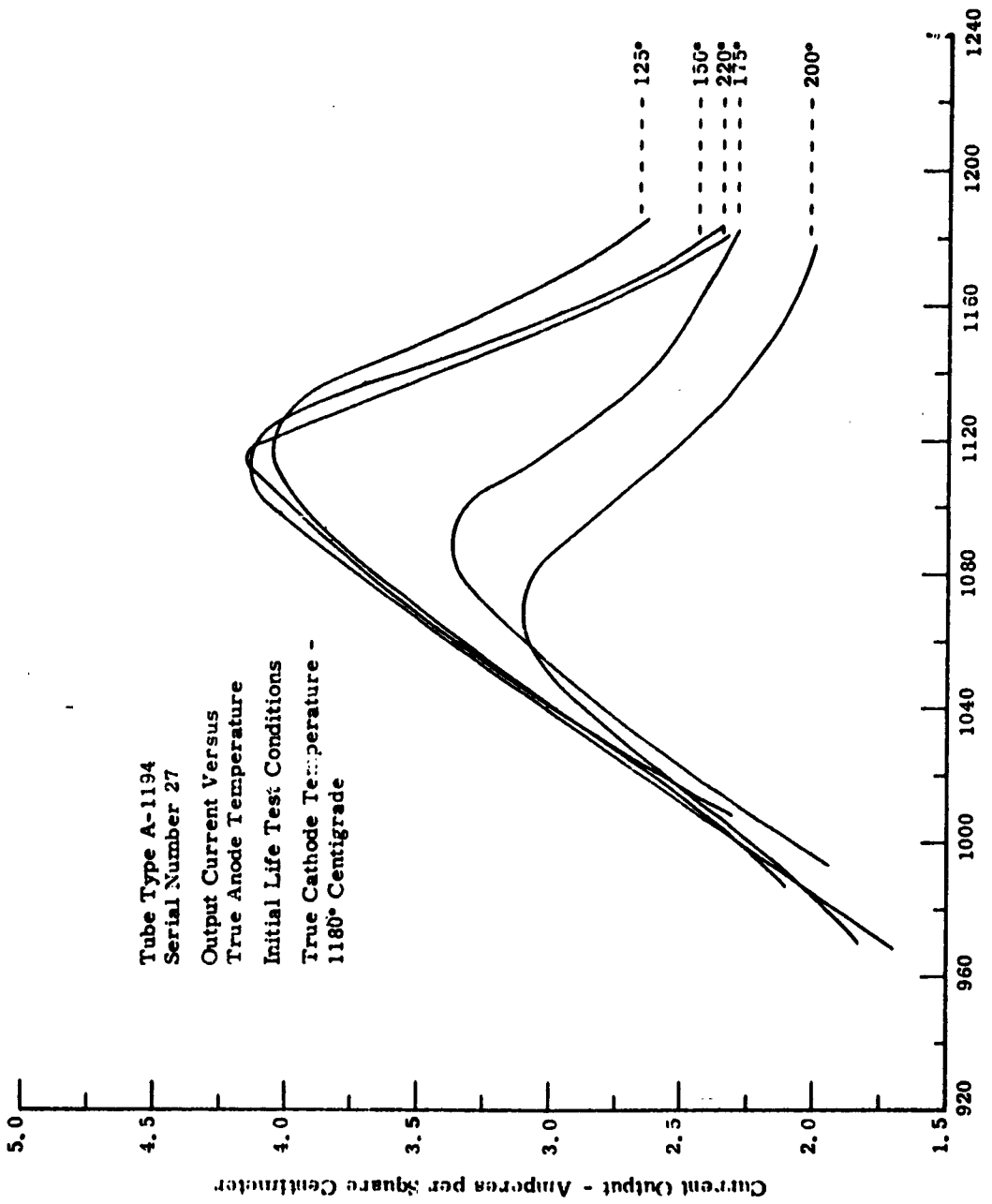

FIGURE 19 - INITIAL OUTPUT VERSUS ANODE TEMPERATURE FOR VARIATIONS IN CESIUM TEMPERATURE

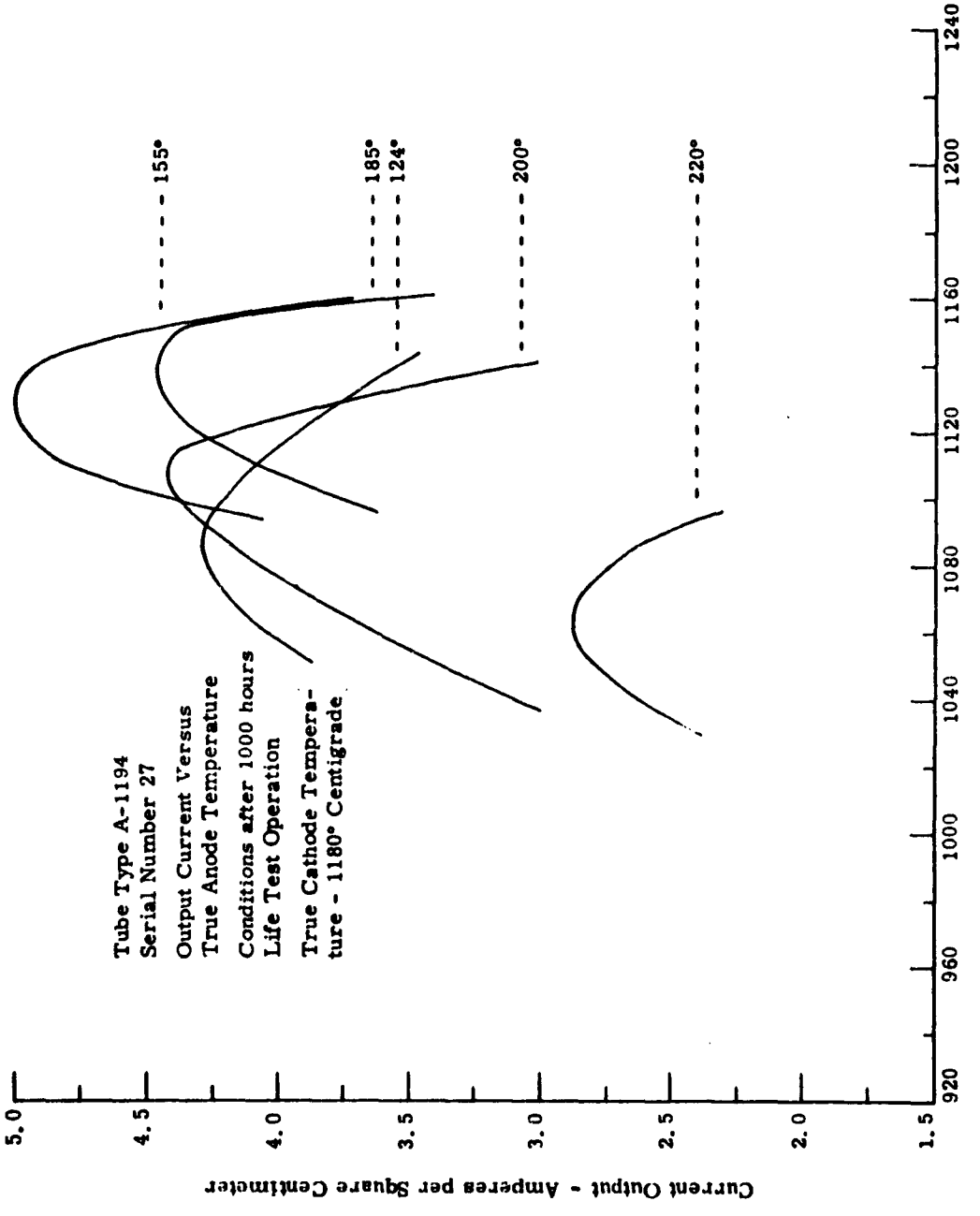

FIGURE 20 - OUTPUT VERSUS ANODE TEMPERATURE FOR VARIATIONS IN CESIUM TEMPERATURE

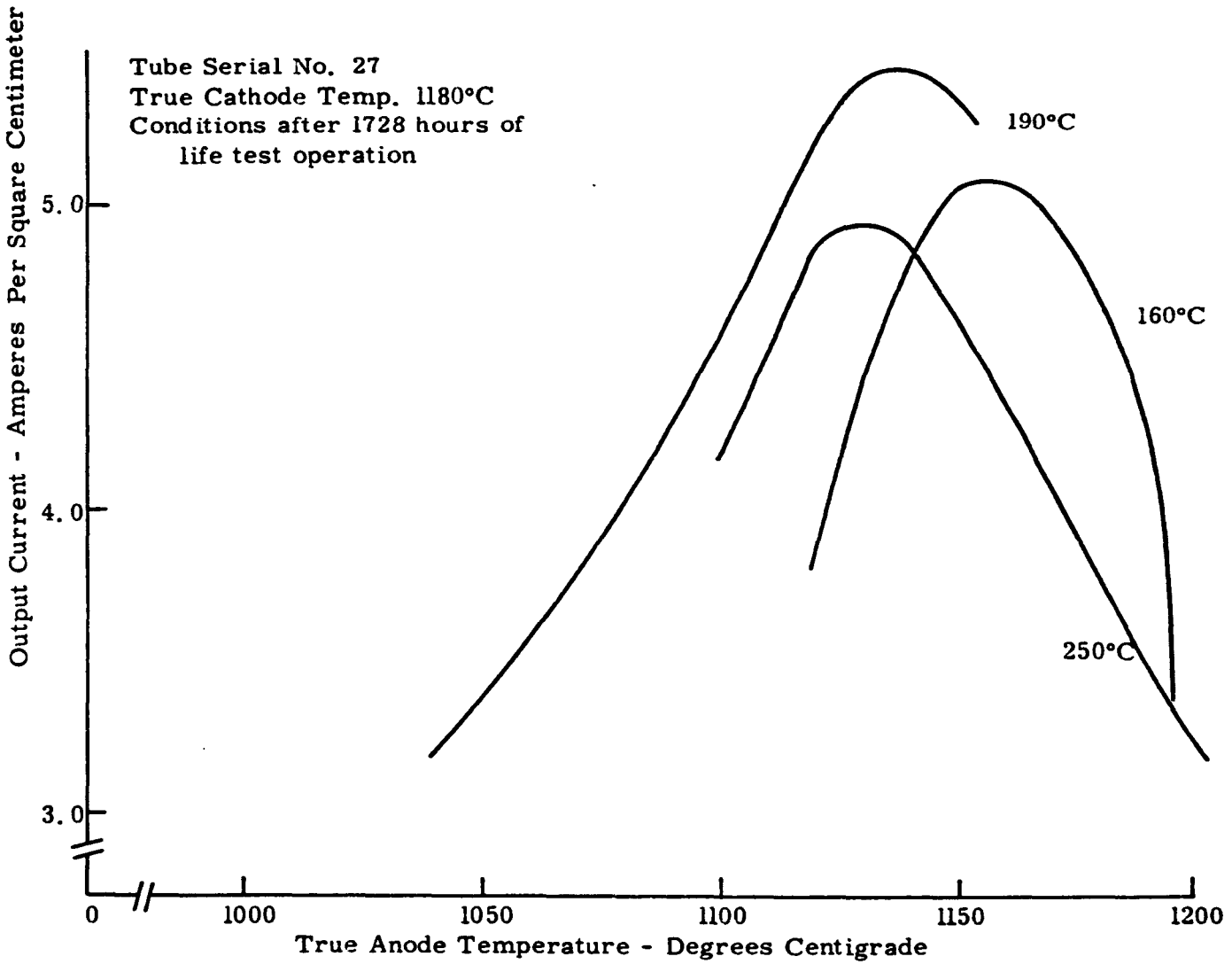

FIGURE 21 - OUTPUT CURRENT VERSUS ANODE TEMPERATURE FOR VARIOUS CESIUM TEMPERATURES

impregnated cathodes remains high, that the ion emission properties of graphite are stable in the presence of the impregnated cathode evaporants, and that envelopes employing metal-to-ceramic seals are reliable in a cesium atmosphere. In addition, it shows that graphite can be used in a cesium atmosphere if proper precautions are taken.

D Laboratory Models

1. Design

The design of the working model converter employs some of the basic features of the duo-emitter diode. These features include a separate evacuated chamber for the heater to prevent the erroneous operation that can be caused by ionization of the cesium from applied heater voltages. The converter was designed to use many of the parts of duo-emitter including the outer shell, outer sleeve, window, cesium reservoir, cathode heater and cathode cup.

The converter consists of an ion-emitter cathode assembly, as described in Section III-B-1 facing a nickel-plated, cold-rolled-steel anode. The ion-emitter cathode assembly is brazed to the heater cup to insure good thermal and electrical conductivity. The anode is made of cold-rolled steel so that by using it as a pole piece, an axial magnetic field can be impressed between the ion-emitter assembly anode gap. The connection to the ion emitters is made through a ceramic insulated feed-through bushing. A picture of the converter, an assembly layout and a cross-sectional drawing of the converter is shown in Figures 22, 23, and 24.

The outer envelope is made of nickel-plated kovar. This material was selected for its good thermal expansion match with the ceramic insulator. In addition, kovar has a high resistance to cesium attack, high strength, and workable properties. Copper is used for the exhaust tubings because of its ability to cold weld under pressure for pinch-off purposes.

2. Construction and Processing

In general, the converter consists of five sub-assemblies, ion-emitter cathode, heater cup assembly, the outer shell assembly, anode assembly, and heater assembly. The outer shell is formed by brazing the ion-emitter cathode heater cup assembly to its envelope parts. The anode assembly and the heater assembly are then heliarc welded into the outer shell assembly to complete the converter. After the window and exhaust tubings are brazed on with induction heating, the converter is exhausted.

3. Test Results

At the start of the contract, plasma-triode converter operation had been demonstrated in glass envelopes with the heating element in cesium vapor. The voltage applied to the heater caused unwanted ionization. Although special care was taken in the testing of the converter to assure that this ionization did not enhance converter operation, it did limit the test results that could be obtained and there was always a question of doubt as to whether the ionization

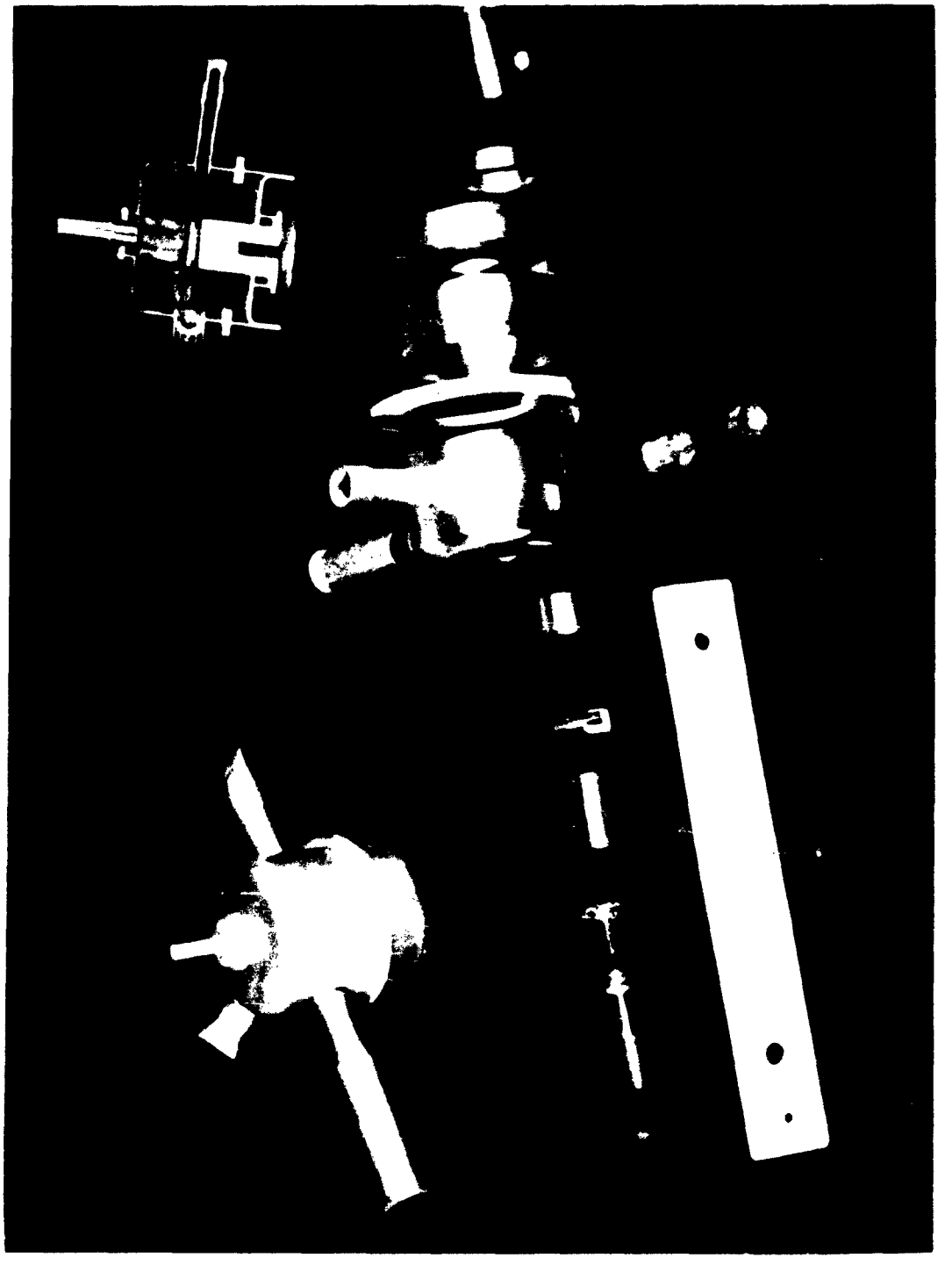

FIGURE 22 - Plasma-Triode Converter

FIGURE 23 - Assembly Layout of the Plasma-Triode Converter

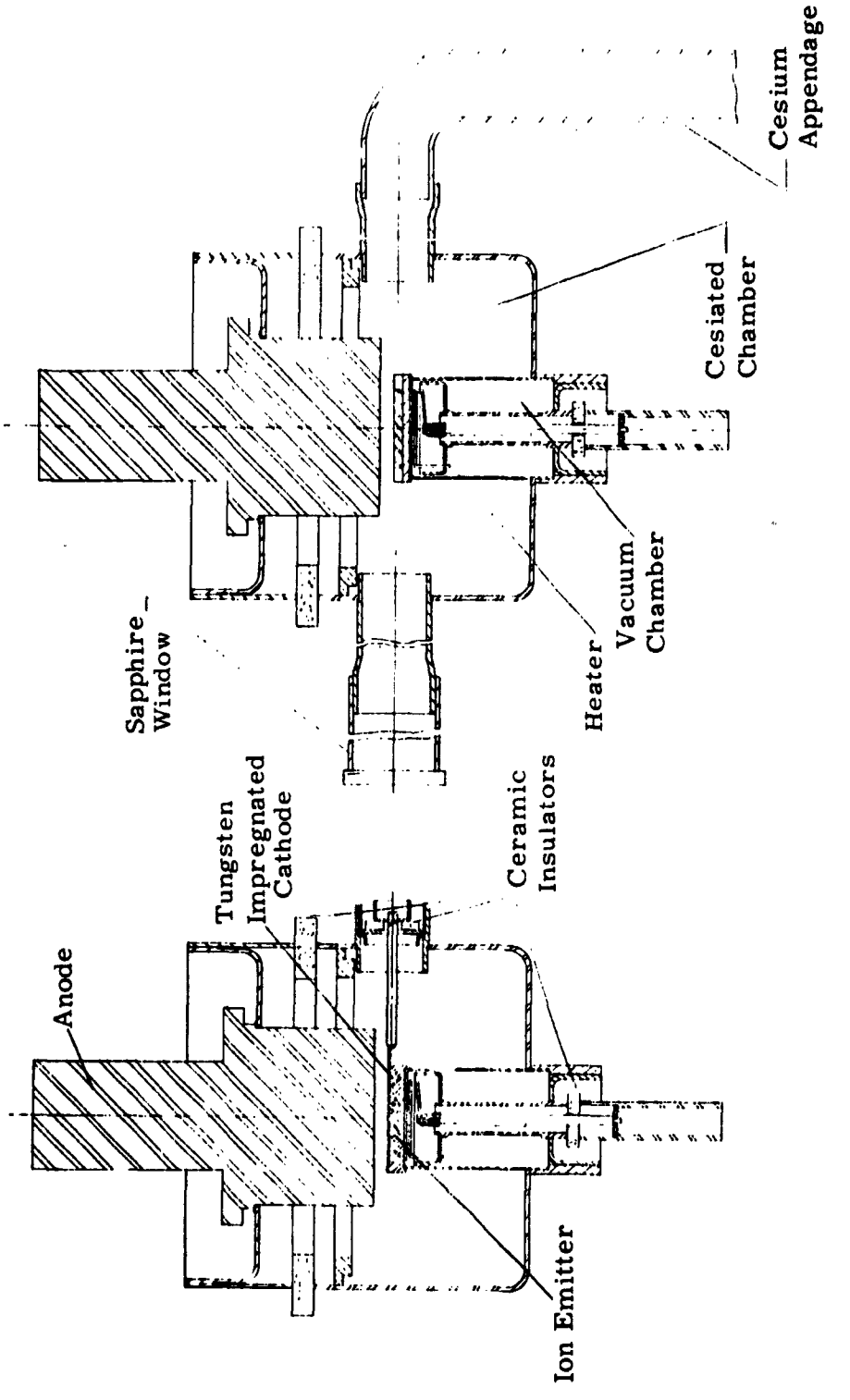

FIGURE 24 - Complete Assembly, "Plasma Triode" Converter

was affecting converter operation. Test results from laboratory model converters has demonstrated, beyond a doubt, that operational theory of a plasma-triode is correct. A power output of 1.2 watts per square centimeter of active cathode area was obtained at a true cathode temperature of 1180° Centigrade with a bias power input of 0.5 watts. Therefore, a total net power of 0.7 watts per square centimeter was obtained. Complete volt-ampere-power characteristics for the plasma triode (A1196), serial numbers 23 and 24, are shown in Figures 25 and 26. The curves show power output, ion emitter power, and output plotted against output voltage at various bias levels with the cathode temperature, anode temperature, and cesium temperature held constant. The optimum anode and cesium reservoir temperatures were found to be 250 and 150° Centigrade, respectively.

In order to reduce the bias power required, a magnetic field was impressed between the anode cathode gap by using the cold-rolled steel anode as a pole piece of an electromagnet. Field pattern tests in the gap showed that the field lines were perpendicular to the cathode and anode. It was felt that such a field would aid the flow of electrons from cathode-to-anode and impede the flow of electrons to the ion emitter since the direction of the flow is normal to the field. Test results confirmed the theory that the ion emitter current would be reduced. At the same time anode current was also reduced, contrary to expectations. The ratio of output power to bias power is improved significantly, however. See Table on following page.

TABLE I

EFFECTS OF MAGNETIC FIELDS

Without Magnetic Field

Tube Number	Output			Bias			P_o/P_{Bias}
	Evolts	Iamps	Pwatts	Evolts	Iamps	Pwatts	
24	0.8	0.7	0.56	1.0	0.21	0.21	2.7
24	0.8	0.75	0.6	1.1	0.29	0.32	1.9
23	0.7	1.5	1.05	1.25	0.68	0.85	1.23
23	0.6	2.6	1.56	1.4	1.5	1.04	1.04

With Magnetic Field

Tube Number	Output			Bias			P_o/P_{Bias}
	Evolts	Iamps	Pwatts	Evolts	Iamps	Pwatts	
24	0.8	0.45	0.36	1.0	0.08	0.08	4.5
24	0.8	0.55	0.44	1.1	0.13	0.14	3.1
23	0.7	1.2	0.84	1.25	0.275	0.34	2.5
23	0.6	1.9	1.14	1.4	0.46	0.64	1.8

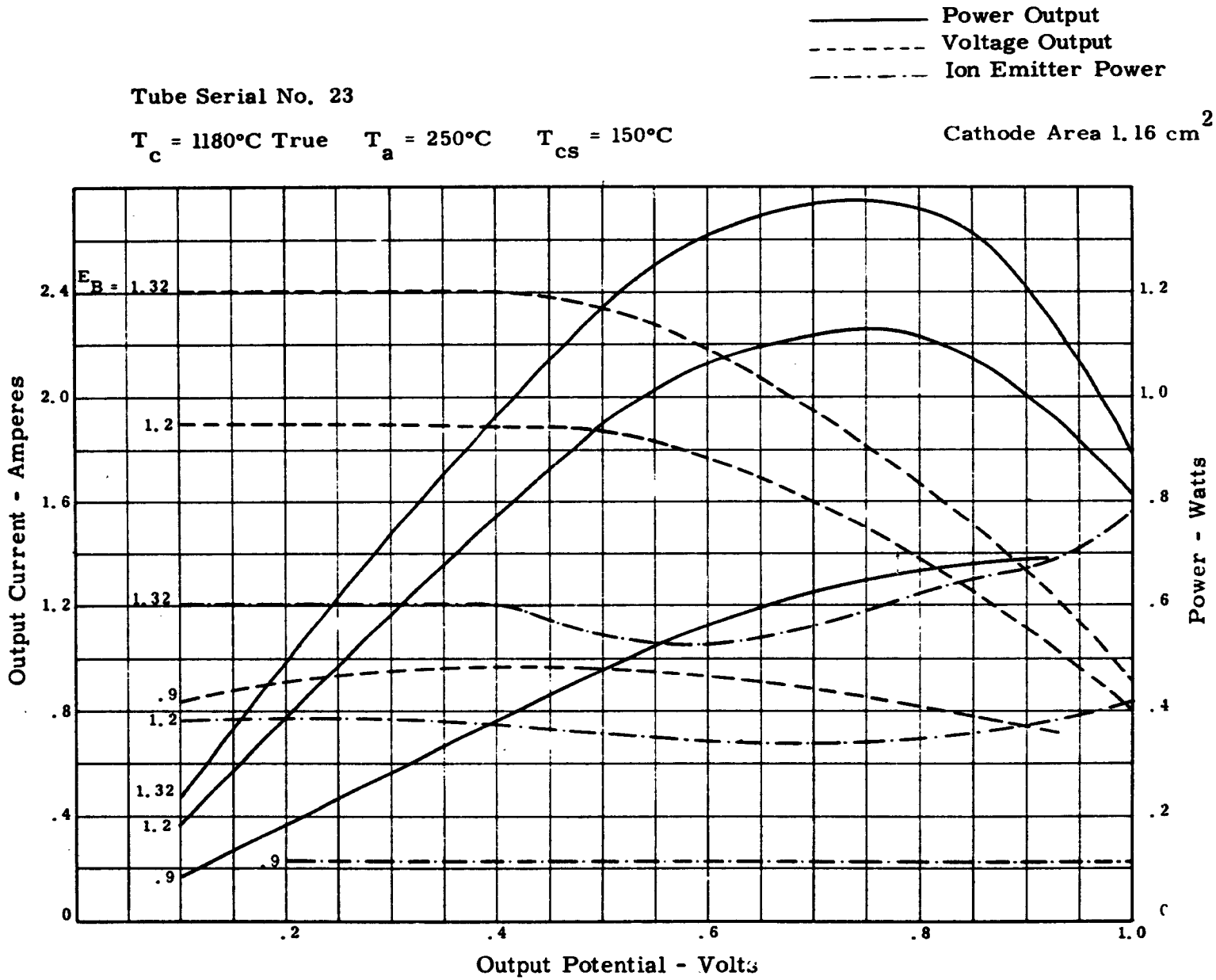

FIGURE 25 - Output Characteristics of the RCA Developmental Type A-1196 At Several Bias Voltages

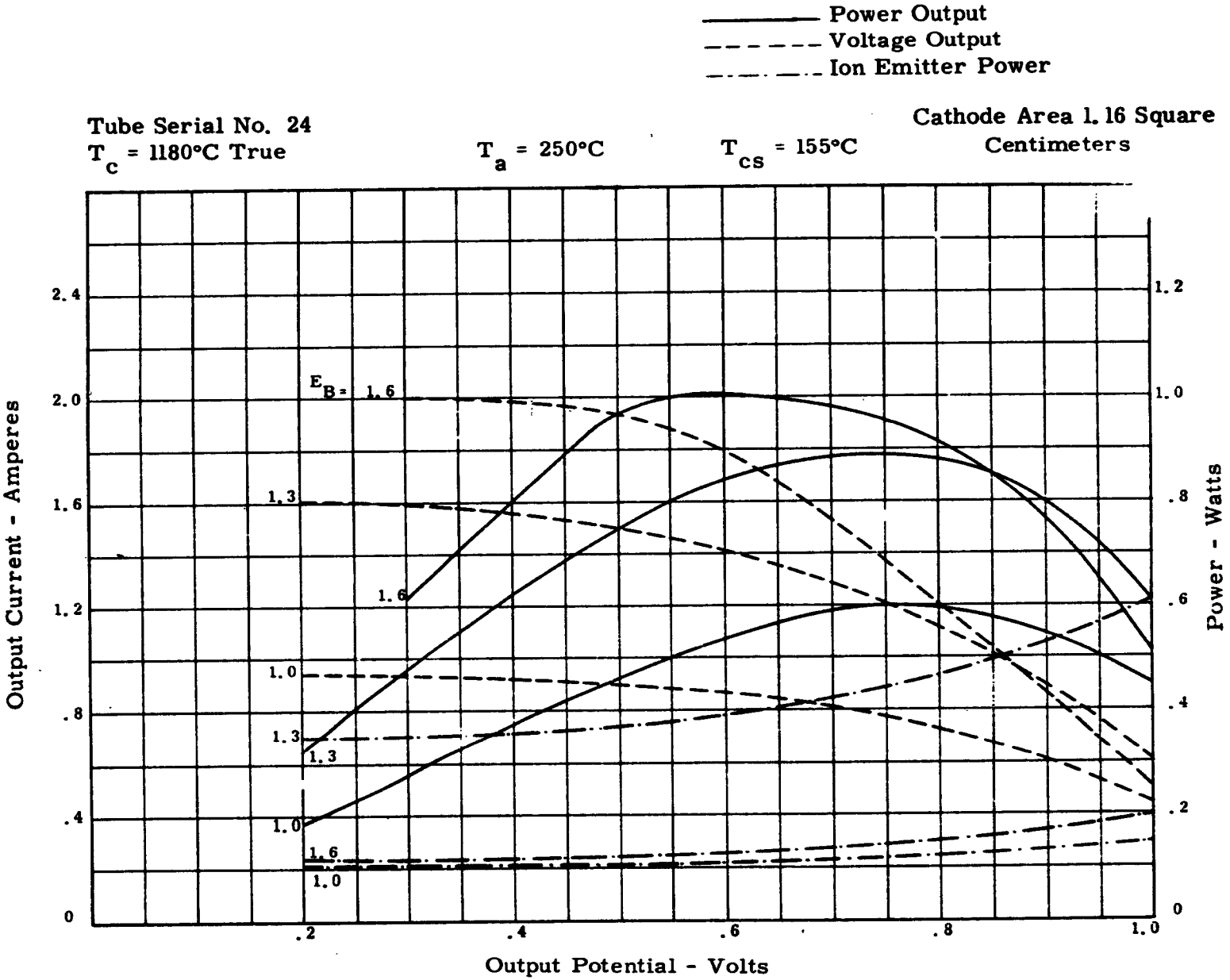

FIGURE 26 - Output Characteristics of the RCA Developmental Type A-1196 At Several Bias Voltages

4. Life Test

Life tests were conducted on two plasma triodes - converters numbers 5 and 9. Both converters employed hafnium ion emitters, nickel anodes, and tungsten impregnated cathodes. The initial volt-ampere-power characteristics are shown in Figures 27 and 28. It can be seen from the curves that the power required for the ion emitter exceeded the power output obtained. Converter number 5 was placed on life without performing tests on the converter to improve this characteristic. An attempt was made to improve this characteristic on number 9. The tests indicated that the ion emitter was giving insufficient ions to neutralize the space charge, probably because it was poisoned by barium deposited on it from the cathode. Therefore, in order to clean the ion emitters of a suspected barium deposit, they were bombarded with ions by applying a negative potential to them. This action poisoned the emission from the impregnated cathode. The cathode was re-aged and the converter retested. An output of 0.112 watts at 0.45 volts and 0.22 amperes was obtained. The ratio of output power to ion emitter power was, however, not improved. The life test was then started on the converter. Converter number 5 ran on life for 130 hours before a vacuum leak caused failure. The power output deteriorated to 0.1 watt during this test. Converter number 9 ran on life for 767 hours before an open heater caused failure. This converter performance was checked on a daily basis during the life test. The output did not improve or decay from its initial value of 0.112 watts. An analysis of both converters after failure revealed that the nickel contained in the nickel-moly brazing material used to attach the ion emitters to

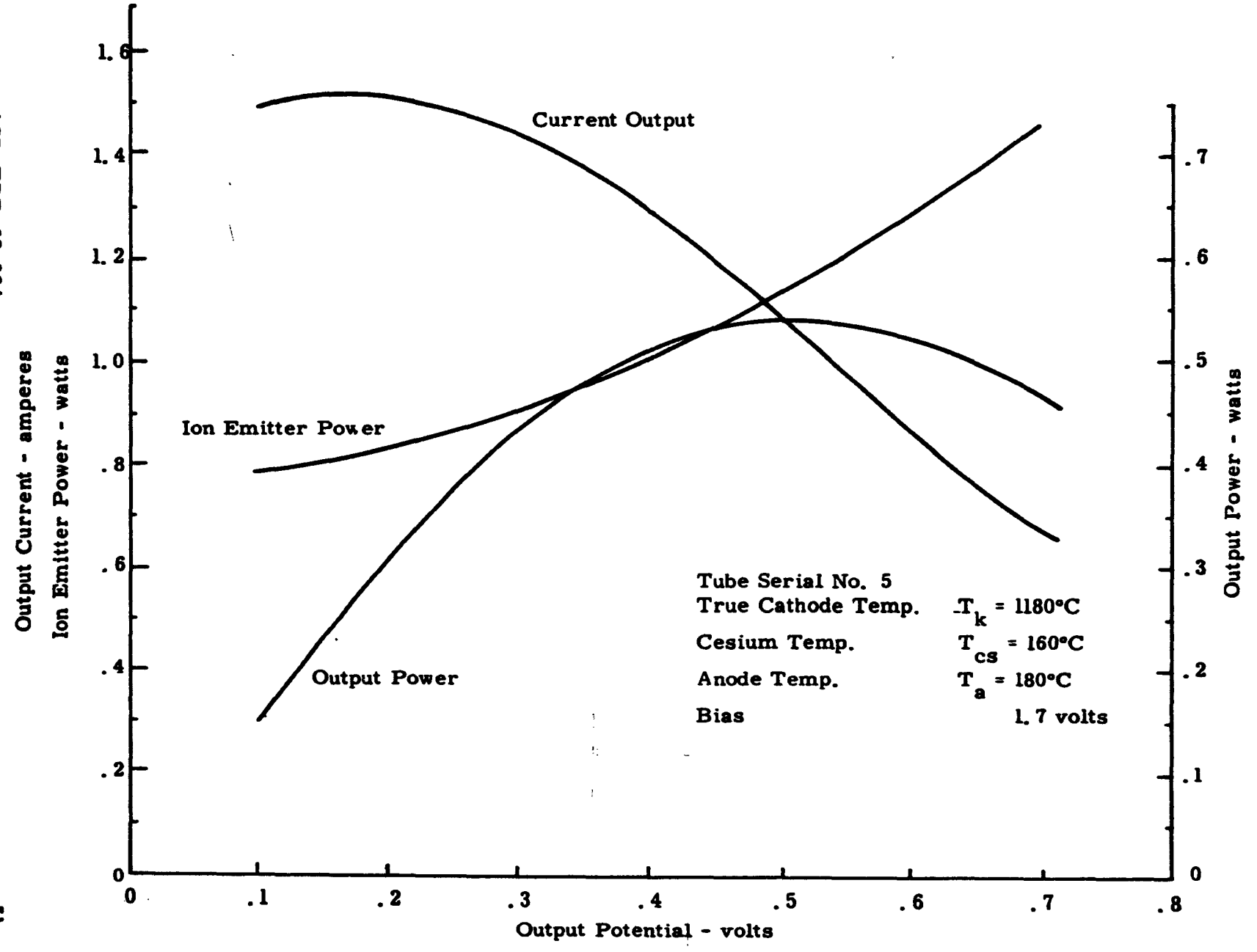

FIGURE 27 - Output Characteristics of Converter No. 5

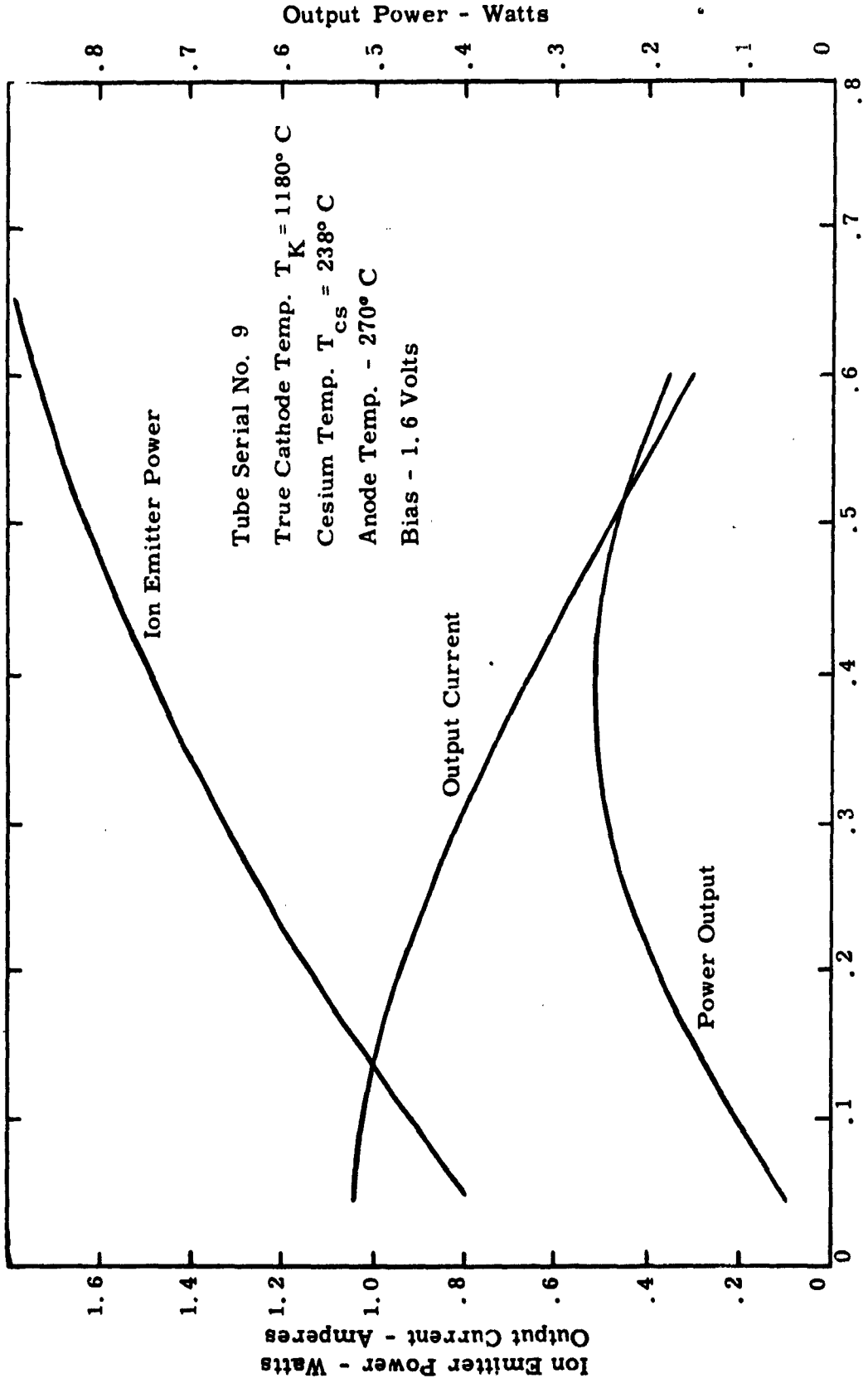

FIGURE 28 - OUTPUT CHARACTERISTICS OF CONVERTER NUMBER 9

the base had migrated across the surface of the hafnium ion emitters. Thus the ion emitter was poisoned, not from the barium deposit as expected, but from a nickel deposit. Problems of hafnium compatibility with brazing material had also been observed on duo-emitter diodes as reported in Section III-C-5 of this report.

5. Efficiency Consideration Plasma Triode

The laboratory model plasma-triode converter was not designed to demonstrate efficiency, but rather to investigate the theoretical aspects of triode converter operation. Therefore, it is necessary to make a theoretical analysis of the efficiency that can be expected from a plasma-triode converter. In order to do this, a converter of sufficient size to minimize end losses must be considered. The size of the converter used and the assumptions made in the theoretical efficiency calculation plus a sample calculation is shown in Appendix IV. The results of these calculations are shown in Figure 29. The theoretical efficiency, at various power densities, was calculated by assuming that the current intercepted by the ion emitter was two percent of the output current. The other two efficiency curves assume that the current intercepted by the ion emitter is the same as was demonstrated by the operation of converter number 23 and converter number 24. The stars on each curve is the best power density that was demonstrated by each of the converters based on total heated area (x) and active cathode area (o). Therefore, with the present State-of-the-Art, based on data from converters number 23 and 24, the best efficiency that can be predicted for a plasma-triode lies between the two points shown on each curve.

o - Power Density obtained from active cathode area
x - Power Density obtained from total heat area

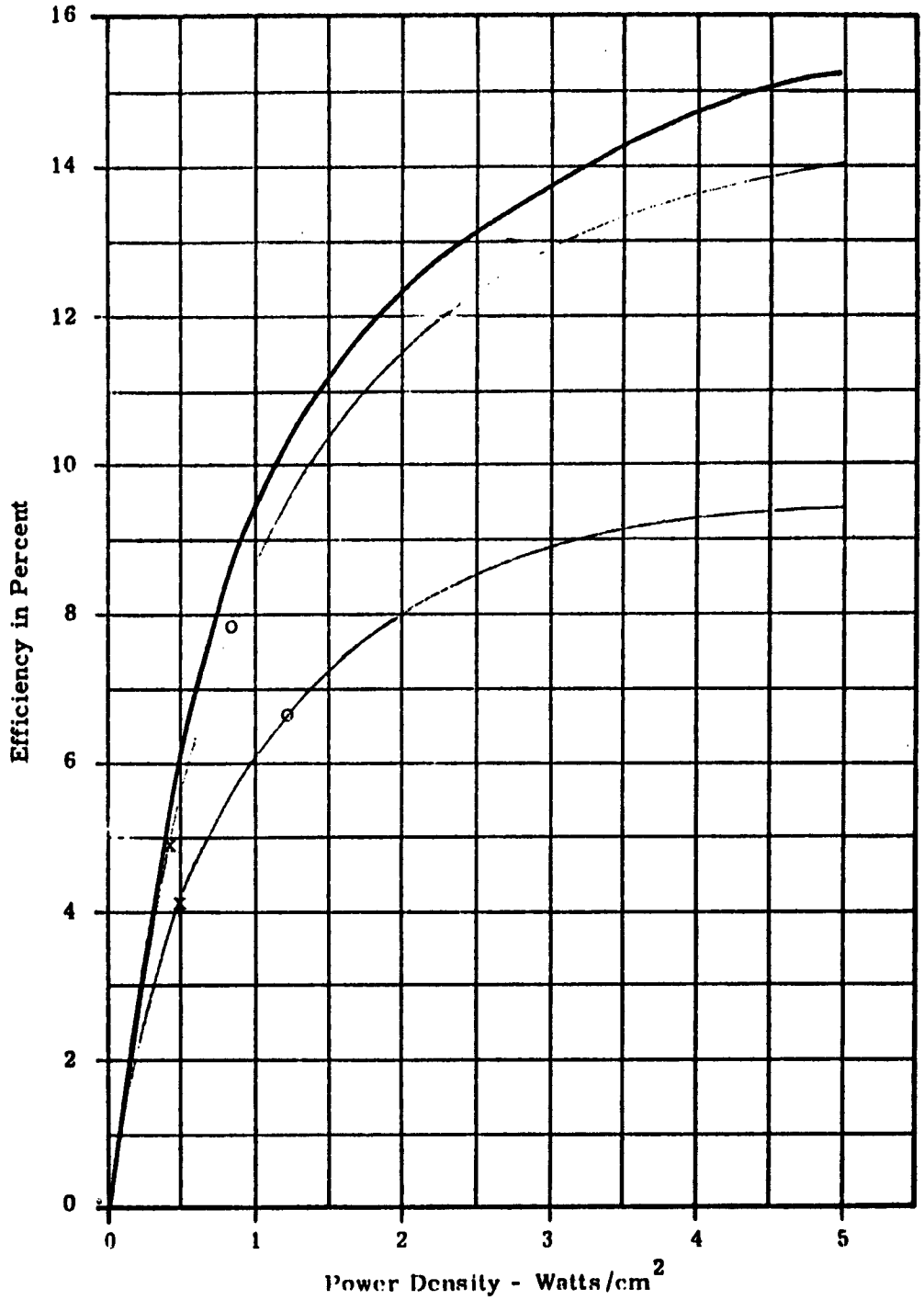

FIGURE 29 - CALCULATED EFFICIENCY VERSUS POWER DENSITY

6. "Ball-of-Fire" Converter Operation

One plasma triode converter, Serial No. 19, was tested as a plasma triode. However, the converter went into the "Ball-of-Fire" mode of operation shown in Figure 30 at a low cesium reservoir temperature (160°C). The cesium reservoir temperature was therefore optimized for the "Ball-of-Fire" mode of operation. The converter operated satisfactorily in this mode. A power output of 2.2 watts per square centimeter was obtained at a true cathode temperature of 1190°C. The volt-ampere power output characteristics are shown in Figure 31. Three additional converters were built and tested in the same mode of operation. A maximum power output of 0.5 watts per square centimeter was obtained from these converters. The reason why Converter No. 19 operated so well has not as yet been explained. It was operated for 20 hours at the 2.2 watts per square centimeter level before the output suddenly dropped to zero. An analysis of the converter revealed that a leak in the vacuum envelope caused failure.

FIGURE 30 - PHOTOGRAPH OF
"BALL-OF-FIRE" OPERATION

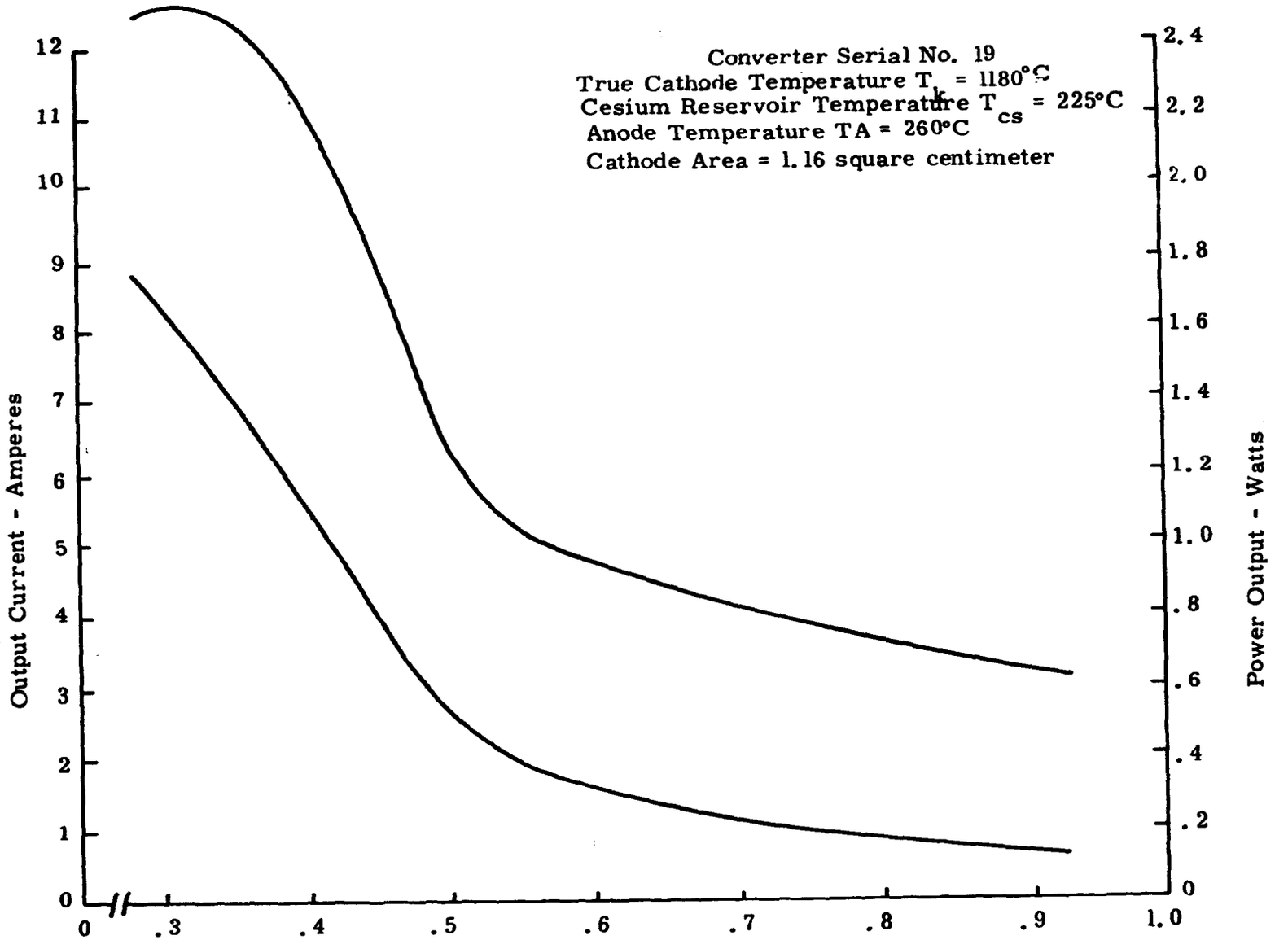

FIGURE 31 Output Characteristics of "Ball of Fire" Operation Of "Plasma Triode" Converter

APPENDIX I

MATERIALS COMPATIBILITY WITH CESIUM

Prepared for:

AERONAUTICAL SYSTEMS DIVISION
United States Air Force
Wright-Patterson Air Force Base
Ohio

Contract AF33(616)-7903
Project Number 3145
Task Number 314509

Prepared by:

J. J. Moscony
F. G. Block

RADIO CORPORATION OF AMERICA
Electron Tube Division
Space Component Engineering
Lancaster, Pennsylvania

MATERIALS COMPATIBILITY WITH CESIUM

TABLE OF CONTENTS

LIST OF ILLUSTRATIONS

LIST OF TABLES

MATERIALS COMPATIBILITY WITH CESIUM

SECTION I

INTRODUCTION

The use of elemental cesium for space-charge neutralization in thermionic converters presents the possibility of deleterious interaction of the element with device construction materials. Due to the chemical reactivity of cesium, it is possible that the injudicious selection of materials may cause a limiting effect on the useful life of a converter.

The strong electropositive character of cesium is due essentially to the small expenditure of energy required to remove an electron from the atom. This fact is directly related to the low-work functions and ionization potential of the metal and also accounts for a high-chemical reactivity.

The literature concerning compounds of cesium with non-metallic elements is extensive; however, little information is available concerning the interaction of cesium with metals, alloys, and ceramics (Ref. 1 and 2). In order to provide information pertinent to the development of a low-temperature thermionic converter, a program was initiated to test various materials in cesium liquid and vapor over a wide range of temperatures.

The program was divided into three phases:

1. Evaluation of materials in cesium liquid at 200° Centigrade and in cesium vapor at 200° Centigrade with the cesium vapor pressure at 10^{-1} millimeters of mercury.
2. Evaluation of materials in cesium vapor at 500° Centigrade with the cesium vapor pressure at 10^{-1} millimeters of mercury.

3. Evaluation of materials in cesium vapor at 1300° Centigrade with the cesium vapor pressure at 10^{-1} millimeters of mercury.

Tests have been performed in each of the above cases and the following sections include a discussion of test procedures, results, and conclusions.

SECTION II

CESIUM COMPATIBILITY TESTS AT 200° CENTIGRADE

A Test Procedure

Since it is possible that a major portion of a device would operate at a temperature of 200° Centigrade, particularly in liquid-cooled application, a wide variety of possible anode and envelope materials were tested at this temperature so as to provide a broad base for comparison. In general, metal and brazing alloy samples consisted of flat stock or wire ranging from 0.003 inch - 0.050 inch in thickness, 1-1/4 inches long and 1/4 inch wide. The ceramic samples were 1/4 inch diameter rods, one inch in length.

In practice, two samples of each material to be tested were carefully degreased, weighed, and placed in an OFHC copper tube along with a glass cesium capsule. (The cesium employed for these tests was analyzed spectrographically and found to be 99.9 percent pure.)

One sample was mounted so that during test a portion of that sample was immersed in cesium liquid, whereas the other sample was mounted so that it would be exposed only to cesium vapor. After mounting the samples, the copper tube was attached to a stainless steel manifold (Figure 1), evacuated to approximately 5×10^{-7} millimeters of mercury and pinched off. After pinch off, the cesium capsule was broken by applying pressure to the outside wall of the copper tube. In order to eliminate possible side effects from glass the cesium was distilled to the opposite end of the tube and after cooling, the end containing the glass was pinched off. Then the copper tube containing only the test samples and the cesium was placed in a controlled oven at 200° Centigrade for 200 hours (cesium vapor pressure 10^{-1} millimeters of mercury). See Figure 2.

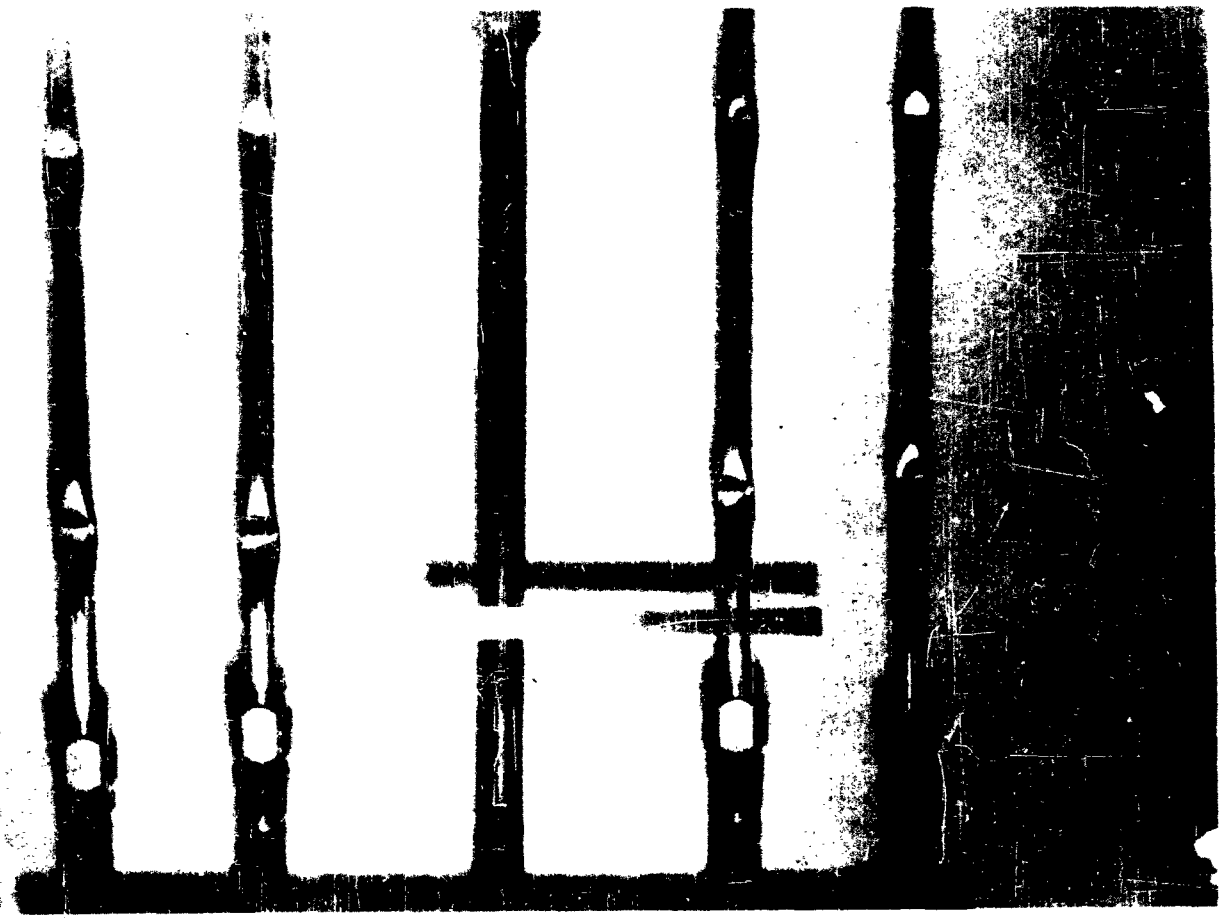

FIGURE 1. STAINLESS STEEL MANIFOLD USED FOR EVACUATING OFHC COPPER TEST CHAMBERS

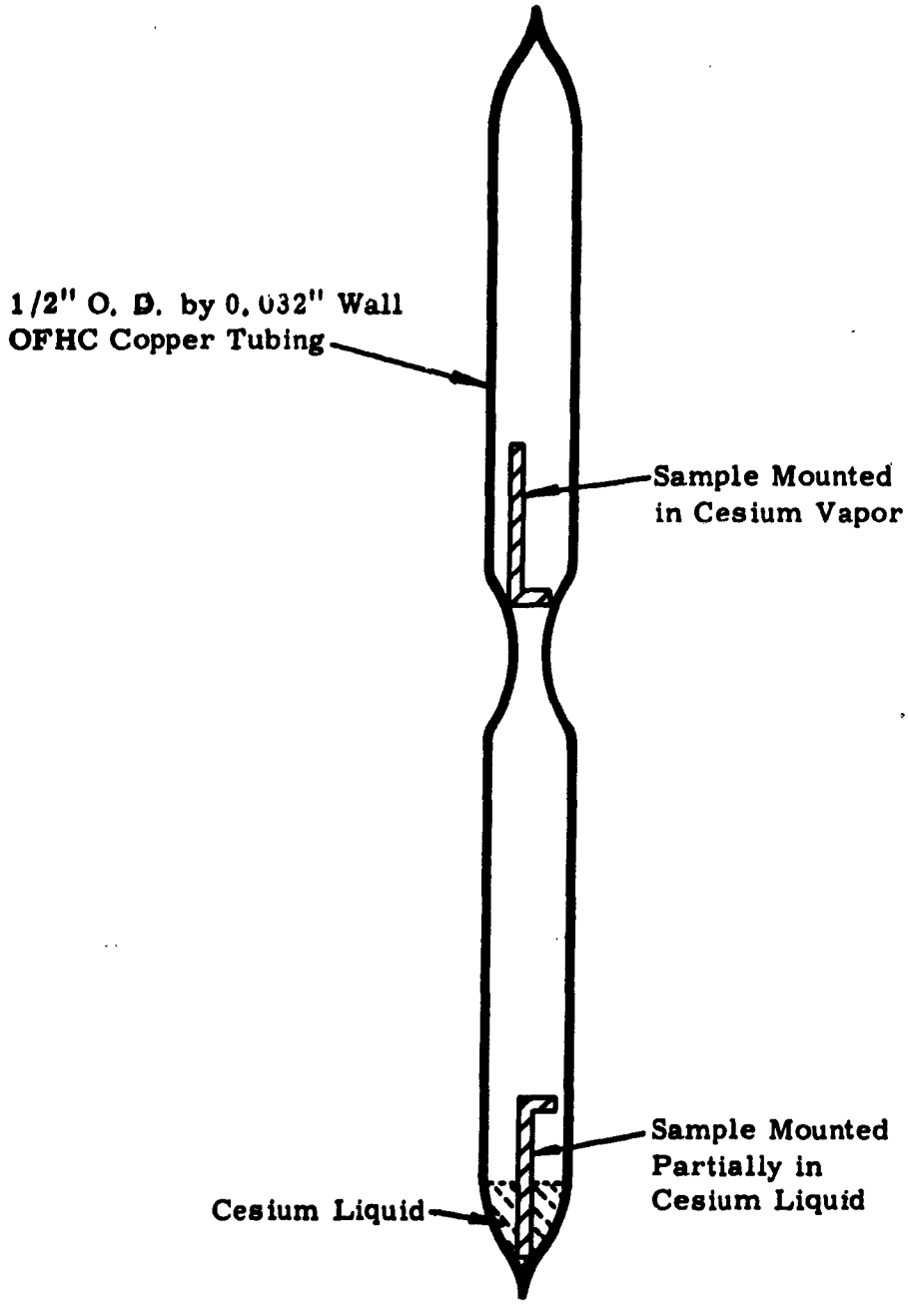

FIGURE 2 - TEST CHAMBER FOR MATERIALS COMPATIBILITY WITH CESIUM AT 200° CENTIGRADE

At the end of the test period, the samples were removed from the copper tube and rinsed thoroughly with water. This was done to remove any soluble compounds that might have been formed and thus more easily detect, by a loss in weight, any interaction with cesium. After the water treatment, the samples were dried in an oven and then weighed. Weight changes were recorded in all cases, and cross section, spectrographic and/or X-ray analyses were made only when interaction with cesium was suspected.

B Results of Tests

The results of these tests are listed for metals in Table I, brazing alloys in Table II, and ceramics in Table III. Exposure time to the test conditions was 200 hours for all materials and those materials with weight changes equal to or less than ± 0.0003 gram are recorded as having no detectable change.

It is possible for metals and brazing alloys that corrosion by intergranular penetration, would not be detected by weight changes or appearance. However, such interaction usually manifests itself by embrittlement of the material. Accordingly, a simple 90° bend test was applied to all the test specimens after final weighing and those cases where embrittlement was evident are noted in the Tables under specimen description.

Table I illustrates that many metals are resistant to attack by liquid and gaseous cesium at 200° Centigrade. Of all the metals tested only platinum and gold show significant attack. In the case of gold the attack was severe in liquid and vapor cesium.

TABLE I

COMPATIBILITY OF CESIUM WITH METALS AT 200° CENTIGRADE

Metal		Weight Change	Specimen Description
Zirconium	Vapor	None Detectable	No Change Evident
	Liquid		
Titanium	Vapor	None Detectable	No Change Evident
	Liquid		
Tungsten	Vapor	None Detectable	No Change Evident
	Liquid		
Niobium	Vapor	None Detectable	No Change Evident
	Liquid		
Tantalum	Vapor	None Detectable	No Change Evident
	Liquid		
Molybdenum	Vapor	-0.03 Percent	No Change Evident
	Liquid	-0.03 Percent	No Change Evident
Nickel	Liquid	None Detectable	No Change Evident
Rhenium	Vapor	None Detectable	No Change Evident
	Liquid		
Nichrome	Vapor	None Detectable	No Change Evident
	Liquid		
302 Stainless Steel	Vapor	None Detectable	No Change Evident
	Liquid		
Silver	Vapor	None Detectable	Slight surface stain in each case.
	Liquid		
Gold	Vapor	-38 Percent	Severe attack evidenced by scale formation.
	Liquid	Dissolved	Spectrographic and x-ray fluorescence analyses of residue show presence of cesium-gold compound.

TABLE I
(Continued)

Metal		Weight Change	Specimen Description
Platinum	Vapor	-0.1 Percent	No Change Evident
	Liquid	-0.2 Percent	No Change Evident
OFHC Copper	Vapor	None Detectable	Surface stain on sample in liquid.
	Liquid	None Detectable	
Beryllium Copper	Vapor	None Detectable	No Change Evident
	Liquid		

For Tables I, II, III, exposure time was 200 hours. One sample of each material was exposed only to cesium vapor, a portion of the second sample was exposed to liquid cesium. In some cases only one entry appears, this is because questionable results due to processing difficulties have not been included. See "Test Procedure Section II-A", in text.

Liquid cesium caused complete degradation of the gold to a brownish powder. This intermetallic compound and/or solid solution was not identified by X-ray diffraction but spectrographic and X-ray fluorescence analyses did reveal the presence of cesium and gold. Cesium vapor, while not as bad as the liquid, showed pronounced interaction with gold. The cross sections in Figure 3 illustrate the effect of the vapor on 0.030 inch wire. In A, a loosely adherent scale is evident on the unetched specimen. In B, the amorphous nature of this adherent scale is contrasted against the crystal structure of the unreacted gold.

While there was no change evident in the appearance of the platinum test specimens, a definite change in weight was observed after test.

Common brazing materials show considerable interaction with cesium. Table II indicates that all the brazing alloys tested are attacked by cesium. In the cases where gold is a constituent of the alloy the degree of attack is roughly proportional to the percent gold present.

Figures 4 and 5 show the effect of cesium vapor at 200° Centigrade (10^{-1} millimeters of mercury pressure) on two common gold-bearing brazing alloys. The before samples show clearly defined crystal patterns for Nicoro and gold-copper solders. After 200 hours exposure, both samples show crystal degradation with the extent of corrosion greater in the case of the gold-copper solder.

In view of the fact that neither pure silver or OFHC copper show interaction with cesium, it is interesting to note that BT (28 percent copper, 72 percent silver) does show noticeable corrosion (see Figure 6). This could be due to oxygen present in the cesium or alloy or, it is possible

TABLE II

COMPATIBILITY OF CESIUM WITH BRAZING ALLOYS AT 200° CENTIGRADE

Brazing Alloy		Weight Change	Specimen Description
Gold Copper (37.5% Au, 62.5% Cu)	Vapor	-1.1 Percent	Surface stains in each case.
	Liquid	-1.1 Percent	
Nicoro (3% Ni, 35% Au, 62% Cu)	Vapor	-0.3 Percent	Surface stains in each case.
	Liquid	-0.3 Percent	
Nioro (18% Ni, 82% Au)	Vapor	-5.5 Percent	Surface darkened and sample embrittled.
	Liquid	Dissolved	
BT (28% Cu, 72% Ag)	Vapor	-0.3 Percent	Surface stains in each case.
	Liquid	-0.2 Percent	Silver appears to have been leached out in the area of the stains.
(50% Au, 50% Cu) Gold Copper	Vapor	3.9 Percent	Surface darkened and slight pitting.

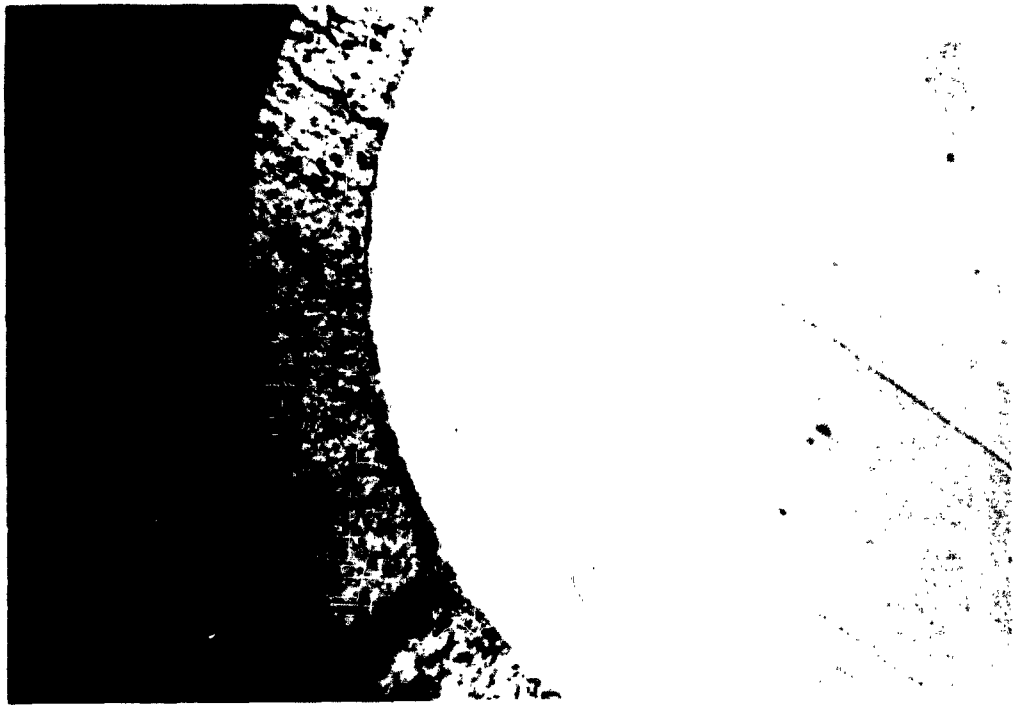

A. Sectioned and Polished

B. Sectioned, Polished and Etched

FIGURE 3 - EFFECTS ON GOLD AFTER 200 HOURS EXPOSURE TO CESIUM VAPOR AT 200° CENTIGRADE

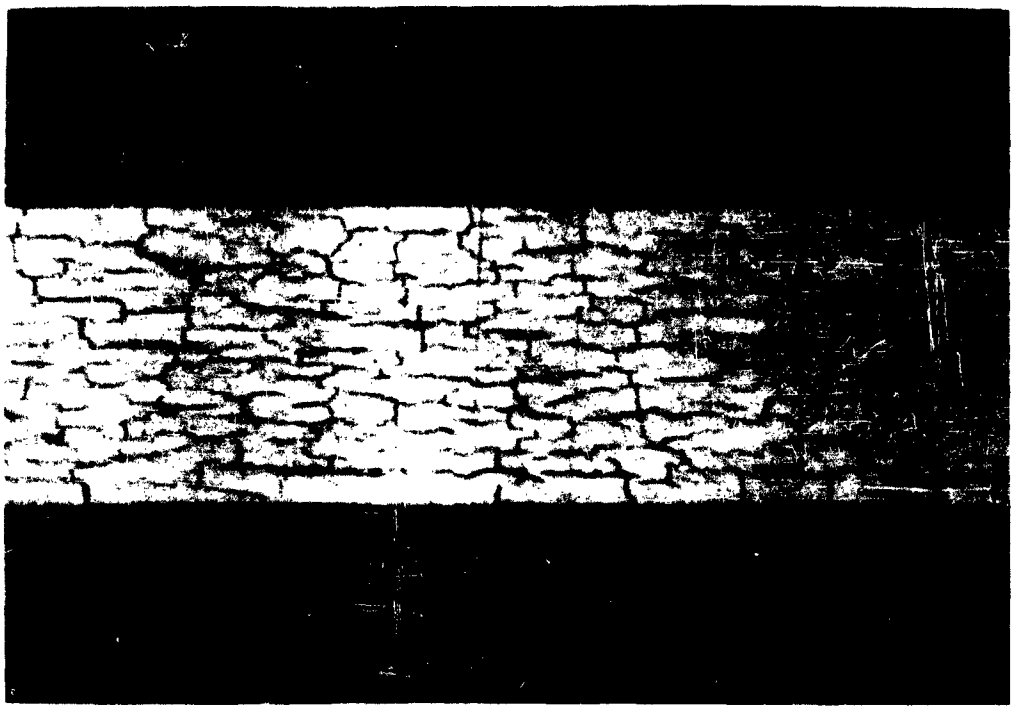

A. Nicoro - Before
3% Ni, 35% Au, 62% Cu

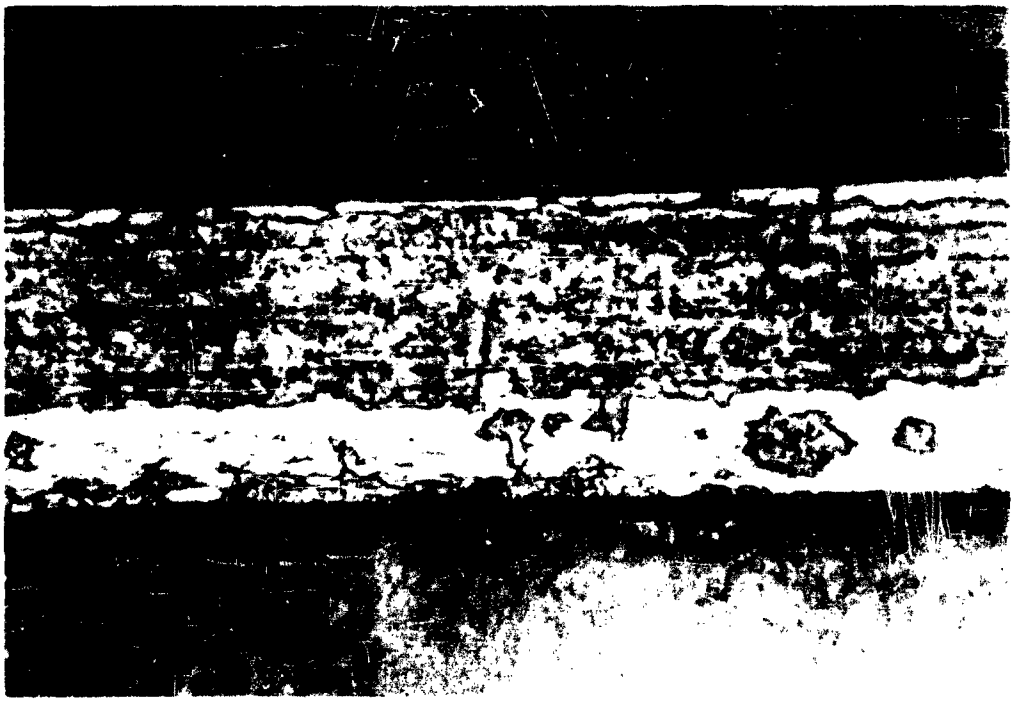

B. Nicoro - After 200 Hours at 200° Centigrade
in Cesium Vapor

FIGURE 4 - EFFECT OF CESIUM VAPOR ON GOLD BRAZING ALLOYS AFTER 200 HOURS AT 200° CENTIGRADE

A. Gold Copper - Before
37.5% Au, 62.5% Cu

B. Gold Copper - After 200 Hours at 200° Centigrade
in Cesium Vapor

FIGURE -5 - ADDITIONAL EFFECTS OF CESIUM VAPOR ON GOLD BRAZING ALLOYS

that the alloy possesses a more favorable crystal structure to cesium attack. Figure 6 illustrates the edge corrosion effect present in the sample that was exposed to cesium vapor, whereas this effect is absent in the unexposed sample.

The test results on ceramic materials are listed in Table III. As indicated, high alumina, steatite, and forsterite ceramics, in general, show little interaction with cesium. The only notable reaction occurred with the Frenchtown 4462 specimen, a portion of which was in contact with cesium liquid. Due to the prevailing use of the Frenchtown ceramic in tube construction practice, further tests at higher temperatures were planned for this material.

A. Before Exposure
BT - 28% Cu, 72% Ag

B. After 200 Hours at 200° Centigrade
in Cesium Vapor

FIGURE 6 - EFFECT OF CESIUM VAPOR ON SILVER BRAZING ALLOY

TABLE III

COMPATIBILITY OF CESIUM WITH CERAMICS AT 200° CENTIGRADE

		Weight Change	Specimen Description
High Alumina			
Diamonite B890	Vapor	-0.02 Percent	No Change Evident
	Liquid	-0.02 Percent	
Diamonite B890-2	Vapor	+0.03 Percent	No Change Evident
	Liquid	+0.03 Percent	
Frenchtown 16536	Vapor	None Detectable	No Change Evident
	Liquid	None Detectable	
Frenchtown 4462	Vapor	-0.02 Percent	No Change Evident
	Liquid	-0.15 Percent	Black residue on surface in contact with cesium.
Coors AD96	Vapor	-0.02 Percent	No Change Evident
	Liquid	-0.02 Percent	
Wesgo	Vapor	-0.02 Percent	No Change Evident
	Liquid	-0.02 Percent	
Steatite			
Paktron L4-A	Vapor	None Detectable	No Change Evident
	Liquid	None Detectable	
Forsterite			
Alsimag 243	Vapor	None Detectable	No Change Evident
	Liquid	None Detectable	

SECTION III

CESIUM COMPATIBILITY TESTS AT 500° CENTIGRADE

A Test Procedure

Anode and envelope materials in radiation-cooled applications can be expected to operate at approximately 500° Centigrade. For this reason a series of tests in cesium vapor at 500° Centigrade were performed.

Since it is not practical, due to oxidation effects, to use copper test envelopes at 500° Centigrade, a system was devised employing stainless steel envelopes. In actual practice, the cesium reservoir of a converter would operate at 200° Centigrade with the anode and envelope materials at 500° Centigrade. Figure 7 illustrates the test set-up that was used in order to simulate these conditions.

The samples to be tested were carefully degreased, weighed, and mechanically attached by means of pre-welded clamps to a stainless steel support rod. The support rod containing the samples was then placed in a 3/4-inch OD x 1/16-inch wall, 304 stainless steel tube. This stainless steel tube was closed at one end by a welded cap and the other end contained a welded female Parker fitting capable of accommodating a 1/2-inch OD x 1/32-inch wall, OFHC copper tubing. The copper tubing contained a glass cesium capsule and was attached to the stainless steel tube by means of the Parker fitting. This assembly was connected to an exhaust manifold by another Parker fitting and the entire assembly was evacuated to approximately 5×10^{-7} millimeters of mercury. After exhaust, the copper tube with the stainless steel appendage was pinched off the system. Then the copper tube was bent as indicated in Figure 7

Note: Letters indicate position of thermocouples

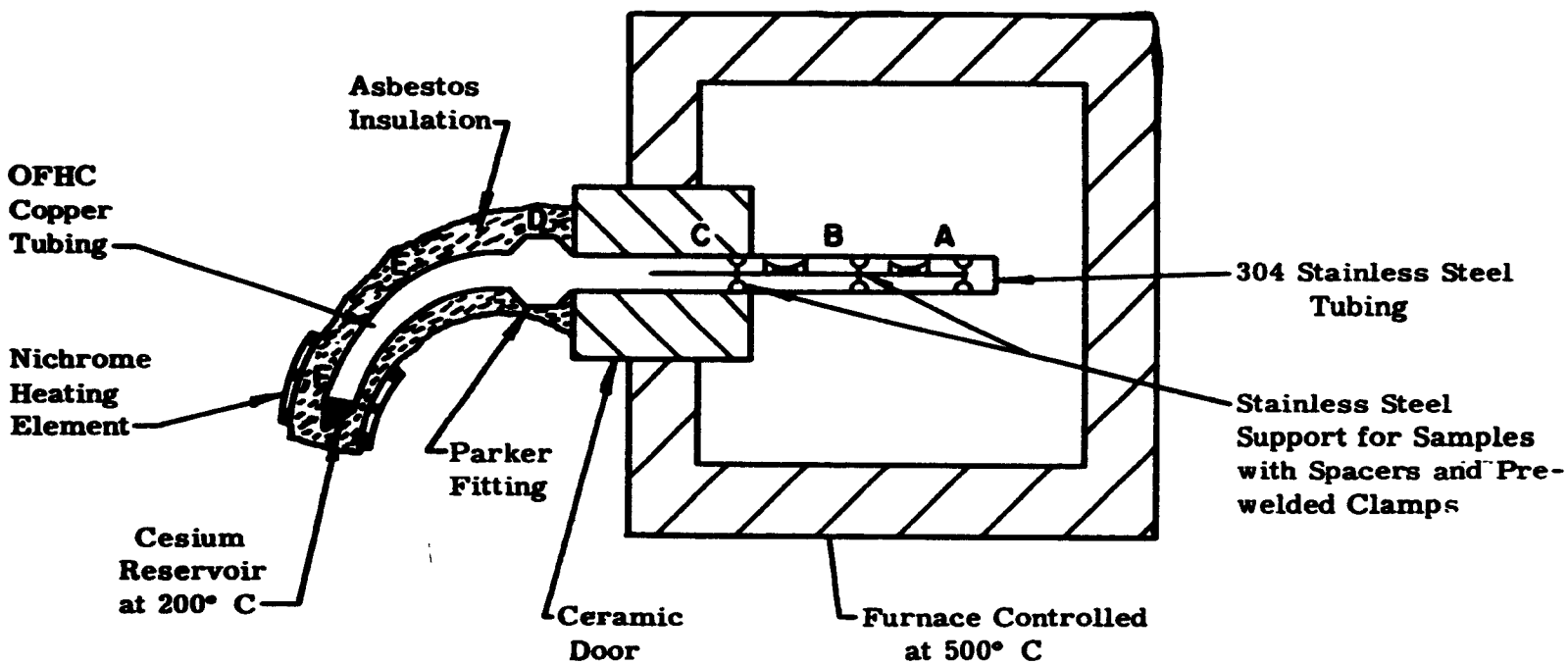

FIGURE 7-TEST CHAMBER FOR MATERIALS COMPATIBILITY WITH CESIUM AT 500° CENTIGRADE

and the cesium capsule was broken. The stainless steel portion of the assembly was placed in a controlled furnace at 500° Centigrade and the copper tube was allowed to remain outside the oven. No difficulty was experienced in keeping the test zone at 500° Centigrade, but it was found necessary to insulate the copper tube and to provide heat through a Nichrome heater tape to maintain the temperature of the cesium reservoir at 200° Centigrade. Using the manifold illustrated in Figure 1, it was possible to process four test assemblies at one time. Each test assembly contained from three to four samples. In general, the metal samples consisted of flat stock ranging from 0.010 inch to 0.050 inch thick, 1 inch long and 3/16 inch wide. The ceramic samples were 1/4 inch diameter rods, 1 inch in length.

At the end of the test period, the samples were removed from the stainless steel tube, washed thoroughly with water and oven dried as in the 200° Centigrade tests. Whereas weight changes were recorded in all cases, cross sections, spectrographic and/or x-ray analyses were made only when interaction with cesium was suspected.

B Results of Tests

The results of these tests are listed for metals in Table IV, brazing alloys in Table V and ceramics in Table VI. It must be emphasized that the test samples were exposed only to cesium vapor at a pressure of 10^{-1} millimeters of mercury. The test duration was 200 hours for all materials and the same procedure was followed for recording weight changes and testing for embrittlement as in the 200° Centigrade tests.

The results in Table IV indicate that many metals used in tube construction practice are resistant to attack by cesium vapor at 500° Centigrade.

TABLE IV

COMPATIBILITY OF CESIUM WITH METALS AT 500° CENTIGRADE

Metal	Heat Treatment	Weight Change	Specimen Description
Zirconium	1500° C - 2 Min. Vacuum	-0.45 Percent	Surface darkened sample. Embrittled intergranular penetration evident.
Zirconium	1300° C - 15 Min. Vacuum	None Detectable	No Change Evident
Titanium	800° C - 15 Min. Vacuum	None Detectable	No Change Evident
Tungsten	1500° C - 2 Min. Vacuum	None Detectable	No Change Evident
Niobium	1500° C - 2 Min. Vacuum	None Detectable	No Change Evident
Tantalum	1500° C - 2 Min. Vacuum	-0.19 Percent	Surface Darkened
Tantalum	1300° C - 15 Min. Vacuum	None Detectable	No Change Evident
Molybdenum	1500° C - 2 Min. Vacuum	None Detectable	No Change Evident
Nickel	800° C - 15 Min. Vacuum	None Detectable	No Change Evident
Kovar	1020° C - 30 Min. Line Hydrogen	None Detectable	No Change Evident
Rhenium	1500° C - 2 Min. Vacuum	None Detectable	No Change Evident
Platinum	1500° C - 2 Min. Vacuum	None Detectable	No Change Evident
OFHC Cpr.	550° C - 2 Min. Line Hydrogen	None Detectable	No Change Evident

For Tables IV, V, VI, exposure time was 200 hours and the cesium vapor pressure was 10^{-1} millimeters of mercury. Each entry represents an individual specimen tested. See "Test Procedure Section III-A, in text.

TABLE V

COMPATIBILITY OF CESIUM WITH BRAZING ALLOYS AT 500° CENTIGRADE

Combination	Weight Change	Specimen Description
Kovar (37.5% Au - 62.5% Cu) Kovar	None Detectable	No Change Evident
Kovar BT (72% Ag - 28% Cu) Kovar	None Detectable	No Change Evident
Kovar Nicoro (3% Ni - 35% Au - 62% Cu) Kovar	None Detectable	No Change Evident

TABLE VI

COMPATIBILITY OF CESIUM WITH CERAMICS AT 500° CENTIGRADE

High Alumina	Weight Change	Specimen Description
Diamonite B890	None Detectable	No Change Evident
Frenchtown 4462	+0.24 Percent	Entire surface covered with black residue; spectrographic and x-ray analysis revealed iron and cesium.
Forsterite		
Alsimag 243	None Detectable	No Change Evident

In order to degas the metals and minimize possible corrosion effects due to intergranular penetration, each sample before test, was subjected to a heat treatment. In an initial test, the refractory metals, i. e., zirconium, tungsten, niobium, tantalum, molybdenum, rhenium, and platinum were fired in vacuum for two minutes at 1500° Centigrade. It can be observed from Table IV that, of the metals fired under these conditions, zirconium and tantalum revealed attack after test. Figure 8 shows the effect that the cesium vapor had on the vacuum treated zirconium. Definite intergranular corrosion can be seen by comparing the before and after samples. It was not possible to obtain a satisfactory etch in the before and after tantalum specimens, indicating indirectly that the tantalum was not sufficiently annealed.

The alteration of the crystal structure in the case of zirconium could have been caused by an insufficient removal of impurity constituents during the vacuum heat treatment or corrosion by contaminants in the cesium itself, e. g., nitrogen, oxygen, hydrogen. The former possibility appeared more likely, consequently, new samples of zirconium and tantalum were vacuum fired at 1300° Centigrade for 15 minutes at a pressure of 5×10^{-4} millimeters of mercury. The test results in Table IV indicate that these metals had no detectable change in weight or appearance and were not embrittled after test. It is possible that the extended vacuum treatment adequately degassed the metals, thereby removing the reason for the cesium attack.

It should not be concluded from Table IV that metals in general are resistant to liquid cesium at 500° Centigrade or cesium vapor in equilibrium with liquid at this temperature. The vapor pressure of cesium under this condition is 10^{2} millimeters of mercury, a thousand times

greater than the vapor pressure in the tests listed in Tables IV, V, and VI.

In comparing the platinum results at 500° Centigrade and 200° Centigrade it can be seen that attack was evidenced at 200° Centigrade, but not at 500° Centigrade. In each case the platinum was from the same source. This at first appears contradictory but it should be noted that the platinum used for the 500° Centigrade test was vacuum fired at 1500° Centigrade for two minutes, whereas the platinum in the 200° Centigrade test was not fired. This vacuum treatment could have removed grain boundry inclusions, as proposed for the tantalum and zirconium, thereby affording the platinum a greater resistance to cesium attack.

A test was made in order to evaluate the effect of cesium vapor in equilibrium with liquid cesium at 500° Centigrade. Four OFHC copper test tubes, each containing cesium and test samples, were prepared in exactly the same fashion as described in Section II-A. After processing these tubes were coated with a 0.001 inch thick Kanigen plating (General American Transportation Company). The Kanigen process will deposit on copper a dense, amorphous nickel-phosphorous coating. In a previous test, two copper tubes containing no cesium or test samples but plated with this nickel alloy coating were found resistant to oxidation and vacuum tight after 150 hours at 500° Centigrade. However, when the copper test tubes containing the cesium were placed in the oven at 500° centigrade, the copper was severely attacked after less than 60 hours and the test samples were destroyed. Evidently the attack was from the inside by cesium rather than from the outside by air.

The test samples listed in Table V were combinations prepared for testing brazing alloy materials. These combinations were brazed units consisting of a 0.003 inch thick strip of a given solder, sandwiched between

two 0.040 inch thick, annealed kovar strips. After 200 hours under test, these samples showed no evident changes in appearance or weight. It must be pointed out that only a very small area of actual braze material was exposed to the test environment, the remainder to the brazed area was covered by the kovar. These results must be viewed as a first approximation, considering the demonstrated corrosion of brazing materials in the 200° Centigrade tests.

The ceramic materials tested at 500° Centigrade are listed in Table VI. Of the materials tested, the Frenchtown 4462 ceramic showed considerable interaction with cesium (Ref. 3). After test, the entire surface of the sample was covered with a conductive black residue. Spectrographic and x-ray diffraction analysis revealed the primary constituents of this residue to be iron, aluminum, manganese, silicon and cesium. Apparently, the metallic oxides present in this ceramic were reduced to the free metal by reaction with the cesium vapor. The other two ceramics tested showed no evident reaction.

The effect of cesium vapor at 500° Centigrade on a ceramic-to-metal seal was evaluated. The medium for this test was an RCA computer diode package. Figure 9-A illustrates that this package consists of a molybdenum metallized ceramic, copper brazed to kovar on either end. Two samples were found to be vacuum tight after 200 hours under test. However, the ceramic was attacked (Figure 9-B) as evidenced by insulation breakdown and a black residue on the surface. It is not surprising that this should occur since the ceramic involved contains five percent manganese. These results are in agreement with those obtained in Table IV for copper and Table VI for the manganese containing Frenchtown ceramic.

A. Before Exposure

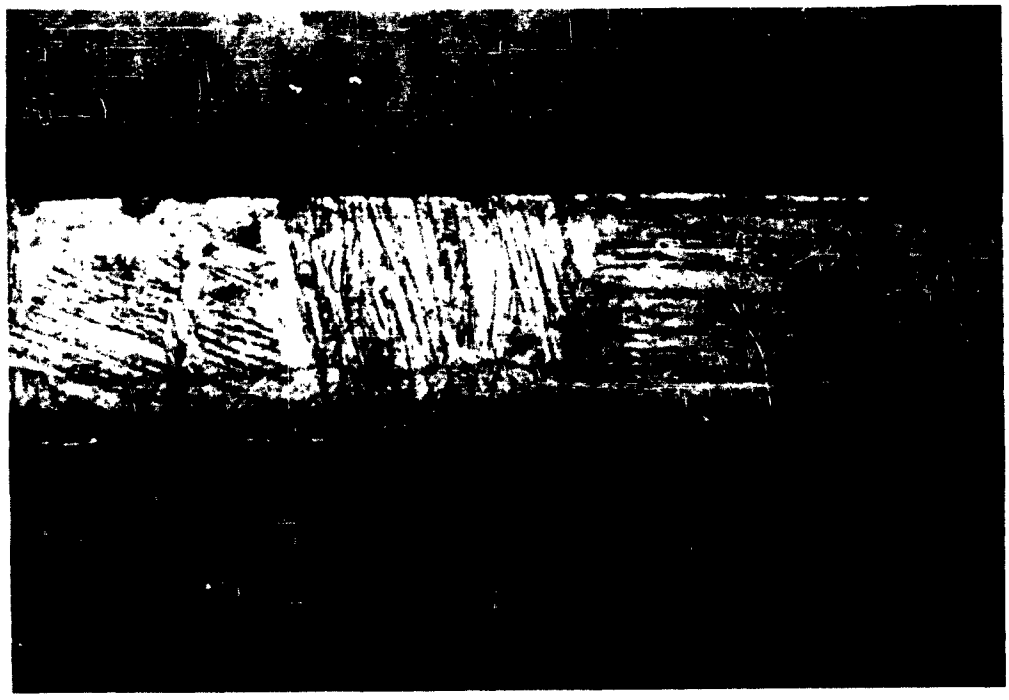

B. After 200 Hours at 500° Centigrade in Cesium Vapor

FIGURE 8 - EFFECT OF CESIUM VAPOR ON ZIRCONIUM

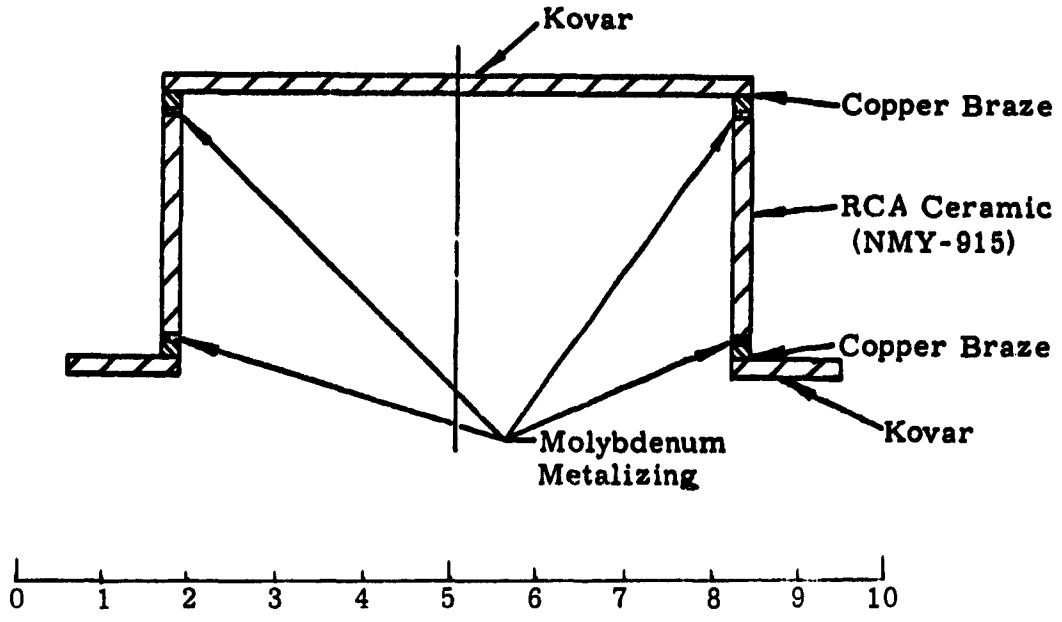

A - Computer Diode Package

B - "Before" and "After" Photograph of
Exposure of the Package to Cesium

FIGURE 9 - EFFECTS ON AN ASSEMBLY OF EXPOSURE TO CESIUM AT 500° CENTIGRADE

SECTION IV

CESIUM COMPATIBILITY TESTS AT 1300° CENTIGRADE

A Test Procedure

A vacuum tube was designed that permits cathode materials of interest to be tested as electrically heated filaments in the presence of cesium vapor at 200° Centigrade and a pressure of 10^{-1} millimeters of mercury. The essential features of this device are illustrated in Figure 10.

In the construction of the tube, filamentary wire, with a diameter of six to eight mils, was welded to kovar stem leads. The external portion of the leads served as electrical connections to the power supply. Each tube can accommodate four samples. After construction, the tube was exhausted to approximately 5×10^{-7} millimeters of mercury and then pinched off. The cesium capsule in the arm of the exhaust tubing was broken and the entire assembly was placed in a controlled oven at 200° Centigrade. The filaments were then adjusted to 1300° Centigrade. The proper temperature was obtained by adjusting the filament power supply until an emissivity corrected, optical pyrometer measurement was made through the glass window.

After allowing the test to run for 200 hours, the filaments were removed from the tube, washed thoroughly with water, oven dried and then cross-sectioned.

B Results of Tests

Two tubes, employing the materials of interest as filaments, were tested for cesium compatibility at 1300° Centigrade and 10^{-1} millimeters

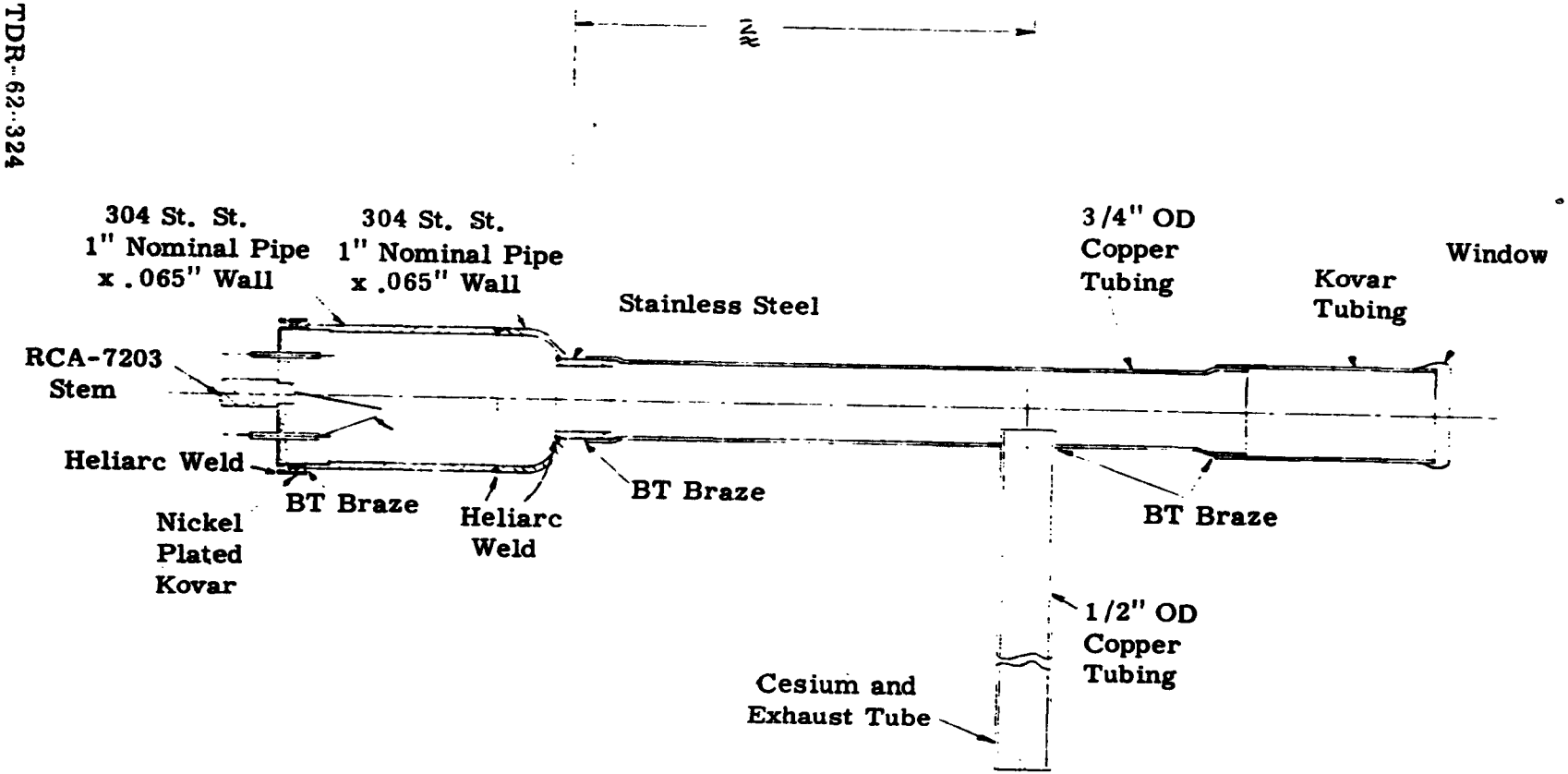

FIGURE 10 - HIGH-TEMPERATURE CESIUM COMPATIBILITY TEST TUBE

of mercury cesium vapor pressure.

In the first test, the filaments consisted of molybdenum, tantalum, rhenium, and tungsten. In this test, the tantalum filament burned out after twelve hours under the test conditions. At the same time, no change was observed in the operating characteristics of the other materials. The test was discontinued at this point, the filaments were removed from the tube, washed, and dried and then cross sectioned.

Figure 11 shows two cross sections obtained from the first test. Both rhenium and tantalum show attack, with the interaction being less severe in the case of rhenium. The cross sections for the tungsten and molybdenum revealed no intergranular corrosion.

In processing this tube, the filaments were given a one hour bakeout at 350° Centigrade. However, they were not degassed at high temperature in vacuum. In addition, liquid cesium accidently came in contact with the hot filaments at the beginning of the test. It is therefore difficult to determine the true cause for the tantalum failure. It could have been the cesium itself, impurities in the cesium or perhaps impurities in the tantalum.

In the second test, the filaments again consisted of molybdenum, tantalum, rhenium, and tungsten. After bakeout, the filaments were degassed at 1800° Centigrade for a few minutes while the tube was on the pumps and no liquid cesium came in contact with the tantalum. After two hundred hours under test all the filaments were still operating but the tantalum filament had increased in resistance. A few hours after 200, the window cracked, the tube went to air and the filaments burned out. Under these circumstances, it was not possible to obtain pertinent information from cross sections.

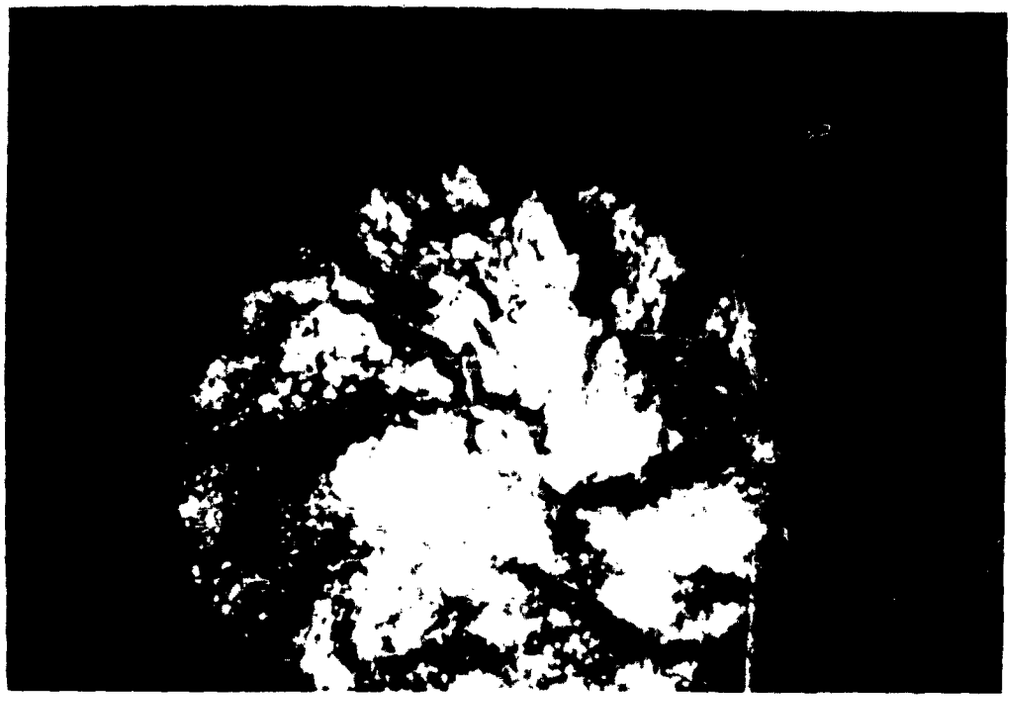

A. Tantalum After 12 Hours at 1300° Centigrade in Cesium Vapor

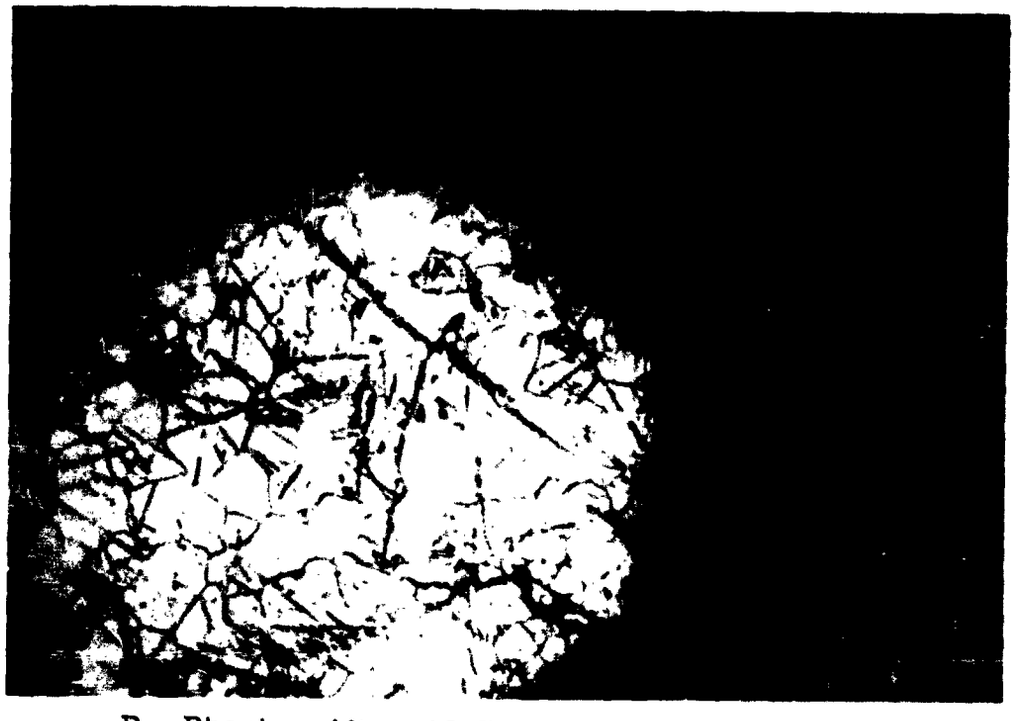

B. Rhenium After 12 Hours at 1300° Centigrade in Cesium Vapor

FIGURE 11 - EFFECT OF CESIUM VAPOR ON TANTALUM AND RHENIUM

Apparently, the precautions taken in the second test, resulted in improved life for the tantalum specimen. Nevertheless the change in resistance of the tantalum could indicate a cesium reaction was taking place.

It is interesting to note that the BT brazed areas in the second tube were leak checked after test and found to be vacuum tight.

SECTION V
CONCLUSIONS

A summary of the resistance of tube construction materials to attack by cesium vapor at 10^{-1} millimeters of mercury pressure appears in Table VII. The results apply for a 200-hour test period. If a material was found to have good resistance at a given temperature and cesium pressure, then it was considered to have good resistance at all lower temperatures and equal or lower cesium pressures. If a material was found to have poor or limited resistance at a given temperature and cesium pressure, then it was considered to have poor resistance at all higher temperatures and equal or higher cesium pressures.

Many metals showed good resistance to cesium vapor at the temperatures tested. Zirconium and tantalum revealed a tendency to be attacked at 500° Centigrade however, with proper degassing, this susceptability appeared to be removed. It is also probable that a vacuum treatment improves the resistance of platinum to cesium attack. Pure gold was found to have poor resistance to cesium vapor.

Brazing alloys containing precious metals such as gold and silver showed poor resistance to cesium attack. In the case of gold-containing brazing alloys the degree of interaction corresponds roughly to the amount of precious metal present in the alloy.

Steatite, forsterite and high-alumina ceramics in general revealed good resistance to cesium vapor. An exception to this statement is found in the fact that high-alumina ceramics, containing manganese, in the order of five percent, were attacked at 500° Centigrade.

TABLE VII

THE RESISTANCE OF MATERIALS TO ATTACK
BY CESIUM VAPOR AT A
PRESSURE OF 10^{-1} MILLIMETERS OF MERCURY

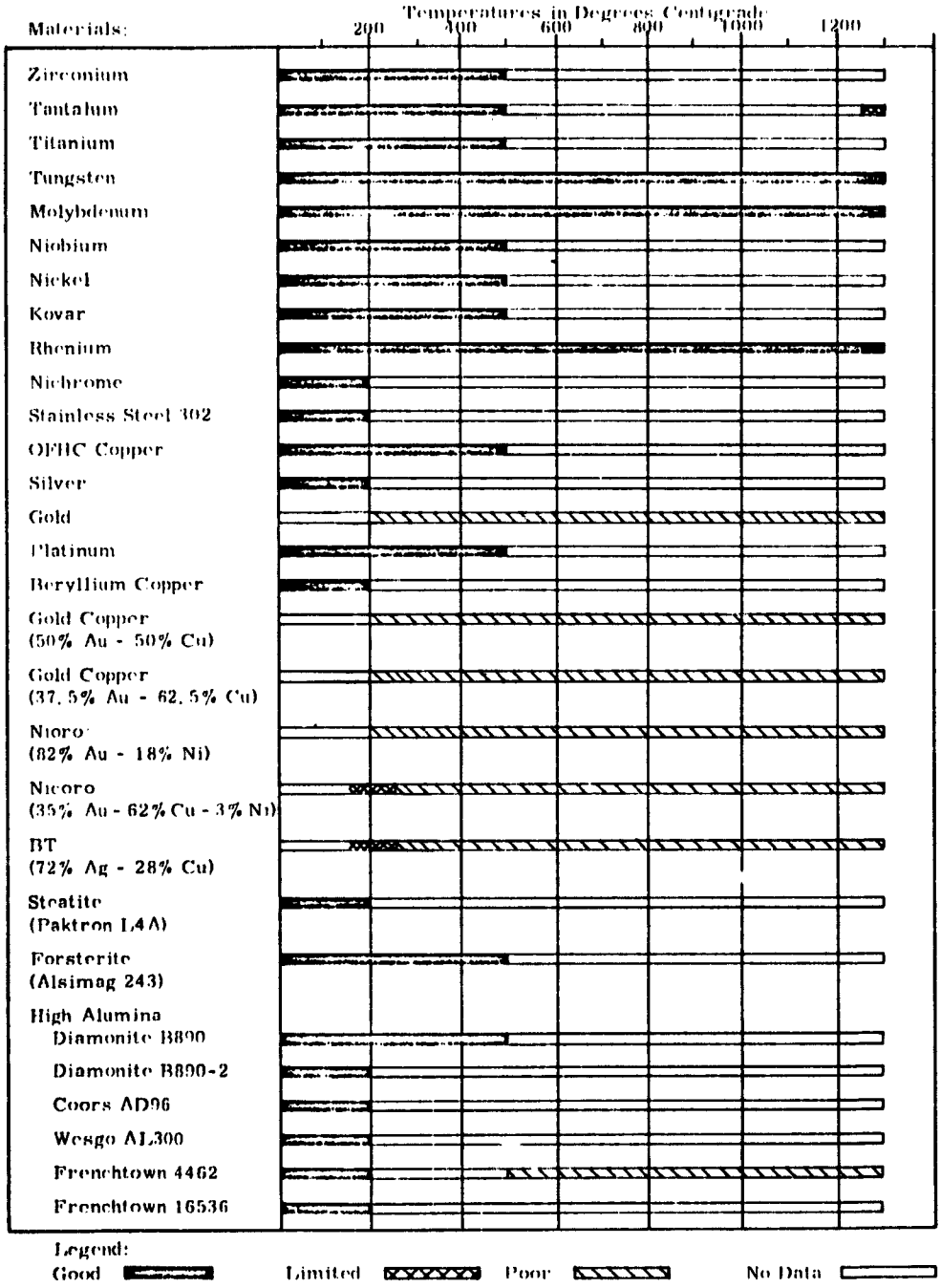

In reviewing the results presented above, a distinction must be made between the effects of cesium vapor at 10^{-1} millimeters of mercury pressure and cesium vapor at some other pressure or cesium liquid. For example, copper was found to have good resistance at 500° Centigrade and 10^{-1} millimeters of mercury, cesium pressure, but was severely attacked by cesium liquid at the same temperature. Similarly at 200° Centigrade, a manganese bearing high-alumina ceramic showed good resistance to cesium vapor but was attacked by the liquid. Meaningful information depends on the purity of the material being tested. Even when materials are considered spectrographically pure, they may contain grain boundry impurities that could lower the resistance to cesium attack. In such cases vacuum treatment at elevated temperatures may be useful.

Since the test period was only 200 hours, the results presented should be viewed as indicating trends in material behavior. Further tests for extended periods should be performed. This is particularly true for cathode and ion emitter materials since they must function at elevated temperatures. Sufficient information has been obtained to demonstrate clearly the need for a more reliable braze material to maintain vacuum conditions.

SECTION VI
LITERATURE REFERENCES

1. Final Report - Analytical and experimental investigation of compact-charge ionization, p. 118-146, 1 June 1960, ARPA Order Number 5-58, Task Number 094-347, Contract Number NOmr-2886(00), published by Curtiss-Wright Corporation Research Division, Quehanna, Pennsylvania.

2. Liquid-Metals Handbook, 1950, Atomic Energy Commission, Department of the Navy, Washington, D. C.

3. Quarterly Status Report of the LASL Plasma Thermocouple Development Program for period ending 20 March 1961, p. 6, Los Alamos Scientific Laboratory of the University of California, Los Alamos, New Mexico.

APPENDIX II

GAS PERMEATION STUDY OF MATERIALS FOR USE IN THERMIONIC ENERGY CONVERTERS

Prepared for:

AERONAUTICAL SYSTEMS DIVISION
United States Air Force
Wright-Patterson Air Force Base
Ohio

Contract AF33(616)-7903
Project Number 3145
Task Number 314509

Prepared by:

L. J. Conklin
J. C. Turnbull

RADIO CORPORATION OF AMERICA
Electron Tube Division
Chemical and Physical Laboratory
Lancaster, Pennsylvania

GAS PERMEATION STUDY OF MATERIALS FOR USE IN THERMIONIC ENERGY CONVERTERS

TABLE OF CONTENTS

LIST OF ILLUSTRATIONS

LIST OF TABLES

GAS PERMEATION STUDY OF MATERIALS FOR USE IN THERMIONIC ENERGY CONVERTERS

SECTION I

INTRODUCTION

The performance of high-temperature vacuum devices may be affected by the presence of gases which diffuse through the walls of the device. Gas permeation is particularly a problem for the thermionic energy converter as energy must flow into the cathode at high temperature during operation of this device. The present study of gas permeability was thus undertaken on envelope materials for a thermionic converter to operate with cathode temperature in the range of 1200-1500° Centigrade. Representative thermally stable envelope materials selected for study in this high-temperature application were: (1) platinum and platinum-rhodium alloy, (2) molybdenum with a protective coating, (3) Inconel, and (4) an alumina ceramic material. Gases selected for the permeation study were air, nitrogen, argon, helium, hydrogen, carbon monoxide, carbon dioxide, and methane.

In the work described below, the metals platinum, platinum-rhodium alloy, molybdenum and Inconel were found to be permeated rapidly by hydrogen. Hydrogen permeation was observed on maintaining molecular hydrogen, methane or water vapor on the outside surface of the test sample. Two molybdenum disilicide coatings tried on molybdenum had no effect on rate of hydrogen permeation; however, a reduction in nitrogen permeation rate of over 100-fold was observed for a disilicide coating of thickness 0.0005 inch. No gases were found to permeate the alumina material. At high temperatures of 1400-1600° Centigrade, a slight evolution of oxygen in the system was found. This may possibly represent dissociation of impurity

oxides in the alumina; however, there has been insufficient investigation to allow the source of oxygen to be defined accurately.

SECTION II
THEORY OF INVESTIGATION

The permeation or diffusion of gases through a solid material (Ref. 1, 2, 3) involves several steps including: (1) absorption and reaction with the gas phase on the incoming surface and solution of the gas in the solid, (2) diffusion of the gas through the solid to the outgoing side, and (3) surface reaction and desorption of molecular gas on the outgoing side of the material. Permeation is the general term used to describe the overall process leading to the transfer of gas from the incoming to the outgoing surfaces. This process in many cases is limited by the diffusion rate of the gas in the solid, the permeability rate constant P being given by:

$$P = D \times S \qquad (1)$$

where D is the diffusion constant and S the solubility of the gas in the solid. The quantity of gas Q (liter-mm. at STP) that will flow through a wall of area A (cm^2) and thickness d (cm) in time t (sec) with a pressure p (atm) on one side of the wall and zero pressure on the other side, is given by:

$$Q = P\,(A/d)\,t\,(p)^n \qquad (2)$$

where n has the value one for monatomic gases and one-half for diatomic gases. If the test material is tubular in shape, with outside radius a, inside radius b, and length ℓ (cm), then Q is given by the expression:

$$Q = \frac{P2\,\pi\,\ell\,t\,(p)^n}{\ln \frac{a}{b}} \qquad (3)$$

SECTION III
FACTUAL DATA

A Experimental Procedure

The materials to be tested for gas permeation were obtained in the form of tubing. The metal samples were heated by passing a heavy 60-cycle current from one end of the tube to the other. Ceramic samples were heated within a similar tubular heating element of disilicide-coated molybdenum. Gases at atmospheric pressure were maintained on the outside of the tube, while the inside of the tube was exhausted. Gases permeating the wall of the tube were measured with a mass spectrometer.

The metal samples were seamless tubing approximately 10 inches long, with an outside diameter of 3/16 to 1/4 inch, and a wall thickness of 0.010 to 0.030 inch. One end was closed with a copper plug brazed with BT solder; the other end was brazed to a 1/4 inch OD copper tubulation. The ceramic samples of the same length were made with one end closed, the other end being metallized and brazed to a kovar collar which in turn was brazed to a 1/4 inch OD copper exhaust tubulation. Figure 1 shows examples of test samples used in this study.

The apparatus and sample holder for permeation measurements is shown in Figure 2. The copper exhaust tubulation of the sample under test is attached by a Parker "Triple-Lok" fitting to a one-inch diameter stainless steel vacuum manifold. The latter, and two water-cooled copper leads for conducting current to heat the sample, are brought out through the bottom plate of the equipment. The sample tube is surrounded by an inner bell jar, through which the test gas flows; this in

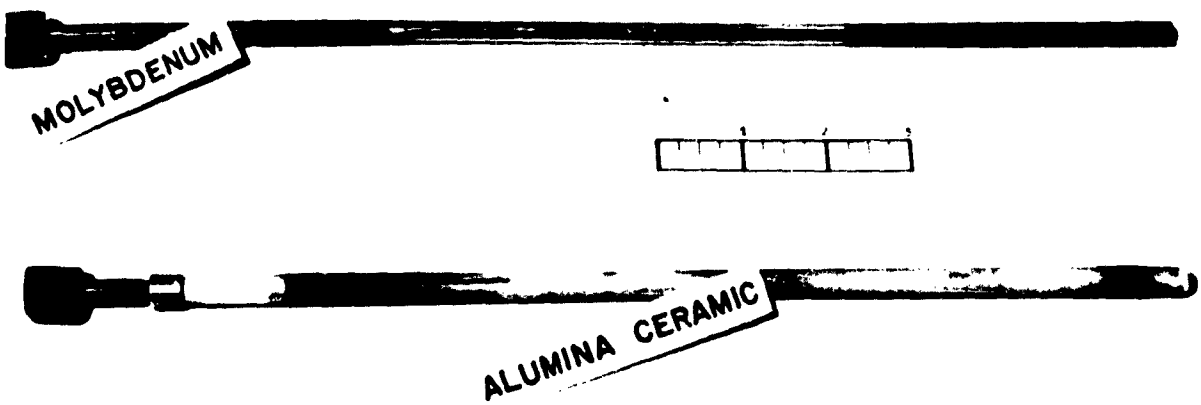

FIGURE 1 - TEST SAMPLES FOR GAS PERMEATION MEASUREMENT

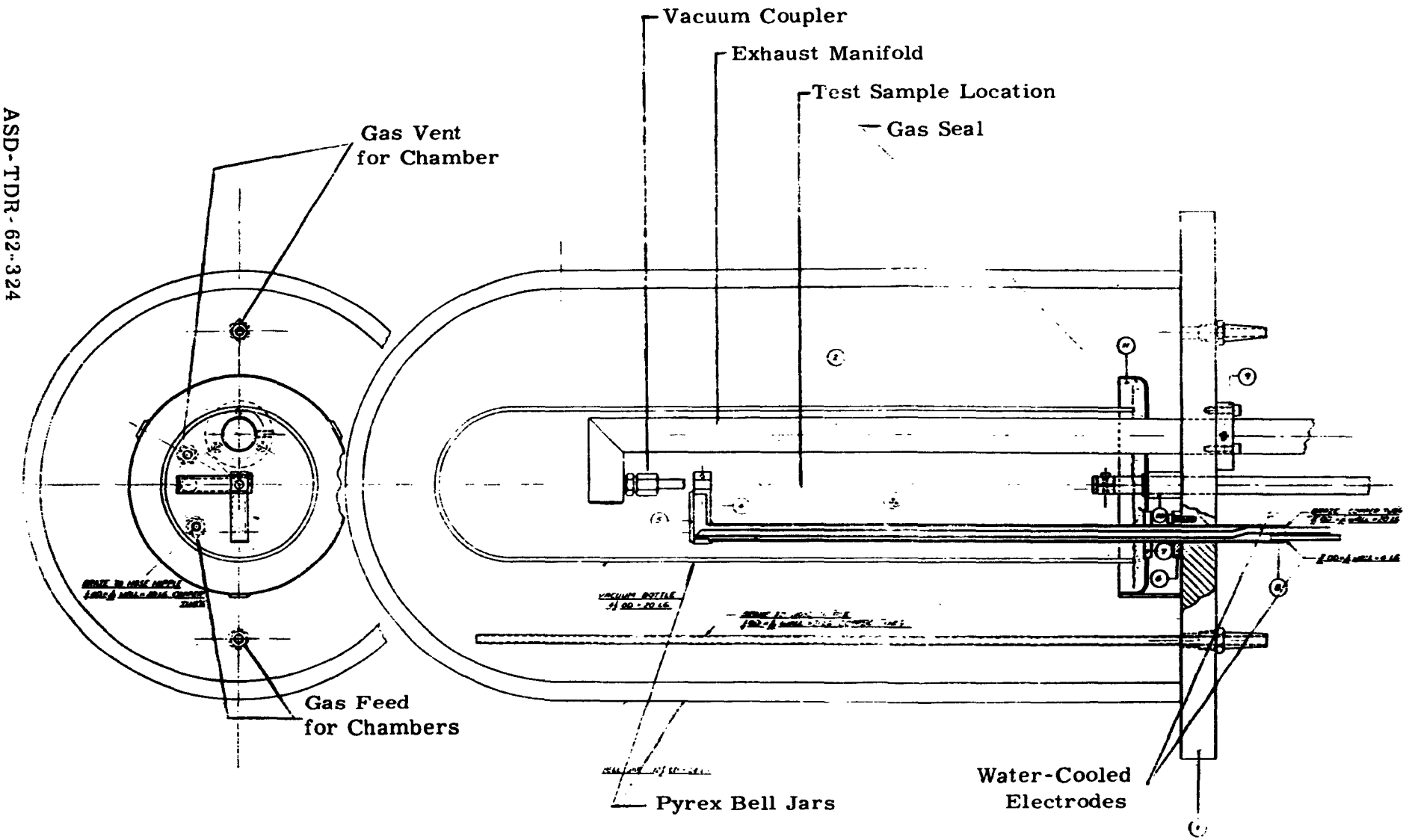

FIGURE 2 - Apparatus for Permeation Measurements

turn is surrounded by an outer bell jar, through which an inert gas (usually helium) flows. Flow rates of these gases were three to five cubic feet per hour. This arrangement was used to minimize contamination of the test gas by air. Commercial tank gases were used for carbon monoxide, carbon dioxide, helium, nitrogen, argon and methane; hydrogen was obtained from the plant gas line. A Lectrodryer (Ref. 4) and liquid nitrogen trap were used to reduce water content of the test gases (excepting CO_2 and CH_4).

The vacuum system for exhaust of the test sample is shown in Figure 3 to consist of a glass mercury diffusion pump, glass "U" trap, and a stainless steel exhaust manifold. Pumping speed of the system at the Parker fitting is estimated to be one liter per second. The system is not baked; lowest pressure during a run, indicated by the ionization gauge, is generally less than 10^{-7} millimeter. As shown, the sample is continuously pumped by the mercury pump. The latter in turn is exhausted either by another mercury pump and fore pump, or, by manipulation of stopcocks, is exhausted by the mass spectrometer vacuum system for determination of gases pumped away from the tubular sample.

The measurement of gases permeating through the sample is made using a Model 21-620 mass spectrometer. For this purpose, the usual gas inlet system of the mass spectrometer is removed. Gases permeating through the sample wall are pumped first by the mercury pump (Figure 3) and then by the mass spectrometer vacuum system (Figure 4). The gases admitted to the spectrometer system diffuse to the ionizing region of the spectrometer ion source, and are recorded as peaks when the mass spectrum is scanned. The height of the peaks measures the relative partial pressures of gas components, which in turn are determined by their rates of permeation through the sample.

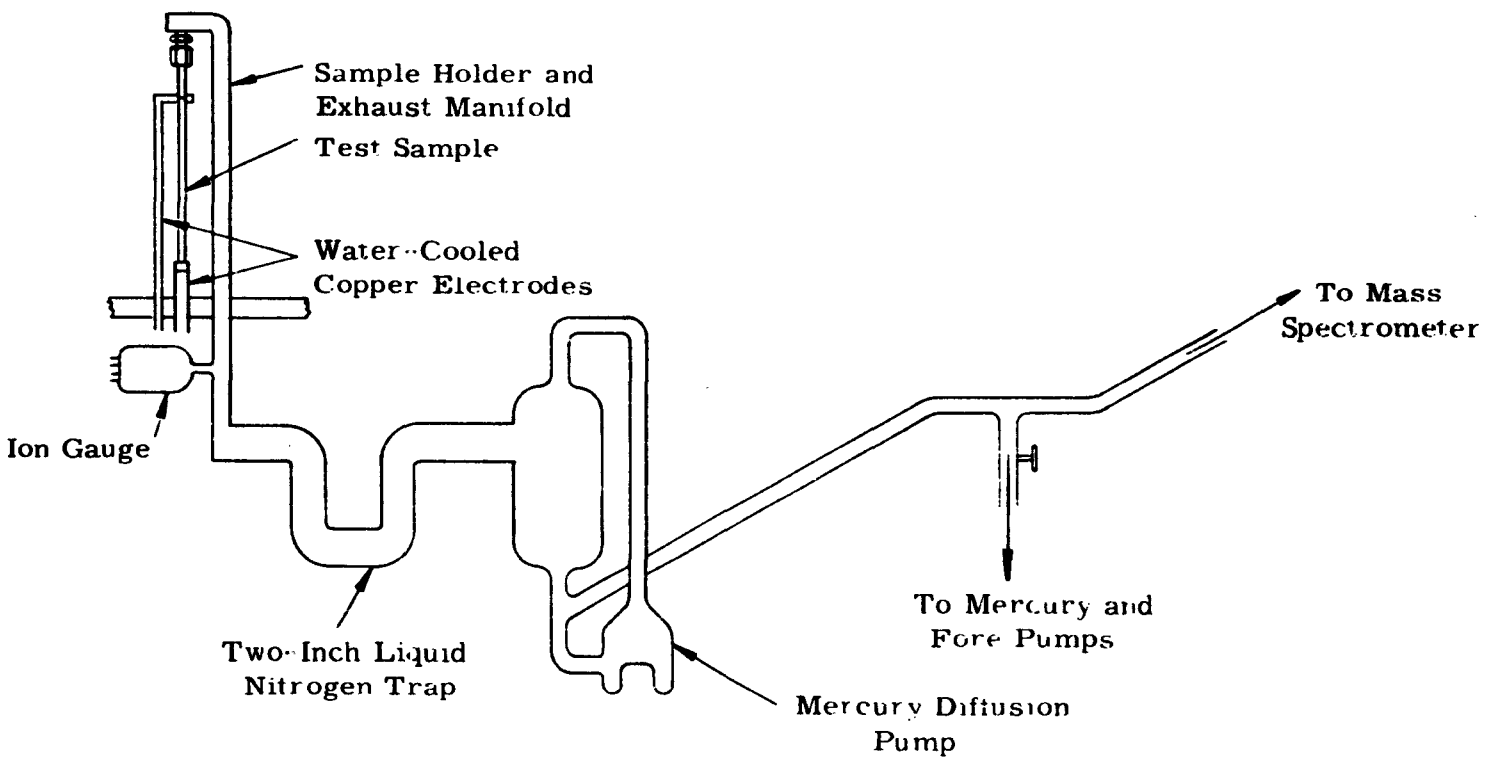

FIGURE 3 - SCHEMATIC OF VACUUM SYSTEM FOR EXHAUST OF TEST SAMPLE

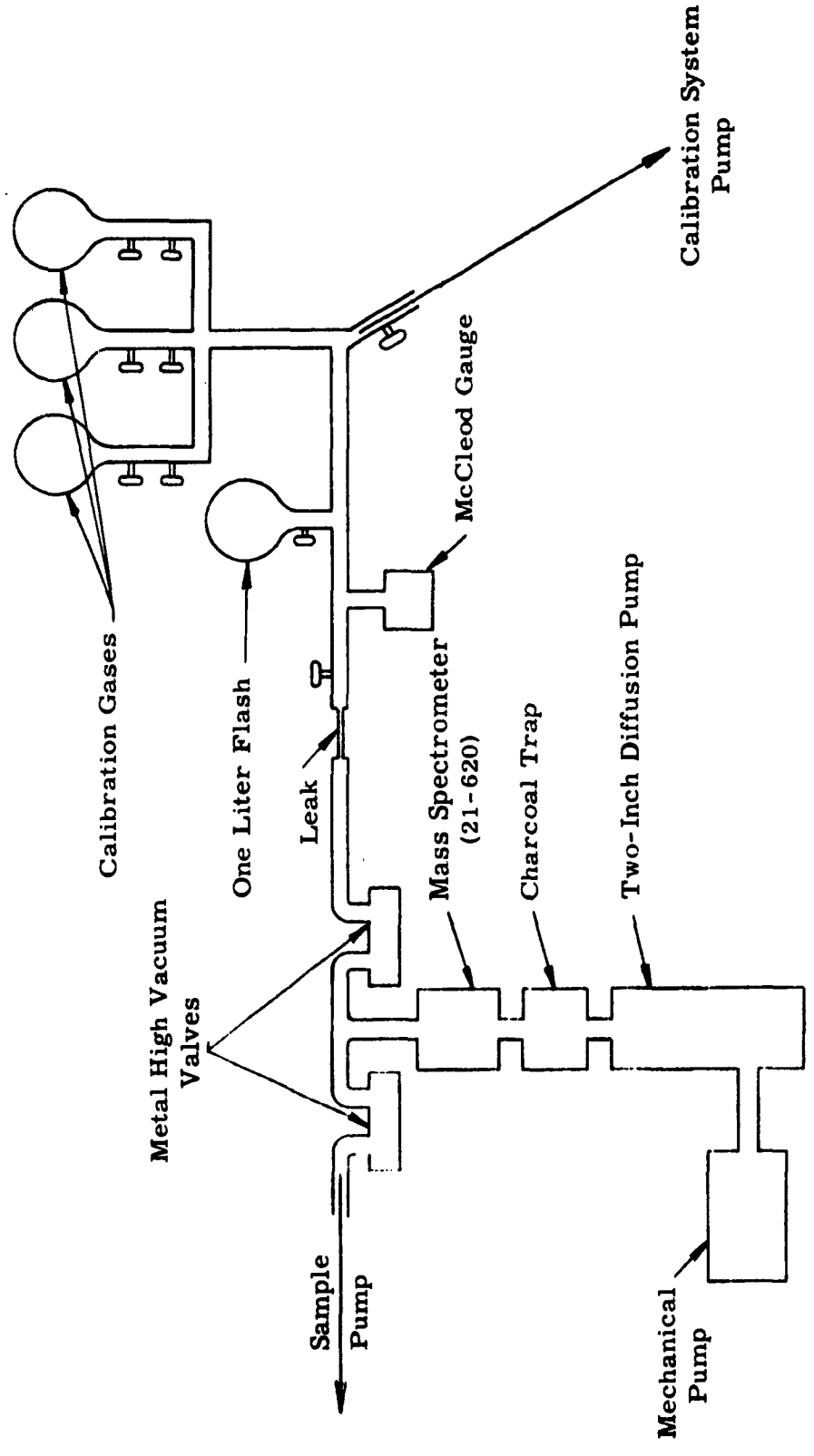

FIGURE 4 - SCHEMATIC OF GAS ANALYSIS AND CALIBRATION SYSTEM

For calibration of the system (Figure 4), pure gases are admitted at known rates into the mass spectrometer, in the same way as are gases under test, and their peak heights recorded. The calibrating gas is obtained from a reservoir which is filled with a gas at an initial pressure determined with a McLeod gauge. The gas is allowed to leak from the reservoir through a glass capillary into the mass spectrometer system. During this time, pressure in the gas reservor falls according to the relation:

$$p = p_o \exp(-St/V) \qquad (4)$$

where p_o = initial reservoir pressure (mm Hg)

p = reservoir pressure (mm) at time t

S = conductance of capillary leak (liter/sec)

V = reservoir volume (liters)

t = time (seconds)

Peak height h is proportional to the quantity of gas being leaked into the mass spectrometer, which is given by p^S (liter-mm/sec). If log h is plotted versus time, a straight line should result, with slope -S/V. From this the conductance of the leak S is readily calculated, which in turn yields the gas quantity p^S and the mass spectrometer sensitivity p^S/h (liter-mm per sec per division).

As a typical example, the reservoir (volume 1.8 liter) was initially filled with CO_2 gas at an initial pressure of 0.26 millimeter. Using the 44 peak, the slope of the log h versus time plot gave a conductance S of 1.2×10^{-4} liters per second. Initial rate of gas leakage was thus 3×10^{-5} liters-millimeter per second. Initial peak height was 16,200

divisions. Thus the sensitivity for CO_2, using the 44 peak was determined to be 1.9×10^{-9} liters-millimeter per second per division. Typical sensitivity values for gases of interest in the present work are given in Table I.

TABLE I

SENSITIVITY OF MASS SPECTROMETER FOR VARIOUS GASES

Gas	Mass No.	Sensitivity (liter-mm/sec per div)
Carbon Dioxide	44	1.9×10^{-9}
Carbon Monoxide	28	2.7×10^{-9}
Hydrogen	2	7.5×10^{-9}

Temperature of the test samples, for Table II, was determined with an optical pyrometer and were corrected for emissivity. The values given in Table II were used for this correction.

TABLE II

EMISSIVITY OF TEST SAMPLE MATERIALS

Material	Emissivity
Inconel (Oxidized Surface)	0.8
Molybdenum	0.4
Disilicide Coating on Molybdenum	0.5
Platinum and Platinum-Rhodium	0.2

B Permeation Measurement

1. Inconel

This material was tested in the form of tubing, of length 11 inches, outside diameter 3/16 inches, and wall thickness 0.010 inch. The length of the uniform hot zone at maximum temperature for the permeation measurement (1225° Centigrade) was 9.5 inches. The samples, heated in helium at 1225° Centigrade, were difficult to outgas, the principal constituents being nitrogen and carbon monoxide. The Inconel sample was oxidized after outgassing, its surface being covered with a very dark green, uniform oxide film. In all cases measurements of gas permeation were carried out with this film present.

Gases tested for permeation through Inconel were methane, nitrogen, carbon monoxide and helium. Results are given in Table III. On exposure to methane at one atmosphere pressure and at temperatures between 710 and 1175° Centigrade, rapid decomposition of methane and permeation of hydrogen was observed, with severe carburization of the Inconel sample at the higher temperatures. The hydrogen permeation rate found with one atmosphere of methane surrounding the sample was of the same order of magnitude as an earlier value reported for hydrogen permeation with hydrogen surrounding the sample (Table III). No permeation of the other gases through the Inconel sample was found.

TABLE III

GAS PERMEATION OF INCONEL

Sample Number	Gas	Temperature	Permeation Rate (Liter-mm/cm^2-sec-mm)
2	Methane	710° C	2.5×10^{-6} (as hydrogen)
3	Methane	810° C	2.0×10^{-6} (as hydrogen)
*	Hydrogen	800° C	5.5×10^{-6}
3	Nitrogen and Carbon Monoxide	1225° C	1×10^{-8}
3	Helium	1225° C	6×10^{-10}

*Note: This value obtained by extrapolation from data given for hydrogen at one atmosphere pressure through Inconel (reference 1).

Sample 2 of Inconel was carburized by running in methane for a short time at 1175° Centigrade. Hydrogen permeation was too high for measurement and sample temperature was reduced to 710° Centigrade. On re-heating to higher temperatures, the sample was lost by accidental melting of the carbide. Sample 3 was run in methane at a maximum temperature of 810° Centigrade in order to minimize carburization during the gas permeation measurement. Metallographic examination of sample 3 shows the formation of carbide (Figure 5); there is also evidence of precipitation of chromium carbide and of the formation of nitride at the grain boundaries.

Strong carbon monoxide and nitrogen degassing of the Inconel sample limits the ability to detect permeation to the upper limit shown

FIGURE 5 - PHOTOMICROGRAPH OF INCONEL
SHOWING CARBURIZATION

in Table III. The outgassing rate (at 1225° Centigrade) has the value 5×10^{-7} liters-millimeter second per square centimeter of sample area, even after heating at this temperature for many hours.

2. Platinum

The platinum test sample was a tube of length 11 inches, outside diameter 1/4 inch and wall thickness 0.020 inch. Permeation tests were carried out at temperatures between 900 and 1400° Centigrade. At maximum temperature, the length of the uniform hot zone was five inches. Gases tested were nitrogen, dry air, moist air, helium, and methane. The sample was degassed by heating at 1400° Centigrade in helium at atmospheric pressure for several hours.

Following degassing, the sample temperature was reduced to 915° Centigrade and methane at atmospheric pressure substituted for helium. As with Inconel, methane decomposed at the hot surface and hydrogen was observed to permeate the sample. The permeation rate of hydrogen at this temperature was 7×10^{-6} liters-millimeter-per square centimeter-second millimeter. This result is lower by an order of magnitude than published data[2] for the permeation of hydrogen through platinum (see Figure 6).

Following further degassing of the platinum sample at 1400° Centigrade in helium, dry air was introduced. No permeation of the components of air was observed, and upper limits of permeation rate are estimated in Table IV. The temperature of the sample was then reduced to 1000° Centigrade and moist air (humidified by bubbling the air through water at room temperature) was introduced.

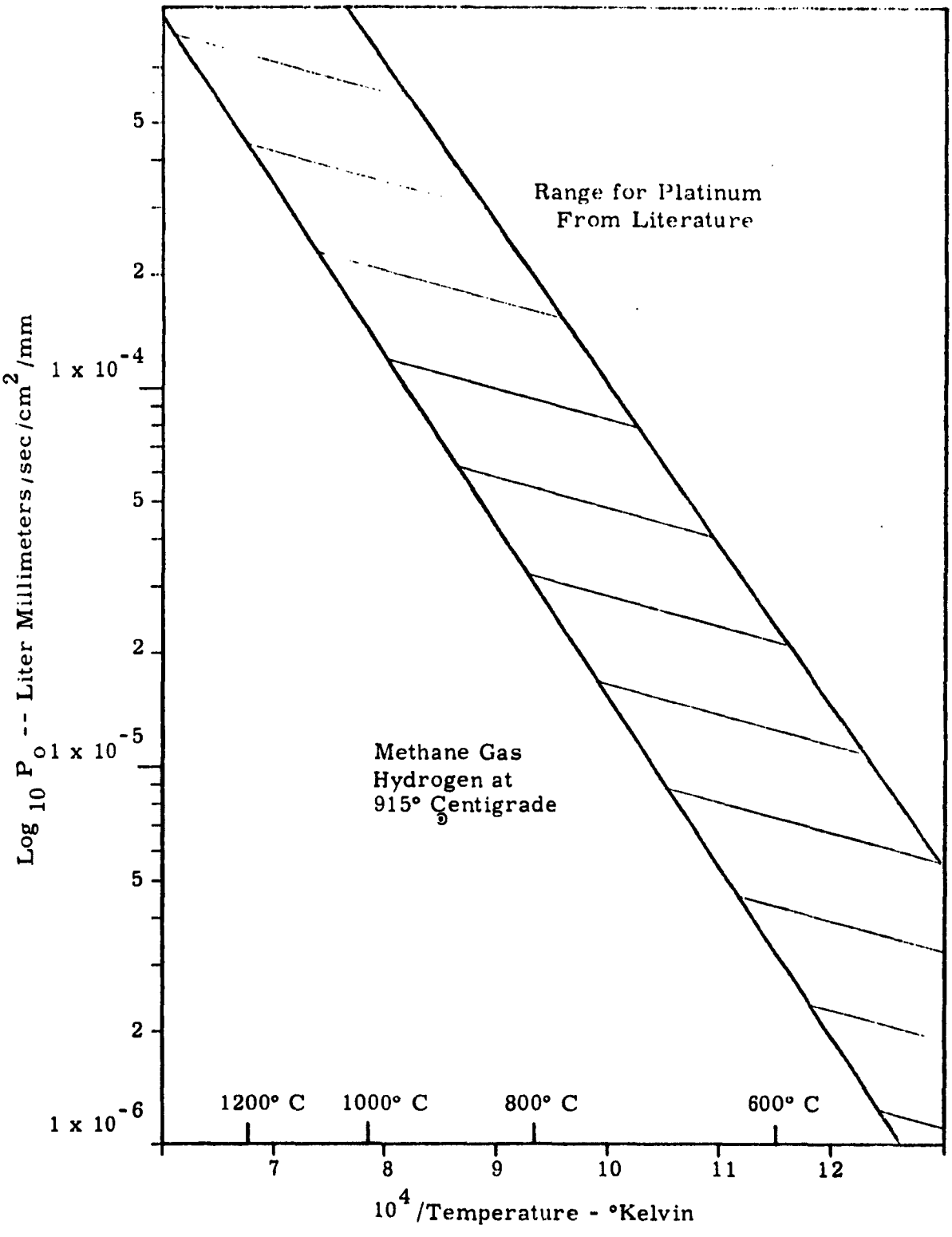

FIGURE 6 - PERMEATION OF HYDROGEN THROUGH PLATINUM

At 1000° Centigrade no permeation of hydrogen was seen, but on raising temperature to 1140° Centigrade dissociation of water vapor and permeation of hydrogen through the platinum was observed. The hydrogen permeation rate over the range 1140-1400° Centigrade is shown in Figure 7.

TABLE IV

GAS PERMEATION OF PLATINUM

Gas	Temperature	Permeation Rate (liter-mm/sec-cm^2-mm)
Nitrogen	1400° C	4×10^{-9}
Dry Air	1400° C	4×10^{-9}
Helium	1400° C	2×10^{-10}
Moist Air	1400° C	2×10^{-7} (as hydrogen)
Methane	915° C	7×10^{-6} (as hydrogen)

3. Platinum-15 Percent Rhodium Alloy

The test sample of platinum-15 percent rhodium alloy was a tube of length 11 inches, outside diameter 1/4 inch and wall thickness 0.020 inch. Permeation tests were carried out at 1400° Centigrade using the gases nitrogen, helium, dry air, and moist air The uniform hot zone at maximum temperature was five inches in length.

Following degassing at 1400° Centigrade in helium, dry air was introduced at atmospheric pressure. No permeation of helium

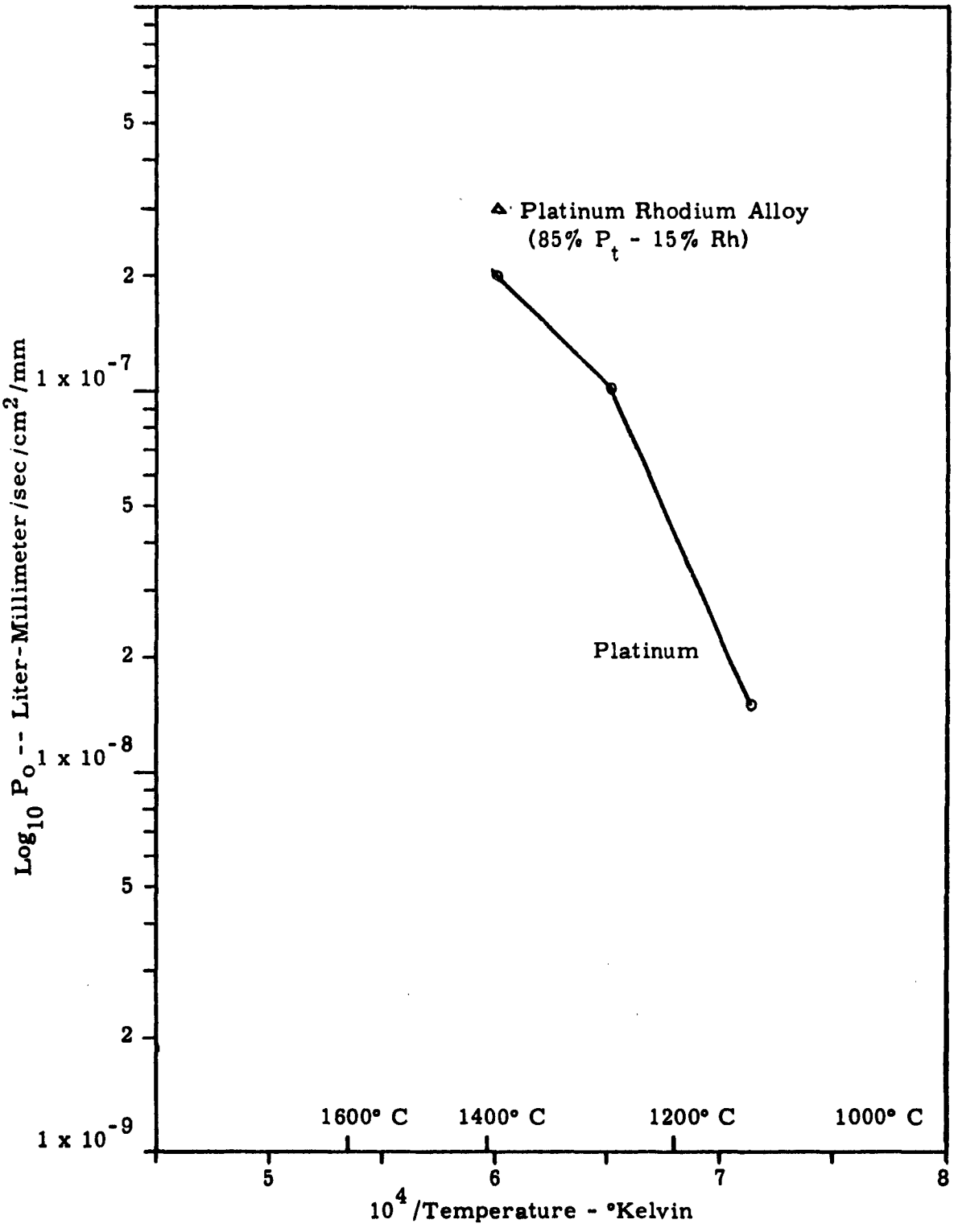

FIGURE 7 - PERMEATION OF HYDROGEN THROUGH PLATINUM DUE TO HEATING IN WATER VAPOR

or air components was found, the upper limits of the permeation rates being given in Table V. On introducing moist air (humidified by bubbling through water) hydrogen permeation was observed; the permeation rate was the same as that found for platinum and shown in Figure 7.

TABLE V

GAS PERMEATION OF PLATINUM-FIFTEEN PERCENT RHODIUM

Gas	Temperature	Permeation Rate (liter-mm/cm^2-sec-mm)
Nitrogen	1400° C	3×10^{-9}
Helium	1400° C	2×10^{-10}
Dry Air	1400° C	3×10^{-9}
Moist Air	1400° C	3×10^{-7} (as hydrogen)

4. Molybdenum

The molybdenum test sample was a tube of length 11 inches, outside diameter 1/4 inch and wall thickness 0.030 inch. Gases tested were nitrogen and hydrogen. Nitrogen permeation was measured at temperatures between 1300 and 1500° Centigrade, hydrogen permeation between 1100 and 2000° Centigrade. The uniform hot section of the molybdenum sample was eight inches long.

Hydrogen and nitrogen permeation is shown in Figures 8 and 9. Satisfactory agreement with published data is shown in these figures. There was no evidence of oxidation of the molybdenum

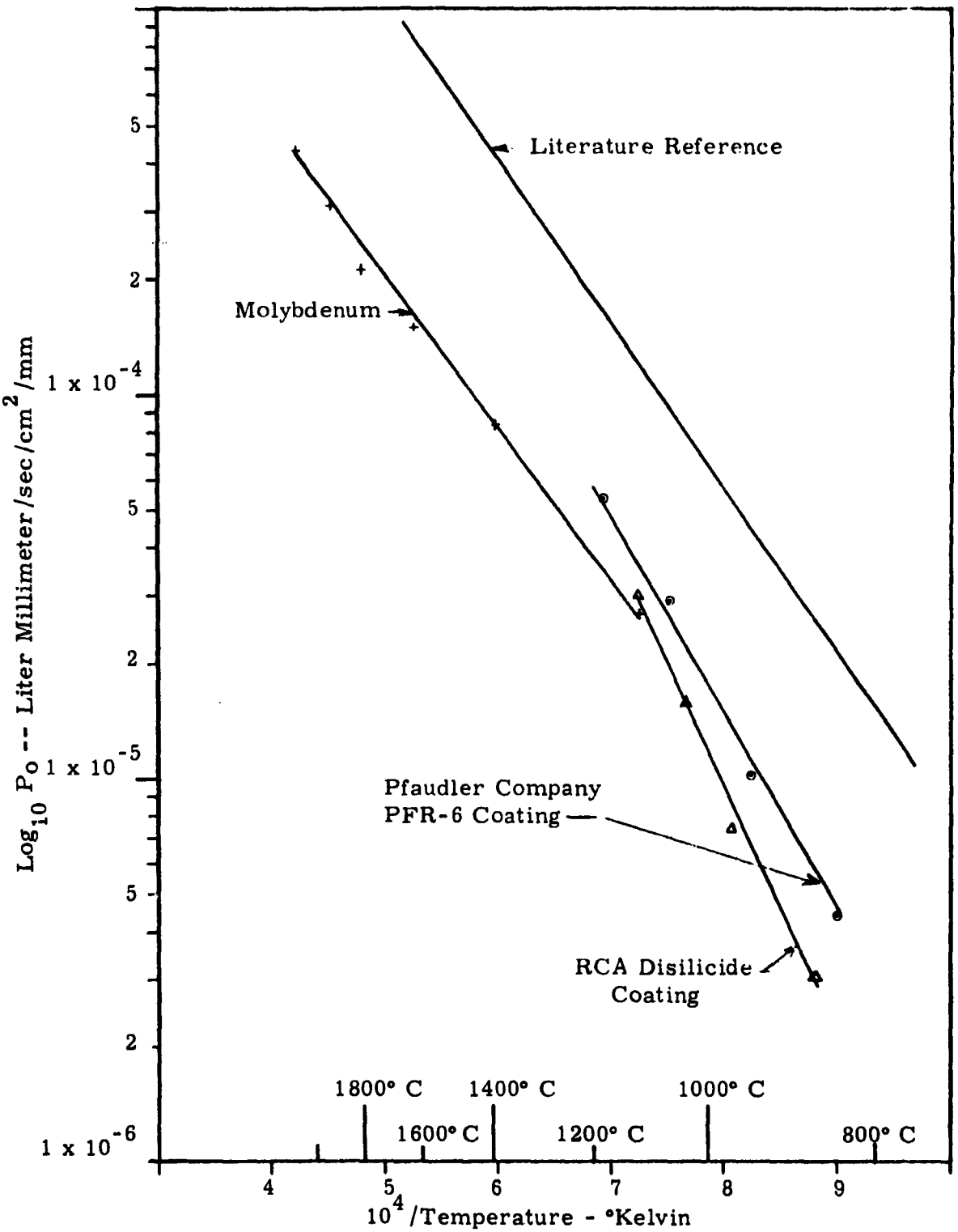

FIGURE 8 - PERMEATION OF HYDROGEN THROUGH MOLYBDENUM AND COATED MOLYBDENUM

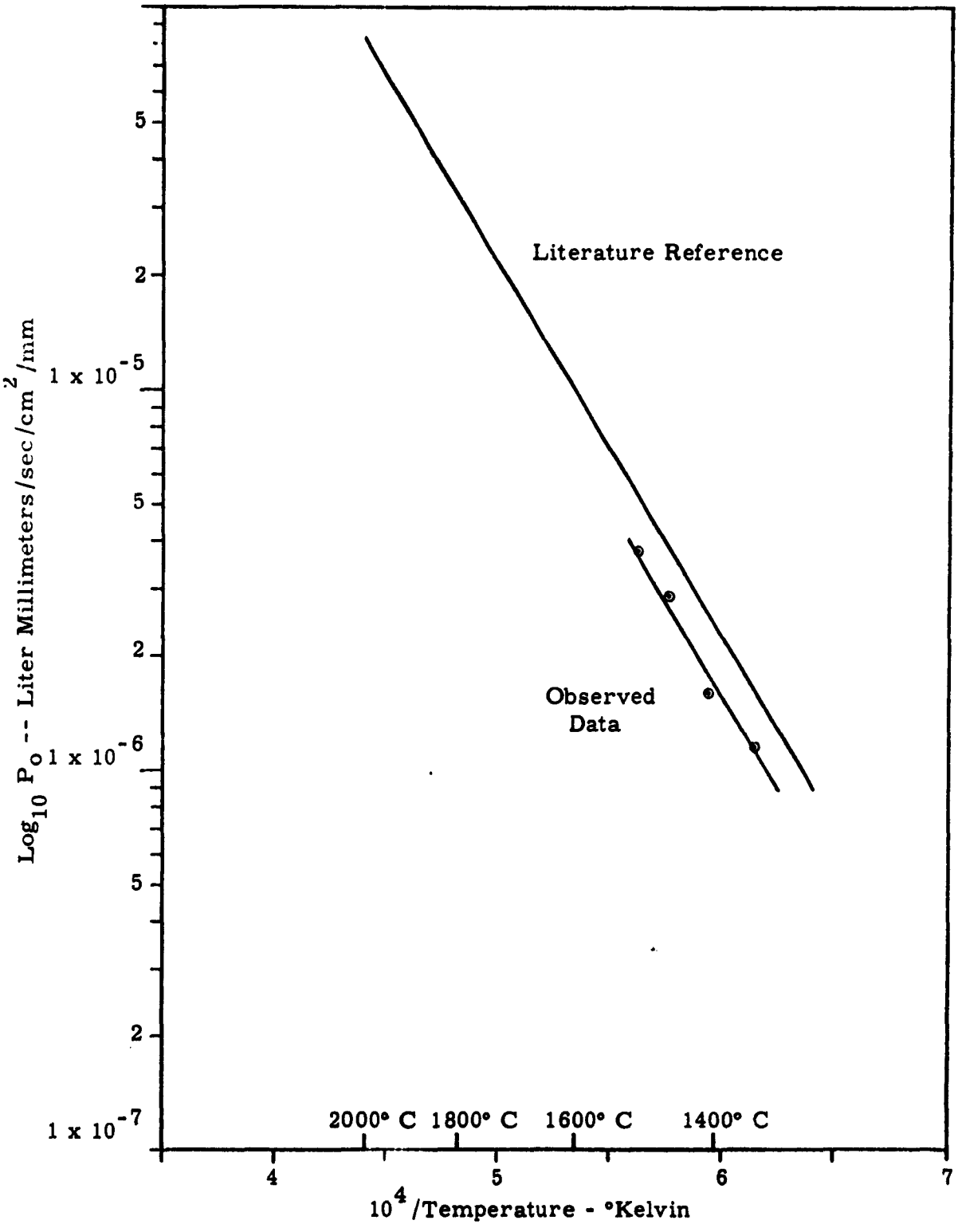

FIGURE 9 - PERMEATION OF NITROGEN THROUGH MOLYBDENUM

sample during the permeation testing with hydrogen or nitrogen, the walls of the bell jar remaining clear and free of discoloration.

5. Molybdenum With a Molybdenum Disilicide Protective Coating

A number of coatings have been developed for the protection of molybdenum against oxidation at high temperatures. One of the best of these selected for study in the present work is a coating of molybdenum disilicide. The disilicide coating was tested in two forms: (1) as applied in these laboratories, (2) as supplied by an outside laboratory (Ref. 5). In both cases, the same lot of molybdenum tubing was used as that in the permeation testing of uncoated molybdenum.

The RCA coating of molybdenum disilicide was applied according to the method described in Rawson (Ref. 6) to a 5.5 inch length of molybdenum tubing. The molybdenum sample is packed in silicon powder, heated to 900° Centigrade in hydrogen, and a mixture of HCl and H_2 gas is then allowed to stream through the batch for 30 minutes. A cross section of a disilicide coating attained in this way and used for permeation testing as described below is shown in Figure 10(a). This section shows the normal fibrous structure of the unrecrystallized molybdenum tubing. Coating thickness is 0.0005 inch.

The coating supplied by the Pfaudler Company was their PFR-6 coating. This is a proprietary coating which consists of molybdenum disilicide. It is applied by a diffusion pack process; details of the coating preparation, however, are not available. A photomicrograph of a cross section in Figure 10(b) shows a coating thickness of 0.003 to 0.004 inch. In addition, the molybdenum has

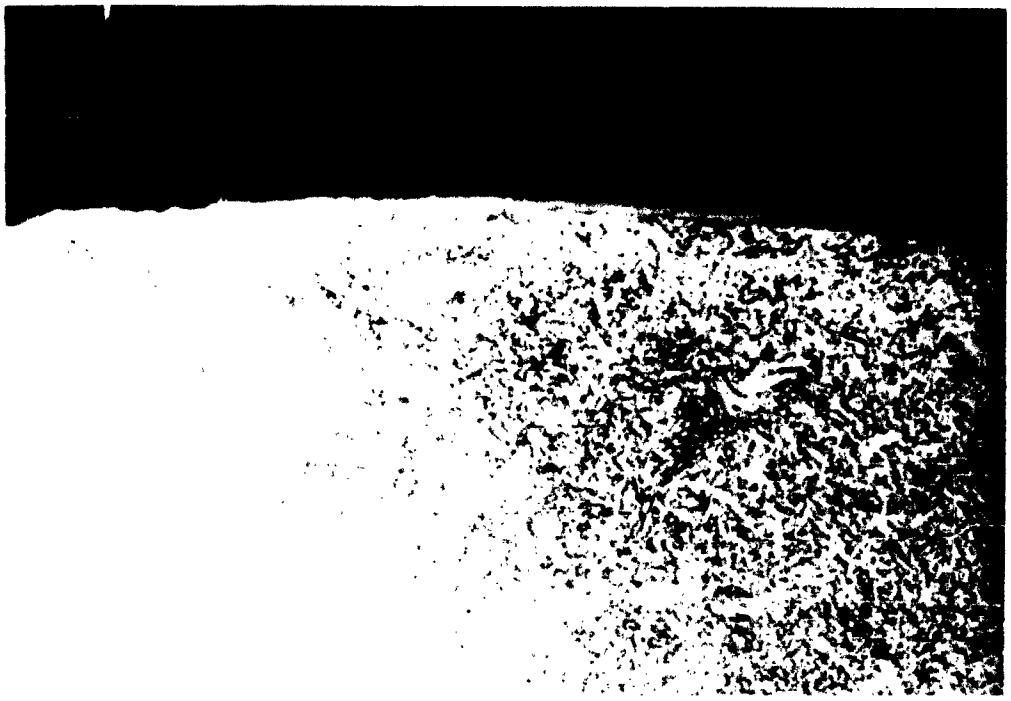

A. Rawson Method

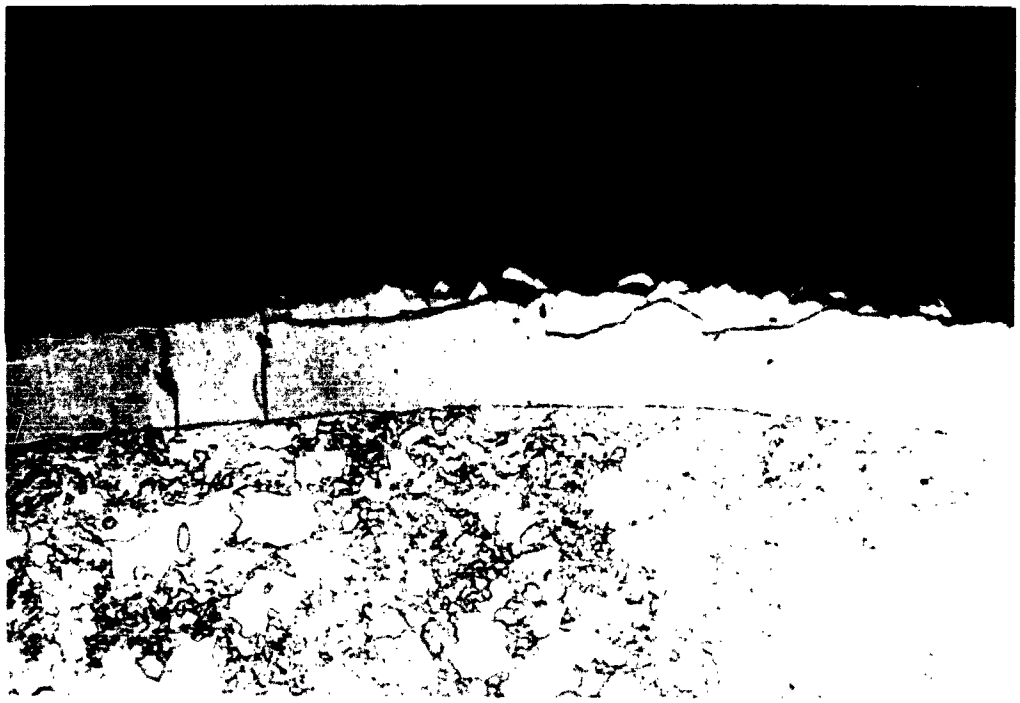

B. Pfaudler Company

FIGURE 10 - PHOTOMICROGRAPH OF A DISILICIDE COATING APPLIED TO MOLYBDENUM

recrystallized indicating temperatures somewhat higher than 900° Centigrade were used during the coating process. The two disilicide coatings in Figure 10 both show uniform thickness of the outside of the molybdenum tubing; the coating on the inside surface is thinner and less uniform. Occasional cracks are seen traversing the coating.

Although commercial resistance heaters made from molybdenum disilicide are designed for continuous operation in oxidizing atmospheres at temperatures as high as 1700° Centigrade, the disilicide coating on molybdenum is restricted to lower operating temperatures. The life of their coatings was stated by the Pfaudler Company to be several hours at 1500° Centigrade, or several hundred hours at 1200° Centigrade. Similar relatively poor life results were experienced with both types of disilicide coatings when tested here at the higher temperatures (1300 to 1500° Centigrade).

The molybdenum sample with the RCA disilicide coating was degassed before test by heating it in helium at 1200° Centigrade. Strong outgassing of carbon monoxide was observed even after heating for a number of hours. Following this, hydrogen was introduced and permeation measured between 850 and 1100° Centigrade. The permeation rates given in Figure 8 and Table VI are of the same order as were found for uncoated molybdenum. The sample was then degassed by heating in helium at 1500° Centigrade, and nitrogen was substituted for permeation test. No permeation was found to the upper limit indicated in Table VI (3×10^{-8} liter-mm/cm^2-sec-mm). This is lower by a factor of 100 than nitrogen

permeation found for the uncoated molybdenum and indicates the disilicide coating has considerable effectiveness as a barrier for nitrogen. Finally, on reheating the sample in air to about 800° Centigrade, severe smoking from its surface was observed, indicating failure of the coating with oxidation and sublimation of molybdenum oxide. The RCA disilicide coating was thus found to retard the permeation of nitrogen but not that of hydrogen; after a few hours of operation at 1500° Centigrade, however, its ability to protect molybdenum from oxidation was lost.

TABLE VI

GAS PERMEATION OF MOLYBDENUM WITH DISILICIDE COATING (RCA)
(Coating - thickness 0.0005 inch)

Gas	Temperature	Permeation Rate (liter-mm/cm^2-sec-mm)
Nitrogen	1500° C	3×10^{-8}
Hydrogen	1100° C	3×10^{-5}
Helium	1500° C	1×10^{-9}

The Phaudler PFR-6 disilicide coating was degassed by heating in air and then in helium for several hours prior to test. Hydrogen permeation tests were carried out over the temperature range of 850 to 1150° Centigrade. The data is shown graphically in Figure 8, which shows the same permeability for molybdenum with the PFR-6 coating as was obtained with uncoated molybdenum. The coating thus is no barrier to the permeation of hydrogen. No steady state permeation of the gases carbon monoxide, nitrogen and air was observed at 1150° Centigrade. (Table VII). At the end

of test, the coated molybdenum sample was cross sectioned; the photomicrograph (Figure 11) shows the coating to have numerous radial cracks. The pockets formed at the base of the cracks illustrate the erosion of the molybdenum by oxidation and sublimation.

TABLE VII

GAS PERMEATION OF MOLYBDENUM WITH DISILICIDE COATING (Pfaudler)
(PFR-6 Coating, 0.0035 inch thickness)

Gas	Temperature	Permeation Rate (liter-mm/cm^2-sec-mm)
Hydrogen	1150° C	5×10^{-5}
Helium	1150° C	3×10^{-10}
Carbon Monoxide	1150° C	1×10^{-8}
Nitrogen	1150° C	1×10^{-8}

6. Alumina Ceramics

Test samples of alumina ceramic material (Ref. 7) were obtained for permeation measurement. This material has high density and high purity (99.7 Al_2O_3) and can be used at temperatures as high as 1950° Centigrade. It is described as having good electrical resistivity at high temperature, as well as high thermal conductivity.

Two samples were prepared for test, having length 12 inches, outside diameter 5/15 inch and wall thickness 1/16 inch. The tubing was closed at one end and molybdenum metallized and brazed to a nickel-plated kovar collar and copper tubulation at

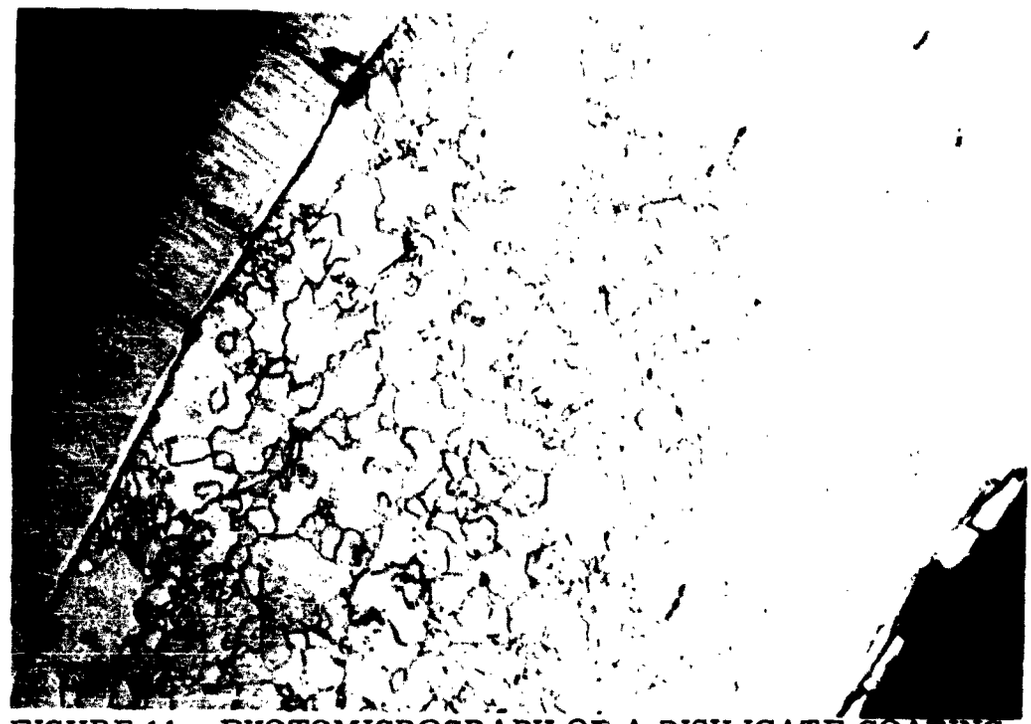

FIGURE 11 - PHOTOMICROGRAPH OF A DISILICATE COATING AFTER FAILURE

the exhaust end. The samples were heated using a PFR-6 disilicide coated molybdenum heater tube. The length of the hot zone was approximately five inches. Gases tested at 1250° Centigrade were hydrogen, nitrogen, helium, argon, methane, carbon monoxide, carbon dioxide, and air. On completion of these tests, hydrogen and helium were also tested at 1600° Centigrade.

The first ceramic sample failed during initial operation in air at temperatures below 1200° Centigrade. Examination showed that a reaction had occurred between the sublimation products of the heater and the alumina tube, changing the exterior appearance of the tube from white to gray. Cross sectioning showed that the reaction extended about half way through the wall of the tubing. Spectrographic and x-ray fluorescence analysis showed both molybdenum and silicon to be present in the ceramic as impurities.

The second alumina sample was tested for permeation of various gases at 1250° Centigrade, with the results shown in Table VIII. In this work the alumina sample was exposed to the test gas for from one to two hours before changing to the next test gas. No permeation of any of the gases was observed. During the test with methane, the gas decomposed and carbon was deposited on the heater and sidewall of the bulb. This test was therefore terminated after twenty minutes, no permeation being observed. The sample exhibited very good outgassing properties at 1250° Centigrade, the system pressure being maintained below 1×10^{-6} millimeter during the permeation testing at this temperature.

Following this, higher temperature tests were made using hydrogen. After heating to 1350° Centigrade for 30 minutes, however,

the disilicide coating decomposed and silicon was deposited on the sidewalls of the bulb and the exhaust manifold. The length of the hot zone was reduced to about 2.5 inches. During this time, the temperature of the heater increased to 1600° Centigrade. Tests were subsequently made using both helium and hydrogen at 1600° Centigrade. As indicated in Table VIII, no permeation of either of these gases was observed. Pressure was, however, found to increase by a factor of two, from 5×10^{-7} millimeter to 1×10^{-6} millimeter, when sample temperature was increased from 1250 to 1600° Centigrade. This increase was found to be caused by an increase in oxygen, and was independent of the gas present on the outside of the sample tube. No increase in nitrogen or argon was noted, and it was concluded that the effect was not due to an air leak.

TABLE VIII

GAS PERMEATION OF ALUMINA CERAMIC MATERIAL

Gas	Temperature	Permeation Rate (liter-mm/cm^2-sec-mm)
Hydrogen	1250-1600° C	3×10^{-8}
Nitrogen	1250° C	5×10^{-9}
Helium	1250-1600° C	5×10^{-10}
Argon	1250° C	1×10^{-11}
Methane	1250° C	- - - - -
Carbon Monoxide	1250° C	5×10^{-9}
Carbon Dioxide	1250° C	1×10^{-9}
Air	1250° C	1×10^{-9}

There is a possibility that the oxygen observed is due to dissociation at these high temperatures of oxides present in the ceramic material. Aluminum oxide itself has a low dissociation pressure, calculated from its free energy of formation (Ref. 8) to be of the order of 10^{-17} millimeters of mercury at 1600° Centigrade. Impurity oxides (present to a level of about 0.3 percent) could have substantial dissociation pressures sufficiently high to account for the observed oxygen pressure.

SECTION IV
CONCLUSIONS

The present investigation of gas permeation was undertaken to help define the best choice of envelope materials for a thermionic energy converter to be heated to temperatures of 1200° Centigrade or slightly higher.

Gases present on the outside of the converter will thus typically contain hydrogen and carbon (as molecular hydrogen, methane, water vapor, carbon monoxide, carbon dioxide, etc.) and oxygen or the gas components of air.

It was found that metals can not be used at high temperatures in contact with gases containing hydrogen, due to the rapid permeation of the metals by hydrogen. A promising high temperature protective coating for molybdenum, consisting of molybdenum disilicide, was found not to prevent hydrogen permeation, although nitrogen permeation was substantially improved. Inadequate oxidation protection of molybdenum by this coating, for a long-lived device, was also observed.

The only material offering protection from gas permeation for all gases was found to be an alumina ceramic. This material should be useful either as a bulk envelope material, or as a protective coating applied to metals. Oxygen evolution was found to be a possibility at higher temperatures (1400-1600° Centigrade). The alumina material was not shown to be the source of oxygen, but if it is, the phenomenon could possibly be controlled by (a) control of oxide impurity content of the alumina or (b) oxygen degassing prior to use of the material.

SECTION V

REFERENCES

1. J. Brous et al, "A Study of High Temperature Microwave Tube Design and Processing", WADD Technical Report 60-324 (pp. 54 to 75). Wright Air Development Division, W-P Air Force Base, Ohio, (June, 1960).

2. Norton, F. J., J. App. Phys., 28, pp. 34-39, (1957).

3. Barrer, R. M., "Diffusion In and Through Solids," Cambridge Univ. Press, (1951).

4. Lectrodryer Division, McGraw Edison Company, Pittsburgh, Pennsylvania.

5. The Pfaudler Company, Rochester 3, New York.

6. Rawson, H., Jour. Soc. Glass Tech., 39, 211T, (1955).

7. Triangle RR Alumina, Manufactured by the Morganite Company, Long Island City, New York.

8. Coughlin, J. P., "Heats and Free Energies of Formation of Inorganic Oxides," Bulletin 542, Bureau of Mines, (1954).

APPENDIX III

ATMOSPHERIC CORROSION OF THE VACUUM ENVELOPE

Prepared for:

AERONAUTICAL SYSTEMS DIVISION
United States Air Force
Wright-Patterson Air Force Base
Ohio

Contract AF33(616)-7903
Project Number 3145
Task Number 314509

Prepared by:

J. J. Moscony

RADIO CORPORATION OF AMERICA
Electron Tube Division
Space Component Engineering
Lancaster, Pennsylvania

ATMOSPHERIC CORROSION OF THE VACUUM ENVELOPE

TABLE OF CONTENTS

LIST OF ILLUSTRATIONS

LIST OF TABLES

ATMOSPHERIC CORROSION OF THE VACUUM ENVELOPE

SECTION I

INTRODUCTION

For some applications, it would be desirable to operate all or a portion of the vacuum envelope of a thermionic energy converter in an oxidizing atmosphere. This type of operation will permit convection cooling of the anode by air and also allow direct heating of the cathode by an open flame or other similar means. In such applications the temperature of external collector surfaces can operate as high as 600° Centigrade, while the cathode temperature will range from 900° to 1400° Centigrade.

In view of the above conditions it is important, for long-life applications, to know the oxidation resistance of the metals and brazing alloys used in the envelope. Accordingly, tests were performed to determine oxidation rates of various materials at 600° and 1000° Centigrade. In addition, methods for coating molybdenum were investigated at 600° Centigrade and in the range of 1000° to 1300° Centigrade.

This metal was given prime consideration as an envelope material because of its low vapor pressure and attractive structural properties at elevated temperatures. However, it is well known that molybdenum oxidizes rapidly above 500° Centigrade and therefore, for such applications, a protective coating is required.

SECTION II

OXIDATION TESTS AT 600° CENTIGRADE AND 1000° CENTIGRADE

A Test Procedure

Samples of the materials to be tested were prepared in one-inch squares from flat stock ranging from 0.003 inch to 0.040 inch in thickness. Each sample had a 1/8-inch diameter hole in one corner for mounting purposes. After degreasing and weighing, the samples were mounted on sapphire rods and placed in a controlled furnace at the temperature of interest. At various time intervals weights were taken and the oxidation in milligrams per square inch was calculated.

B Test Results

Results obtained from oxidation tests at 600° Centigrade and 1000° Centigrade appear in Figures 1 and 2, and in Table I.

Figure 1 illustrates the effect after 40 hours at 600° Centigrade on various materials. Although it is known that molybdenum and copper cannot withstand this temperature, these metals were included for comparison purposes. While Inconel X shows only slight oxidation, Kovar and the brazing alloys G605 (37.5% Au, 62.5% Cu) and Nicoro (3.0% Ni, 35.0% Au, 62.0% Cu) show severe oxidation. In addition, tests were made on the oxidation resistance, at 250° Centigrade, of metal-to-ceramic vacuum seals. These seals employed molybdenum-metalized, high-alumina ceramic, brazed to nickel-plated Kovar. In one case where the braze material was Nicoro 80 (3.0% Ni, 15.5% Cu, Bal. Au) a leak was detected in the braze area after 83 hours as a result of oxidation effects. It is clear that gold-copper brazing alloys and Kovar will require adequate protection against oxidation if they are to be used at 600° Centigrade.

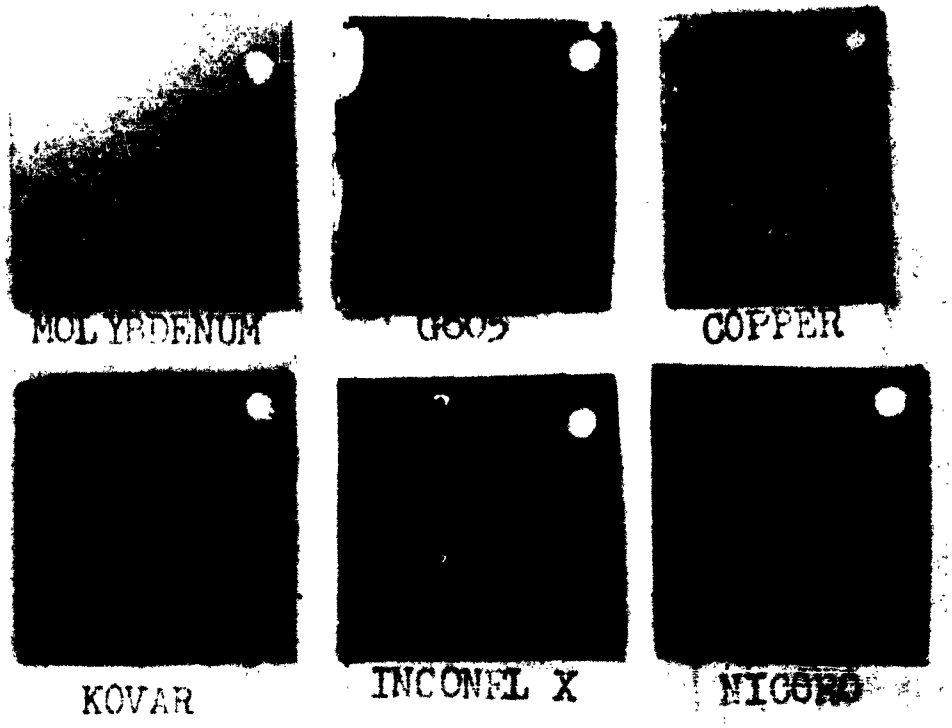

A. Appearance Before Exposure

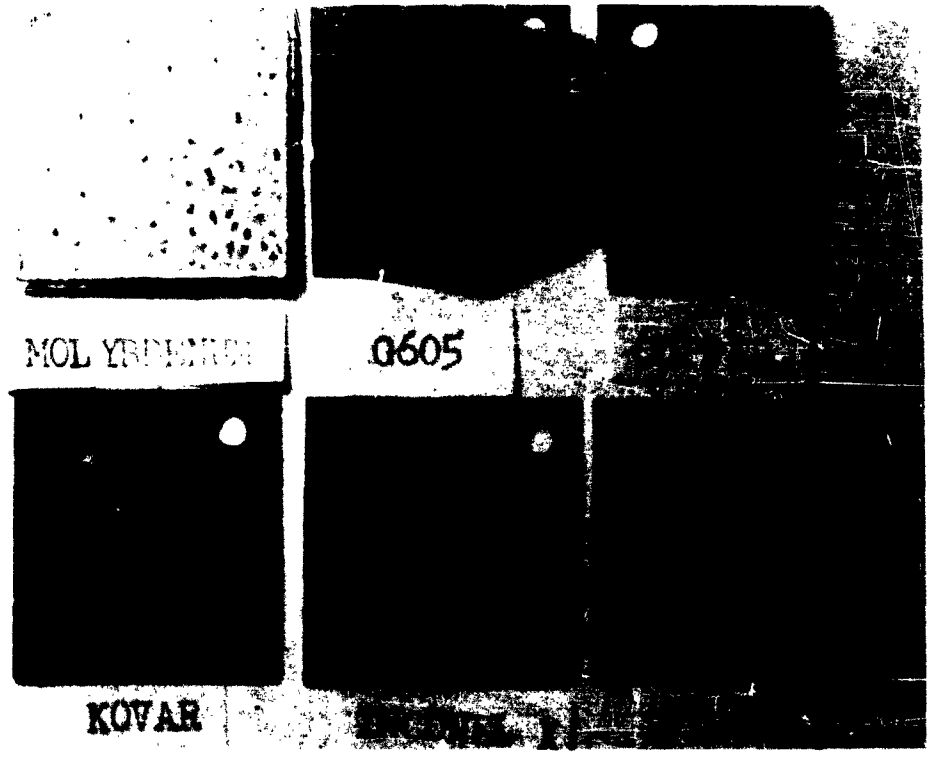

B. Appearance After 40-Hours Exposure

FIGURE 1 - EFFECT OF AIR AT 600° C ON VARIOUS MATERIALS

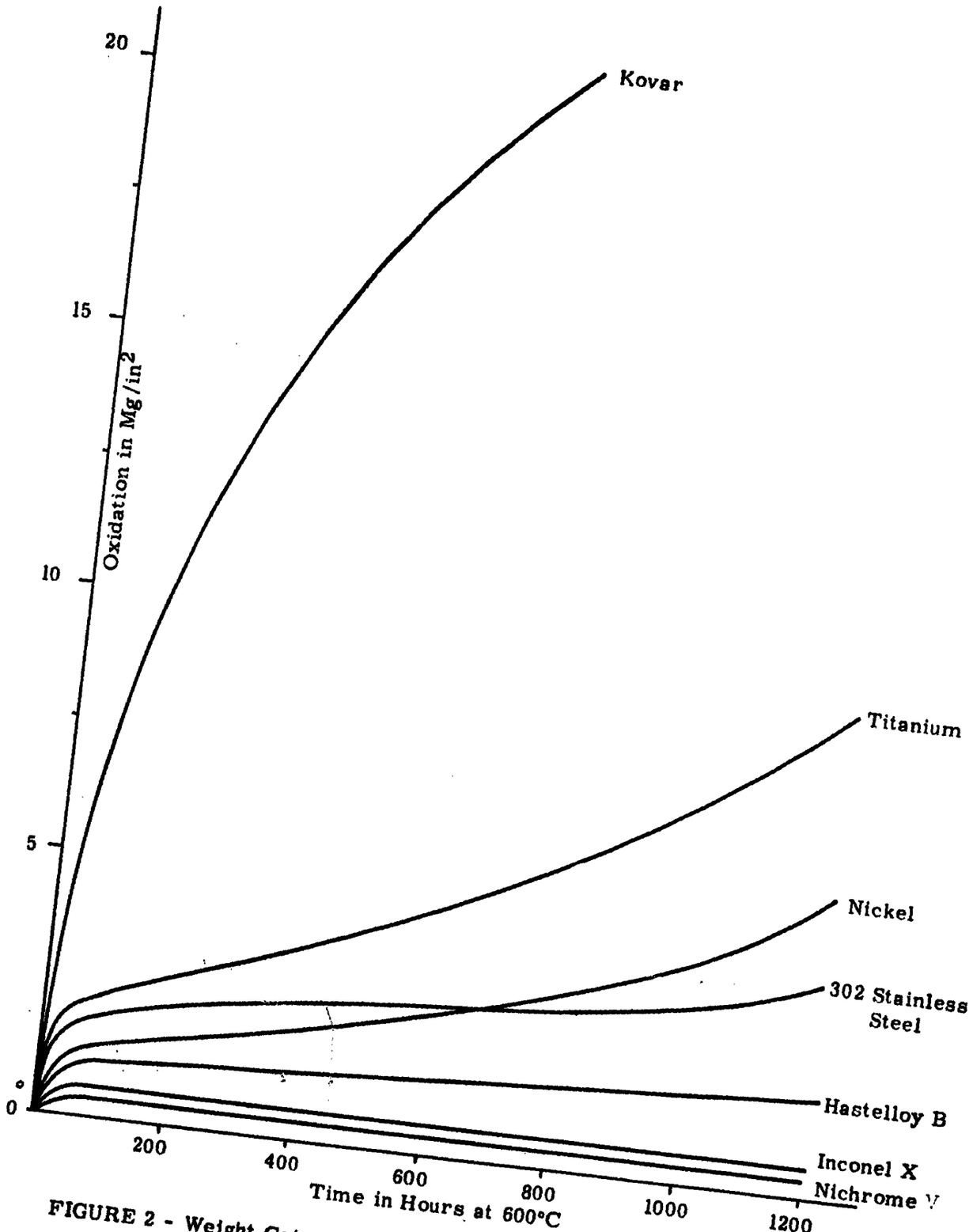

FIGURE 2 - Weight Gain in Mg/in^2 vs Time in Hours for Various Materials at 600°C

TABLE I

Weight Change (Mg/in^2) at 1000° C for Various Materials at the Indicated Exposure Time in Hours

	Exposure Time in Hours		
Material	75.0	126.0	265.0
Nichrome V	5.0	5.3	5.0
Hastelloy B	111.0	129.0	159.0
302 Stainless Steel	157.0	-	-
Inconel X	2.2	2.2	2.2
Kovar	450.0	-	-
Platinum	- 0.4	- 0.5	- 0.8
Nickel	59.0	80.0	-

The oxidation rate observed for various materials at 600° Centigrade has been depicted in Figure 2. Platinum was included in these tests, but no oxidation of this material was observed after an exposure of 1200 hours. The resistance to oxidation of Inconel X, Nichrome V, and Hastelloy B is good, of 302 stainless steel nickel, and titanium is fair, and of Kovar, is poor.

Data presented in Table I illustrates the oxidation rate in Mg/in^2 - hour for various materials at 1000° Centigrade. In those cases where no weight change is recorded, oxide flaking occurred causing further measurements to be irrelevant. Nichrome V, Inconel X and platinum show good oxidation resistance as opposed to the relatively fast oxidation of Hastelloy B, 302 stainless steel, nickel and particularly Kovar.

SECTION III
PROTECTIVE COATINGS FOR MOLYBDENUM

The cross-rolled and fully-annealed molybdenum used for test samples in the following sections conformed to the RCA Material Specifications 33-M-37F.

A Platinum Plating

A method was developed that affords good protection for molybdenum against oxidation by air at 600° Centigrade. This is accomplished by electroplating platinum in alternate plating and hydrogen firing operations. In one test a molybdenum sample having a 0.001 inch thick platinum coating exhibited a weight gain of only 0.8 milligrams per square inch after 500 hours at 600° Centigrade in static air. Figure 3 shows the visual appearance of this sample after 500 hours on test as compared to an unprotected molybdenum sample after 40 hours at 600° Centigrade. A cross section of the plated sample made after test appears in Figure 4. In this figure, the 0.001 inch platinum plating appears as the light area directly above the etched surface of the molybdenum. Note that the plating shows little sign of deterioration and has offered good protection to the molybdenum.

In actual practice, a 0.001 inch thick platinum plating can be deposited according to the following schedule:

1. Degrease;
2. Electropolish in a one-to-one solution of sulfuric acid and phosphoric acid for three minutes at 250 amperes per square foot. Bath temperature should be approximately 50° Centigrade;
3. Water rinse;
4. Dip for one minute in alkaline ferricyanide solution. This

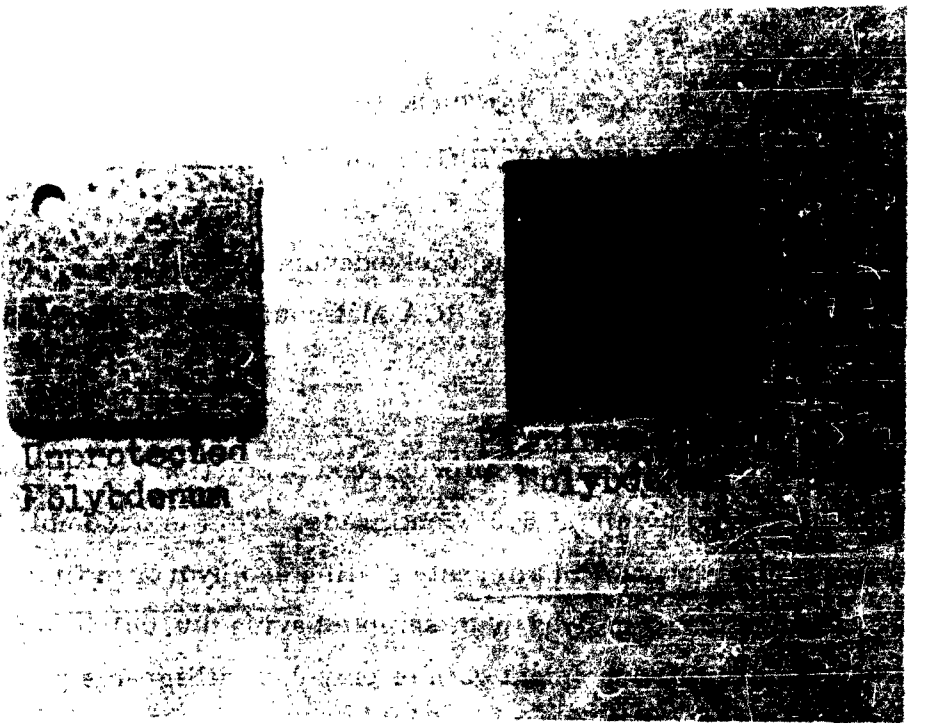

FIGURE 3 - MATERIALS AFTER EXPOSURE AT 600° C
(A - 40 Hrs. - B - 500 Hrs.)

FIGURE 4 - PLATINUM-PLATED MOLYBDENUM
AFTER 500 HOURS AT 600° C

solution consists of 300 grams per liter of potassium ferricyanide and 100 grams per liter of potassium hydoxide;

5. Water rinse;
6. Platinum plate to a thickness of 0.001 inch. This plating can be accomplished at a current density of 20 amperes per square foot and a temperature of 80° Centigrade;
7. Vacuum fire at 1000° Centigrade for 30 minutes at a pressure of 10^{-4} millimeters of mercury;
8. Platinum plate to a thickness of 0.001 inch using the conditions described in 6 above;
9. Vacuum fire as described in 7 above.

A molybdenum test specimen employing a platinum plating 0.003 inch thick, was tested at 1000° Centigrade in air and showed extreme oxidation after two hours. The rapid oxidation was probably due to the increased difference in thermal expansion of the two metals causing exfoliation of the plating and resulting in oxidation of the unprotected molybdenum.

B Silicized Molybdenum

The effect of molybdenum silicide as an oxidation resistant coating for molybdenum at 1000° Centigrade in air was evaluated. Samples were prepared by direct reaction of molybdenum with silicon. The method consisted of packing, in a ceramic boat, several samples of molybdenum rod with 99.99 percent silicon powder (150 mesh) so that the powder completely enveloped the rod. The mixture was then heated to 1000° Centigrade in line hydrogen. When 1000° Centigrade was reached, hydrochloric acid vapor was allowed to stream over the mixture for an hour, after which time the flow of hydrochloric acid was shut off and the mixture was allowed to cool to room temperature.

Using the above procedure, it was possible to develop a molybdenum silicide coating 0.0005 inch thick. After applying the coating, the samples were placed in a static air oven at 1000° Centigrade. This coating showed better protection ability than the platinum coating at 1000° Centigrade. Figure 5 shows a molybdenum slug with a 0.0005 inch thick silicized coating before and after exposure to air at 1000° Centigrade for 200 hours. While there is definite evidence of deterioration, the coating has offered a substantial measure of protection at this high temperature. It is probable that thicker silicized coatings will afford better protection for more extended periods.

A commercial silicide coating for molybdenum,[1] containing small amounts of columbium was tested at 1300° Centigrade and 1200° Centigrade in static air using a globar furnace. This 0.002 to 0.004 inch coating was developed to protect molybdenum-alloy, reentry-vehicle components against oxidation at temperatures near 1650° Centigrade.

Visual inspection of two samples after 24 hours at 1300° Centigrade revealed no evident change in appearance. However, after 50 hours, severe attack was evidenced by cracking and scaling of the coating in each case. Another sample tested at 1200° Centigrade showed oxidation attack after 45 hours, but not so severe as in the 1300° Centigrade test.

[1] ASD Technical Report 61-241, Development of a Cementation Coating Process for High-Temperature Protection of Molybdenum. P. J. Chao, B. S. Payne, Jr., D. K. Priest, June 1961. The Pfaudler Company, a Division of Pfaudler Permutit Inc., Rochester 3, New York.

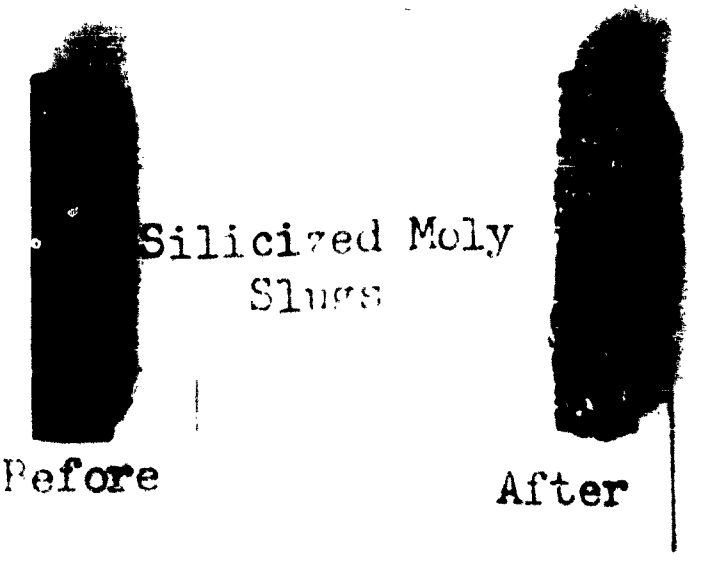

FIGURE 5 - Silicized Molybdenum Slug Before and After Exposure to Air at 1000°C for 200 Hours

SECTION IV
CONCLUSIONS

Some common construction materials such as gold-copper brazing alloys, Kovar, copper, nickel and titanium show atmospheric oxidation rates at 600° Centigrade and 1000° Centigrade in excess of that required for long-term applications. Protective coatings and/or suitable substitutes must be found to insure extended life.

A method was developed that affords good protection for molybdenum against oxidation by air at 600° Centigrade. This is accomplished by electroplating platinum in alternate plating and hydrogen firing operations. This method is applicable in providing an external envelope material with a good thermal expansion match for high-alumina ceramics.

Silicized coatings for molybdenum are useful for long-term applications at 1000° Centigrade in air. However, tests indicate that this type coating, in the present "State-of-the-Art", is not practical for extended use at 1300° Centigrade.

APPENDIX IV

CALCULATION OF EFFICIENCY

Prepared for:

AERONAUTICAL SYSTEMS DIVISION
United States Air Force
Wright-Patterson Air Force Base
Ohio

Contract AF33(616)-7903
Project Number 3145
Task Number 314509

Prepared by:

RADIO CORPORATION OF AMERICA
Electron Tube Division
Space Component Engineering
Lancaster, Pennsylvania

CALCULATION OF EFFICIENCY

Efficiency is calculated by means of the following equation:

$$\eta = \frac{\text{power output}}{\text{power input}} = \frac{I(\phi_C - \phi_A - V_L)}{P_e + P_L + P_r}$$

when I = total current

ϕ_c = cathode work function

ϕ_a = anode work function

V_L = voltage drop in cathode lead

P_e = electron emission cooling

P_L = cathode lead power loss

P_r = radiation power loss

A sample unit was selected having the following characteristics and the efficiency was calculated by means of the subsequent equations.

Dimensions and Constants

Cathode diameter - 3.19 cm

Cathode area - 8 cm^2

Current density, (J) varied from 1-10 amps/cm^2

$\phi_C = 2.3$, $\phi_A = 1.68$

$T_c = 1175°$ C, $T_A = 150°$ C

Thermal conductivity of tantalum = .586 watts/°K-cm

Resistivity of tantalum = 40×10^{-6} ohm-cm

Cathode emissivity = $\Sigma_c = 0.6$

Anode emissivity = $\Sigma_A = 0.25$

Sample Calculation

A. $J = 10 \text{ amps/cm}^2$

1. Reduction of Current by Magnetic Field

$I_o = JA = 10 \times 8 = 80$ amperes

$$\frac{I_o a}{R\sqrt{T_c}} = \frac{80 \text{ amps} \times .0762 \text{ cm}}{1.595 \times \sqrt{1450}} = .1015$$

from Figure C-1 of RCA Appendix C of this report

$I = .84\, I_o = .84 \times 80 = \underline{67.2 \text{ amperes}}$

2. Voltage Drop in Cathode Lead

$V_c = \frac{IPL}{A}$ A = cross-sectional area of lead

L = length of lead

η_o = efficiency calculated before correction for lead loss. When lead loss is optimized, $\eta_o \rightarrow \eta$. For an optimum lead

$$\frac{A}{L} \cong I\sqrt{\frac{\rho}{KBT\,\eta_o}\left(1 - \frac{\eta_o}{2}\right)}$$

assumption $\eta_o = 10$ percent

$$\frac{A}{L} \cong 67.2\sqrt{\frac{40 \times 10^{-6}}{586 \times 1 \times 10^{3} \times .1}\left(1 - \frac{.1}{2}\right)} = .0542$$

then $V_L = \frac{IPL}{A} = \frac{67.2 \times 40 \times 10^{-6}}{0.0542} = \underline{.0496 \text{ volts}}$

3. Electron Emission Cooling

$P_e = I\left(\phi_c + \frac{2K}{e} T_L\right)$ where K = Boltzmann's K

e = electronic charge

T_L = Lead Temperature

$P_e = 67.2\,(2.3 + 1.72 \times 10^{-4} \times 1450) = \underline{172 \text{ watts}}$

4. Lead Power Loss

$$P_L = k \Delta T \frac{A}{L} - \frac{IV_L}{2}$$

k = thermal conductivity

$\Delta T = T_c - T_A$

$$P_L = .586 \times 1000 \times .0542 - \frac{67.2 \times .0496}{2}$$

$$P_L = 31.8 - 1.66 = \underline{30.14 \text{ watts}}$$

5. Radiation Power Loss

$$P_r = \sigma \Sigma \text{eff.} A(T_c^4 - T_A^4)$$

where $\sigma = 5.67 \times 10^{-12} \frac{\text{watts}}{\text{cm}^2 - {}^\circ\text{K}}$

$$\Sigma \text{eff.} = \left(\frac{1}{\Sigma_c} - \frac{1}{\Sigma_a} - 1 \right)$$

$$P_r = 5.67 \times 10^{-12} \times 8 (1450^4 - 425^4) \times .214$$

$$P_r = 5.67 \times 10^{-12} \times 8 (4.38 \times 10^{12}) \times .214$$

$$P_r = 204 \times .214 = \underline{43 \text{ watts}}$$

6. Efficiency

$$\eta = \frac{I(\phi_c - \phi_a - V_L)}{P_e + P_L + P_r}$$

$$\eta = \frac{67.2 (2.3 - 1.68 - .0496)}{172 + 30.14 + 43} = \frac{38.3}{245.14} = \underline{15.56 \text{ percent}}$$

The original assumption for efficiency

$$\eta_o = 10 \text{ percent}$$

was in error. A recalculation after correction to

$$\eta_o = 15 \text{ percent}$$

will proceed as follows:

2a. Correction of V_L

$$\frac{A}{L} = 67.2 \sqrt{\frac{40 \times 10^{-6}}{.586 \times 10^{+3} \times .15} (1 - \frac{.15}{2})} = .042$$

$$V_L' = \frac{67.2 \times 40 \times 10^{-6}}{0.042} = \underline{.064 \text{ volts}}$$

4a. Correction of Lead Loss

$$P_L' = .586 \times 10^3 \times .042 - \frac{67.2 \times .064}{2}$$

$$P_L' = 24.6 - 2.15 = \underline{22.45 \text{ watts}}$$

6a. Corrected Efficiency

$$\eta' = \frac{67.2 (2.3 - 1.68 - .064)}{172 + 22.45 + 43} = \frac{37.4 \text{ watts out}}{237.45 \text{ watts in}}$$

$$\eta' = \underline{15.85 \text{ percent}}$$

7a. Addition of Power Loss for Third Element. (assume I_{bias} = 2 percent of I and E_{bias} = 1 volt.)

$$P_{bias} = .02 \times 67.2 \times 1\ V = 1.34 \text{ watts}$$

$$\eta = \frac{37.4 - 1.34}{237.45} = \underline{15.2 \text{ percent}}$$

TABULATED DATA

Theoretical
(Bias Current Assumed to be 2% of Output Current)

$J \frac{amp}{cm^2}$	I amp	V_L volts	P_e watts	P_L watts	P_r watts	P_{bias} watts	P_{out} watts	P_{out} watts/cm^2	P_{in} watts	Percent
10	67.2	0.064	172.0	22.45	43	1.34	36.06	4.5	237.45	15.2
8	56.3	0.0618	143.5	19.56	43	1.13	30.27	3.8	206.06	14.65
6	43.6	0.0541	111.0	17.72	43	0.87	23.83	3.0	171.70	13.6
4	29.7	0.0436	75.8	15.35	43	0.594	16.7	2.1	134.15	12.4
2	15.2	0.0486	38.8	6.95	43	0.304	8.4	1.05	88.75	9.4

Tube Number 23
(Bias Current Observed to be 17% of Output Current)

$J \frac{amp}{cm^2}$	P_{bias} watts	P_{out} watts	Percent
10	14.7	22.7	9.6
8	12.3	19.1	9.3
6	9.55	15.15	8.8
4	6.5	10.8	8.1
2	3.33	5.37	6.05

Tube Number 24
(Bias Current Observed to be 4.0% of Output Current)

$J \frac{amp}{cm^2}$	P_{bias} watts	P_{out} watts	Percent
10	4.19	33.21	14.0
8	3.51	27.89	13.5
6	2.72	21.98	12.8
4	1.85	15.45	11.5
2	0.95	7.75	8.7

APPENDIX V

SPACE CHARGE NEUTRALIZATION BY RESONANCE IONIZATION

Prepared for:

AERONAUTICAL SYSTEMS DIVISION
United States Air Force
Wright-Patterson Air Force Base
Ohio

Contract AF33(616)-7903
Project Number 3145
Task Number 314509

Prepared by:

RADIO CORPORATION OF AMERICA
Electron Tube Division
Space Component Engineering
Lancaster, Pennsylvania

SPACE CHARGE NEUTRALIZATION BY RESONANCE IONIZATION

Assume the presence of a gas within the converter structure whose ionization potential, V_i, is lower than the work function of the cathode, ϕ_c. Since the condition $\phi_c > V_i$ is satisfied, neutral atoms striking the hot cathode will be ionized and injected as positive ions into the interelectrode space. In this way a plasma beam which extends from the cathode to the anode is formed. For complet neutralization, the ion density must equal the electron density, or, for a plane parallel geometry,

$$\frac{I_p}{C_p} = \frac{I_A}{C_e} \tag{1}$$

where I_p is the ion current and C_p and C_e are the average Maxwellian ion and electron velocities, respectively. Assuming the ion and electron temperatures to be equal, Equation 1 may be written

$$I_p = I_A \sqrt{m_e/m_p} \tag{2}$$

where m_e/m_p is the electron-to-ion mass ratio. The power lost in ion generation is $(\phi_c - \phi_a) \sqrt{m_e/m_p}$, which may be of the order of a few hundredths of a watt per ampere.

The required gas pressure may be computed as follows: The number of atoms striking the cathode surface per unit time is $(1/4) A_e N_g C$ where N_g is the gas density and C is the average Maxwellian particle velocity. Assuming an ion yield of the order of unity, the ion current becomes

$$I_p = \frac{e}{4} A_e N_g C \tag{3}$$

Combining Equations 1 and 3 yields

$$N_g = 4 \frac{C_p}{eCC_e} \frac{I_A}{A_e} \tag{4}$$

or, expressed in terms of pressure p in mm of Hg

$$p = 4.12 \times 10^{-6} \sqrt{T_g} j_A \tag{5}$$

where T_g = the gas temperature in °K and j_A is the electron current density in amperes per square centimeter.

The ratio f+ of the number of ions evaporated off the heated surface to the number of neutral atoms impinging on the surface is believed to be given by the Saka equation[4]:

$$f+ = \frac{1}{1 + e^{-\frac{e}{kT_c}(\phi_c - V_i)}} \tag{6}$$

A plot of this equation is shown in Figure 1. This figure shows that $(\phi - V_i)$ should be made as large as possible when large ion currents are desired. It also indicates the weak dependence of f+ on the temperature of the emitter (hot surface).

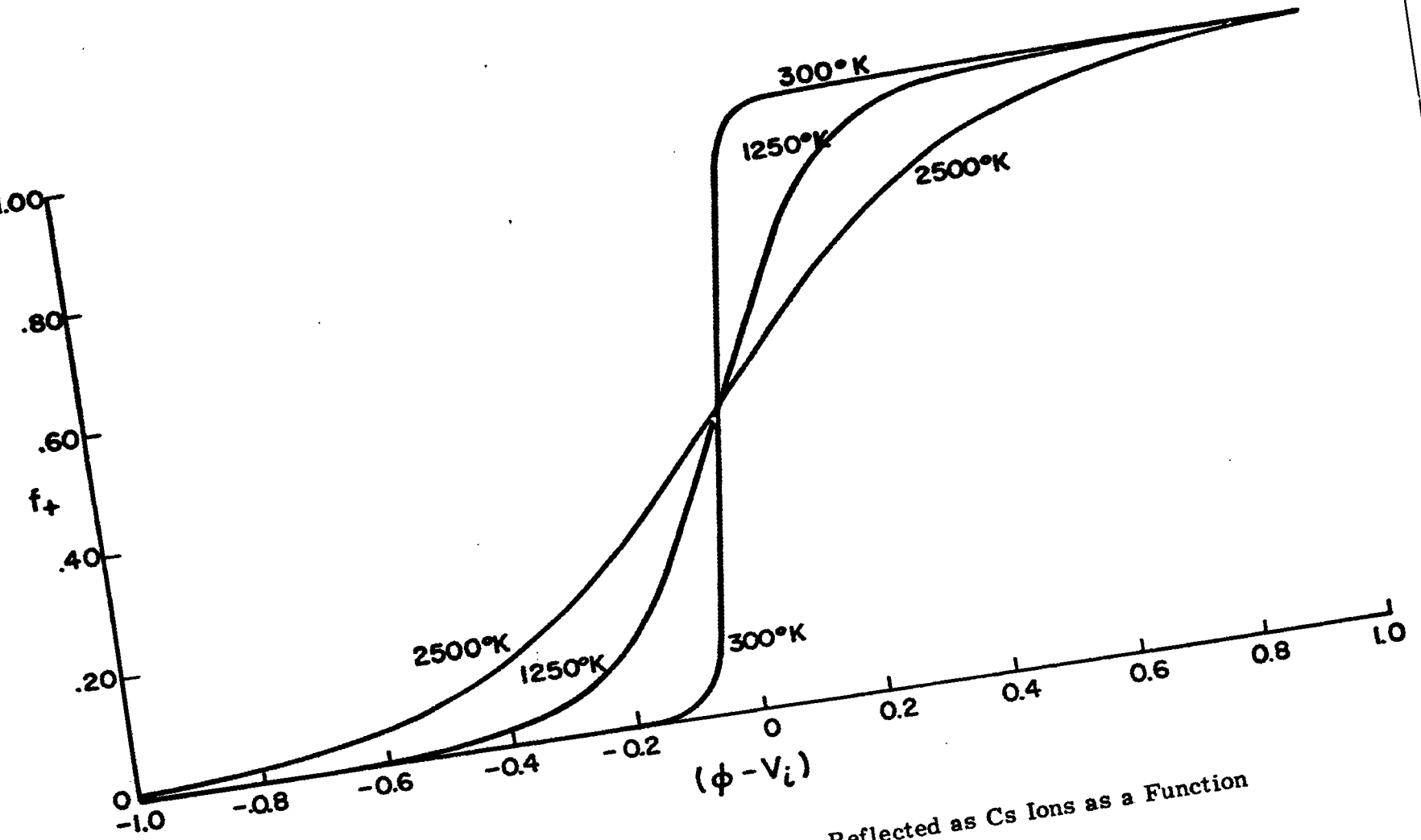

FIGURE 1 - Fraction of Incident Cs Atoms Reflected as Cs Ions as a Function of (ϕ - V_i) and of Emitter Temperature.

APPENDIX VI

EFFECTS OF MAGNETIC FIELD ON EFFICIENCY

Prepared for:

AERONAUTICAL SYSTEMS DIVISION
United States Air Force
Wright-Patterson Air Force Base
Ohio

Contract AF33(616)-7903
Project Number 3145
Task Number 314509

Prepared by:

RADIO CORPORATION OF AMERICA
Electron Tube Division
Space Component Engineering
Lancaster, Pennsylvania

EFFECTS OF MAGNETIC FIELD ON EFFICIENCY

To illustrate the effect of the magnetic field, two different geometries will be discussed. In one geometry the cathode and anode are concentric cylinders. Here the current is drawn out at one end of the cylinder only. In the other geometry two circular discs are considered, one serving as the cathode and the other the anode. It is assumed that the current is drawn out uniformly along the cathode periphery.

In Figure 1 the computed results for these two geometries are shown. In this figure the ratio I/I_o of actual current to emission current is plotted as a function of the parameter $I_o a/R^o \sqrt{T_c}$, where a is the cathode-to-anode separation and R the cathode radius. It is seen from Figure 1 that in order not to reduce the current and the efficiency by more than about 10%, the parameter $I_o a/R \sqrt{T_c}$ should not exceed 0.075. If we assume a separation, a, of approximately 0.075 cm this means that $I_o \precsim R\sqrt{T_c}$. Furthermore, I_o is related to the current density j. For the cylindrical geometry $I_o = 2\pi RLj$, where L = length of cathode. Thus one obtains for the cylindrical geometry

$$L = \frac{\sqrt{T_c}}{2\pi j}$$

and

$$I_o = \frac{R}{2L}\left(\frac{c}{\pi j}\right) \qquad (1)$$

for the disc geometry $I_o = \pi R^2 j$. For the same separation distance, a, of 0.075 cm as assumed above

$$R = \frac{\sqrt{T_c}}{\pi j}$$

and

$$I_o = \frac{T_c}{\pi j} \qquad (2)$$

An examination of equations 1 and 2 reveals that they are different only by the factor R/2L. Clearly R/L must be less than unity in order to reduce end losses and thus the disc geometry allows much higher currents per unit cell.

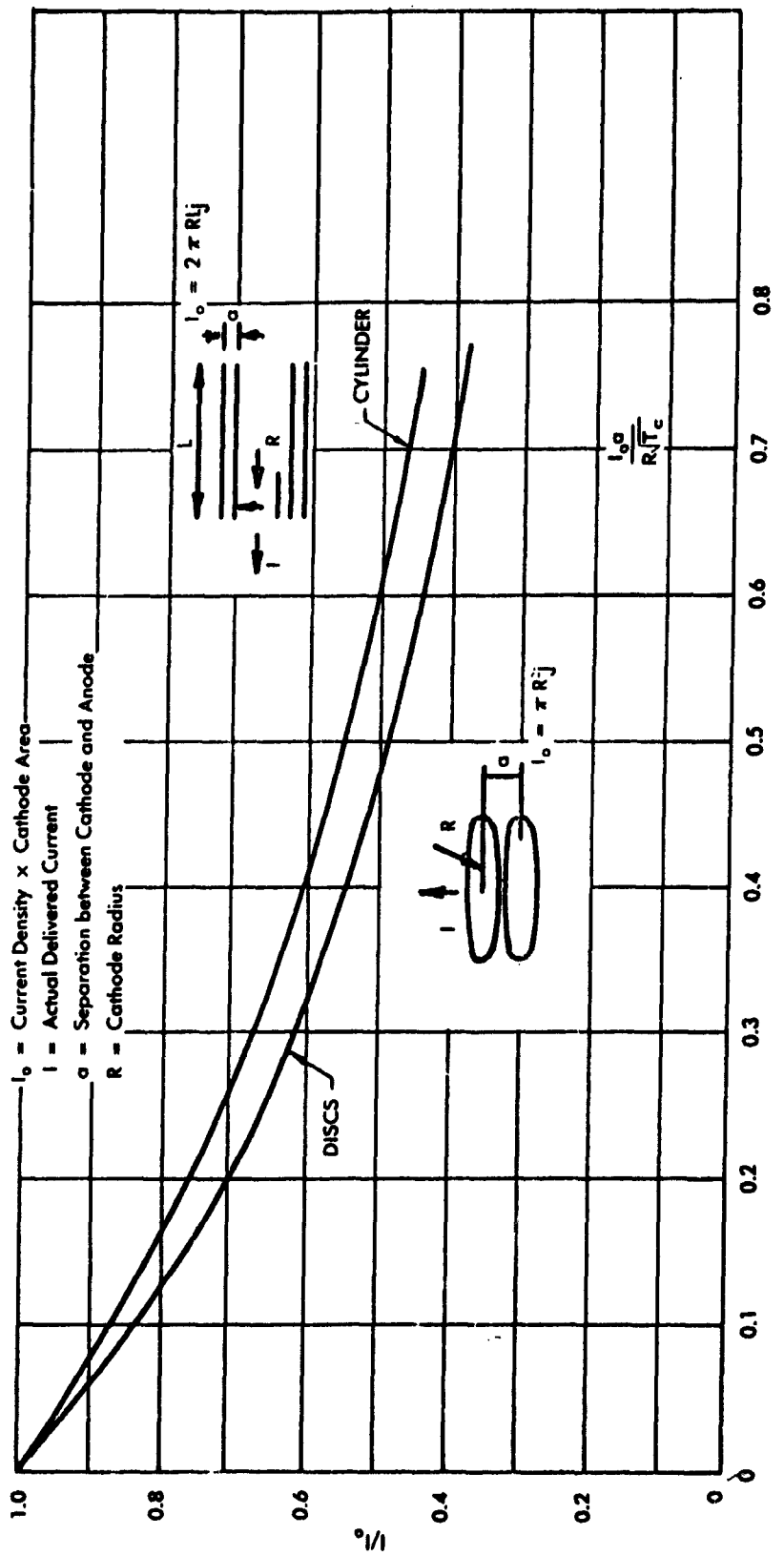

FIGURE 1 - The Effects of Internal Magnetic Fields

APPENDIX VII

EFFECT OF CATHODE LEAD DIMENSION ON EFFICIENCY

Prepared for:

AERONAUTICAL SYSTEMS DIVISION
United States Air Force
Wright-Patterson Air Force Base
Ohio

Contract AF33(616)-7903
Project Number 3145
Task Number 314509

Prepared by:

RADIO CORPORATION OF AMERICA
Electron Tube Division
Space Component Engineering
Lancaster, Pennsylvania

EFFECT OF CATHODE LEAD DIMENSION ON EFFICIENCY

The total power lost in the cathode lead, P_L, is equal to the arithmetic sum of several factors.

P_L = conduction loss + radiation loss -joule heat returned to cathode

Usually the radiation loss in the lead can be included in the total radiation losses from the cathode by appropriate adjustment of the cathode area. Then, the lead loss is the sum of the first and third terms.

$$P_L = \frac{K \Delta T A}{L} - 1/2 \frac{\rho_L}{A} I^2 \qquad (1)$$

Including this loss in the efficiency equation (1) the expression can be written

$$\eta = \frac{(\phi_c - \phi_a)I - \frac{\rho_L}{A} I^2}{\phi_c I + P_r + K \Delta T \frac{A}{L} - 1/2 \frac{\rho_L}{A} I^2} \qquad (2)$$

where

ϕ_c = cathode work function

ϕ_a = anode work function

I = current

P_r = total radiation losses from cathode

ρ = resistivity

L = lead length

A = cross section

K = thermal conductivity

ΔT = temperature drop along lead; or approximately cathode temperature minus anode temperature

Since the voltage drop along the lead is

$$V = \rho \frac{L}{A} I \tag{3}$$

The efficiency can be written

$$\eta \frac{\phi_c - \phi_a - V}{\phi_c + \frac{P_r}{I} + \frac{\kappa \rho \Delta T}{V} - \frac{V}{2}} \tag{4}$$

For optimum lead design $\frac{\delta \eta}{\delta V} = 0$, resulting in the expression

$$\eta = \frac{V^2/\rho}{\kappa \Delta T + 1/2\, V^2/\rho} \tag{5}$$

The optimum voltage drop in the lead is

$$V = \sqrt{\frac{\kappa \rho \Delta T \, \eta}{1 - \eta/2}} \tag{6}$$

and the optimum dimensions are

$$\frac{A}{L} = I \sqrt{\frac{\rho}{\kappa \Delta T \eta} \left(1 - \frac{\eta}{2}\right)} \tag{7}$$

If the lead design is optimized then $\eta \rightarrow \eta_o$ where η_o is the efficiency calculated without consideration of lead loss. Then one obtains

$$\frac{A}{L} \cong I \sqrt{\frac{\rho}{\kappa \Delta T \eta_o} \left(1 - \frac{\eta_o}{2}\right)} \tag{8}$$

for an approach to the optimum lead dimension. If the lead is used as a cathode support it must, for practical reasons, have structural rigidity. This latter requirement calls for a large A/L ratio. It also turns out that a nuclear heat source calls for a large A/L ratio since this will minimize the amount of dead space per unit cell. Since the quantities under the square root sign in Equation 8 are more or less predetermined, a large A/L ratio requires a large current I per unit cell. However, as discussed in the proposal, the magnetic field effect puts an upper limit on I. It is of interest, therefore, to evaluate the reduction in efficiency resulting from a deviation from the optimum lead design.

Consider, as a specific example, a converter operating with the following characteristics: T_c = 1475°K, ϕ_c = 2.30 volts, ϕ_a = 1.75 volts, I = 67 amperes (j = 50 amperes/cm^2), P_r = 76.4 watts, K = .59 watts/°K-cm, ρ = 4.0×10^{-5} ohm-cm, ΔT = 900°K, and from equation (1) η_o = 16.0%. Using these values in equation D-4 one obtains

$$\eta \cong \frac{0.55 - V}{3.44 + \frac{.0211}{V} - \frac{V}{2}} \qquad (9)$$

In Figure 1, η is plotted as a function of V for these conditions.

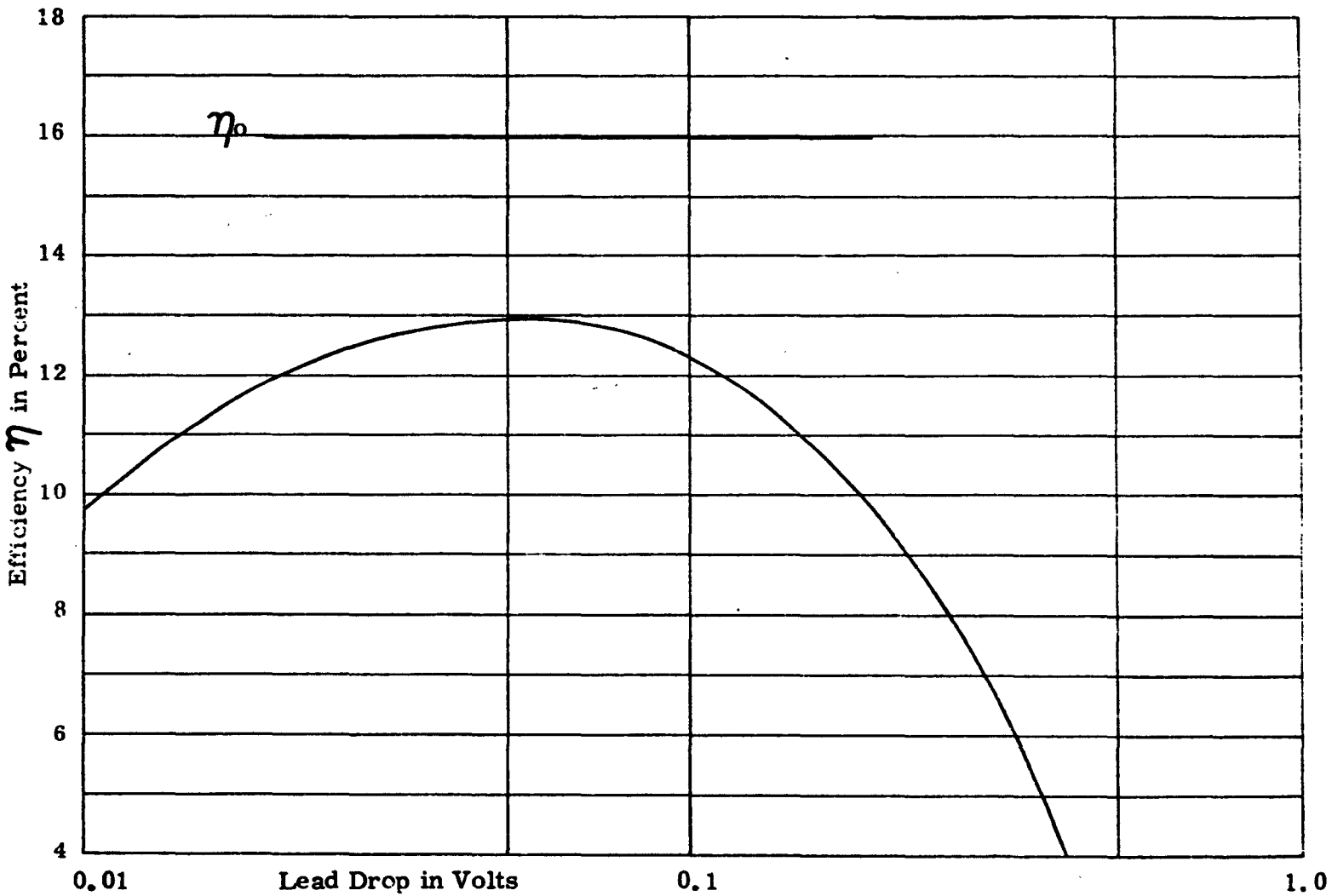

FIGURE 1 - Efficiency as a Function of Lead Drop

Aeronautical Systems Division, Dir/Aeromechanics, Flight Accessories Lab, Wright-Patterson AFB, Ohio.
Rpt Nr ASD-TDR-62-324. THE DEVELOPMENT OF A LOW TEMPERATURE VAPOR FILLED THERMIONIC CONVERTER. Final report, Jun 62, 168p. incl illus., tables, 12 refs.

Unclassified Report

This report covers a one year program of applied research toward developing a low-temperature, plasma, thermionic converter. The converter uses a third electrode to ionize plasma so as to neutralize the space charge. The lower temperature thus achieved should significantly prolong

(over)

the life of the converter and contribute to the development of a more reliable power supply for space application.

The program was directed toward optimizing geometry and operating characteristics and investigating the effects of temperature and pressure, starting pulse, magnetic fields, and operation in both series and parallel circuitry. Materials were investigated to achieve practical electrodes by determining compatibility of material, atmospheric corrosion, and gas permeation. Converters were fabricated, evaluated, and life tested with the parameters optimized by the test program.

1. Thermionic emission
2. Cesium compounds
3. Gas ionization
4. Corrosion

I. AFSC Project 3145, Task 314509
II. Contract AF33(616)-7903
III. RCA-Lancaster, Pa.
IV. F. G. Block, J. J. O'Grady
V. Aval fr OTS
VI. In ASTIA collection

Aeronautical Systems Division, Dir/Aeromechanics, Flight Accessories Lab, Wright-Patterson AFB, Ohio.
Rpt Nr ASD-TDR-62-324. THE DEVELOPMENT OF A LOW TEMPERATURE VAPOR FILLED THERMIONIC CONVERTER. Final report, Jun 62, 168p. incl illus., tables, 12 refs.

Unclassified Report

This report covers a one year program of applied research toward developing a low-temperature, plasma, thermionic converter. The converter uses a third electrode to ionize plasma so as to neutralize the space charge. The lower temperature thus achieved should significantly prolong

(over)

the life of the converter and contribute to the development of a more reliable power supply for space application.

The program was directed toward optimizing geometry and operating characteristics and investigating the effects of temperature and pressure, starting pulse, magnetic fields, and operation in both series and parallel circuitry. Materials were investigated to achieve practical electrodes by determining compatibility of material, atmospheric corrosion, and gas permeation. Converters were fabricated, evaluated, and life tested with the parameters optimized by the test program.

1. Thermionic emission
2. Cesium compounds
3. Gas ionization
4. Corrosion

I. AFSC Project 3145, Task 314509
II. Contract AF33(616)-7903
III. RCA-Lancaster, Pa.
IV. F. G. Block, J. J. O'Grady
V. Aval fr OTS
VI. In ASTIA collection